ELECTROPHYSIOLOGICAL AND BEHAVIORAL
MECHANISMS OF *CAENORHABDITIS ELEGANS* FEEDING

APPROVED BY SUPERVISORY COMMITTEE

Dr. Leon Avery, Ph.D., M.B.A.

Dr. Dean Smith, M.D., Ph.D.

Dr. Thomas Sudhof, M.D.

Dr. Jane Johnson, Ph.D.

ACKNOWLEDGEMENTS

I would like to thank all the people who helped me in getting though the graduate school. Leon Avery is a superb scientific advisor. He has created a lab, in which whoever wants to become a scientist, actually can become a scientist. Members of his lab: Sarah, Jim, Alan, Young, Mark and Ohnjo, have all offered some valuable advice, criticism, and support. I enjoyed collaborating with Katherine Steger. Much of my voltage clamp stuff would not have been possible without the work of Wayne Davis. Anton Maximov has helped me learn basic techniques. Cori Bargmann and Yun Zhang, as well as many other people whose names I do not remember, have provided useful input on C.elegans meetings. Thanks to Sue Lott for great administrative support. My dissertation committee members: Jane Johnson, Thomas Sudhof, Dean Smith, Ralph Dileone and Jim Waddle have done a good job too. Many thanks to my parents for providing me with the genome keen to inquiry, many thanks and love to my wife Ira and to my daughter Masha.

ELECTROPHYSIOLOGICAL AND BEHAVIORAL MECHANISMS OF *CAENORHABDITIS ELEGANS* FEEDING

by

BORIS BORISOVICH SHTONDA

DISSERTATION

Presented to the Faculty of the Graduate School of Biomedical Sciences

The University of Texas Southwestern Medical Center at Dallas

In Partial Fulfillment of the Requirements

For the Degree of

DOCTOR OF PHILOSOPHY

The University of Texas Southwestern Medical Center at Dallas

Dallas, Texas

November, 2004

ELECTROPHYSIOLOGICAL AND BEHAVIORAL
MECHANISMS OF *CAENORHABDITIS ELEGANS* FEEDING

Publication No. _____

Boris Borisovich Shtonda

The University of Texas Southwestern Medical Center at Dallas, 2004

Supervising Professor: Leon Avery, Ph.D., M.B.A.

The nematode (roundworm) *Caenorhabditis elegans* lives in soil and eats bacteria. Its feeding organ is a neuromuscular pump called the pharynx.

First, I developed a voltage clamp preparation for the pharynx and recorded native ionic current in the pharyngeal muscle. I showed that a T-type Ca channel CCA-1, an L-type Ca channel EGL-19 and a potassium channel EXP-2 shape pharyngeal action potentials. CCA-1 works in the pharyngeal muscle to boost its response to neurotransmission from the MC pharyngeal neuron. Next, EXP-2 is not an inward rectifier in the pharynx; it generates large currents upon hyperpolarization and has nearly linear voltage dependence. Finally, the

pharynx adapts to the loss of MC excitatory inputs by raising its resting membrane potential, which makes it more excitable.

Second, I studied food seeking and food preference behaviors in *C.elegans.* In the laboratory, *C.elegans* is routinely kept on plates seeded with *E.coli*, and it is not known how worms behave in an environment where diverse food is available. I identified additional food sources, such as *Bacillus megaterium*, *Comamonas sp.*, and *Bacillus simplex*, and showed that bacterial food varies in quality. *C.elegans* hunts for the food of higher quality, the one that better supports growth. This seeking activity is further enhanced in animals that have already experienced good food. Next, the food regulates *C.elegans* locomotion, particularly the equilibrium between two locomotion modes, known as roaming and dwelling. On good food, dwelling is more common, on poor food, roaming is predominant. The normal balance between these states is essential for the food seeking behavior. In *ttx-3* and *osm-6* mutants the food-dependent equilibrium between locomotion states is impaired: worms tend to spend less time roaming on poor food. *ttx-3* defects are partially reproduced by laser ablation of AIY interneurons, suggesting that AIY functions to inhibit the roaming-to-dwelling transition and to extend food-seeking periods. On the other hand, *tax-6* mutants show increased roaming even on high quality food. *tax-6*, *osm-6* and *ttx-3* mutants are defective in food choice behavior.

C.elegans may serve as a new system to uncover mechanisms that enable animals to find high quality food in diverse environments.

CONTENTS

PUBLICATIONS RELATED TO THIS WORK

Avery L. and Shtonda B.B. (2003) Food transport in the *C elegans* pharynx. J Exp Biol, 206: 2441-2457.

Shtonda B.B. and Avery L. CCA-1, EGL-19 and EXP-2 currents shape action potentials in the *Caenorhabditis elegans* pharynx (*accepted by the Journal of Experimental Biology*).**

Steger K.A.*, Shtonda B.B.*, Thacker C., Snutch T.P., Avery L. The *Caenorhabditis elegans* T-type calcium channel CCA-1 boosts neuromuscular transmission (*accepted by the Journal of Experimental Biology*).

* Equal contribution.
** This paper, including text and figures, was adapted for chapter 2 of this thesis.
.

LIST OF FIGURES AND TABLES

SUPPLEMENTARY MATERIAL

- Food preference movie: preference.mpg. Food choice of *eat-2(ad465)* naïve L1 larvae between two *E.coli* strains, DA837 (bottom) and HB101 (top) was recorded for 90 min.
- Leaving behavior movies: leaving of the wild type L1s on *Comamonas sp.* (comamonas.mpg), *E.coli* HB101 (HB101.mpg) and *B.megaterium* (megaterium.mpg). Approximately 2-hour recordings.

All movies are at 30 frames per minute; thus, if played at 30 frames per second they are 60 times the real speed.

- The worm tracking program, B_Player.exe, (Appendix, Fig.7). The Microsoft Visual C++ 6 source code is available at http://eatworms.swmed.edu/~boris/B_Player.
- Labview programs: for voltage clamp experiments, VClamp-1x.vi, and analysis, VAnal.vi (Appendix, Fig. 2); for analysis of current clamp recordings, intracell_anal.vi and intracell_viewer.vi (Appendix, Fig. 3); for the trajectory analysis, traject_anal.vi and bulk_traject_anal.vi (Appendix, Fig. 6). Labview programs are available for download at http://eatworms.swmed.edu/~boris/Labview. Note that there are additional VIs in this folder that are used by the VIs listed above, so all VIs need to be downloaded.

1. Introduction.

We want to understand how excitability and behavior works in animals. In the laboratory of Dr. Leon Avery, we use as a model system a nematode (roundworm) *Caenorhabditis elegans* to achieve this goal. The most fundamental difference of the worm from other systems is that the number of somatic cells in this organism is very small (about a thousand) and constant between individuals. In particular, the nervous system of an adult hermaphrodite consists of 302 neurons. More than that, the position and the pattern of connectivity of individual neurons is reproducible from animal to animal (White et al., 1986), which is a unique advantage of the worm from a neurobiologist's point of view. Another advantage of *C.elegans* is that it is extremely amenable to genetic analysis, but this advantage is of course not unique as people who study *Drosophila* also enjoy it. Some scientists, including some worm researchers, would say that worm behaviors are too simple, too primitive and thus uninteresting. Probably to stress this point, *C.elegans* behaviors were named "taxes", like behaviors of unicellular organisms, rather than "reflexes" or "instincts". Nematodes were thought of as one of the most primitive metazoans that have branched off very early in the metazoan evolution. But recently evidence has emerged that they are related to arthropods and other molting animals in a super-phylum *Ecdysozoa* (Aguinaldo et al., 1997). Therefore, *C.elegans* and *Drosophila* are distant relatives, and it is accepted that *Drosophila* exhibits fairly complex behaviors (Sokolowski, 2001). I think the reason many perceive worm behavior as "primitive" is due to our insufficient knowledge of *C.elegans*

native, "wild", biology. Apart from obvious things, such as chemotaxis, thermotaxis or locomotion, we simply do not know what behaviors they exhibit in the wild. Since worms' laboratory environment (a Petri dish seeded with the intestinal bacterium *Escherichia coli*) in unlikely to model the natural environment well, it is not surprising that many worm behaviors are simply not observed. Mice, on the other hand, are more "anthropomorphic", and in this way their behavior is easier to understand intuitively. They do almost everything humans do, and paradigms like spatial learning, circadian rhythm, or drug addiction, are naturally extrapolated from humans to mice. Their natural environment is similar to our own; whereas the worms' environment is very different. Novel *C.elegans* behaviors are still being actively discovered. A few described in the last 10 years are social behavior (de Bono and Bargmann, 1998; de Bono et al., 2002), association of an attractive odor with a noxious chemical (Morrison and van der Kooy, 2001; Morrison et al., 1999; Rose et al., 2003), habituation to mechanical stimulation (Rose et al., 2003; Rose and Rankin, 2001), area-restricted search (Hills et al., 2004), slowing response upon entering food or substrate (Sawin et al., 2000), swimming (Pierce-Shimomura and McIntire, 2004), response to oxygen (Gray et al., 2004b), association of odors and soluble chemicals with the presence of food (Nuttley et al., 2002; Saeki et al., 2001) ; reviewed in (Hobert, 2003). Despite these potential difficulties, the worm is still an extremely attractive system for the study of behavior because of its versatility and speed. Once a behavioral paradigm is established and understood, its mechanisms can be studied using powerful genetic and molecular techniques available in worms. The network that controls behavior can be pinpointed to the level of single neurons (at least in theory).

The native worm environment is soil where it feeds on soil bacteria (Yeates et al., 1993). Like almost any other wild environment, soil is diverse in many ways: factors such as various chemicals, temperature, different food sources, vary in space and time. To complicate the issue, there are worm pathogens, predators and other competing (and friendly?) nematode species. All these stimuli must be assessed and integrated to produce optimal behavioral decisions. One of the interesting environmental factors that has been, to my opinion, underutilized, is the variability of bacterial food. Food regulates most *C.elegans* behaviors that have been studied (Hobert, 2003). However, except for the efforts of Steger (Steger, 2003), there were no attempts to understand how natural variability of bacterial food regulates *C.elegans* behavior. One of the projects that I pursued was to investigate this.

Generally, feeding behavior in animals can be divided into two stages: the *food seeking* behavior and the *food consumption* behavior *. Chapter 2 of my thesis deals with the mechanisms of food consumption: I describe my efforts in developing the voltage clamp preparation for the worm feeding organ, the pharynx. With the help of this technique, I study ionic currents that shape action potentials in the pharynx. I find that the T-type Ca channel CCA-1 boosts neurotransmission from a pharyngeal neuron by acting in the pharyngeal muscle. This work was done in collaboration with Kate Steger. Chapter 2 deals with food-seeking behavior in *C.elegans.* In mammals, food seeking behavior is a form of motivated behavior. Its mechanisms are poorly understood, so, it is of great interested to establish a genetic system for it. To look at food-seeking behavior in worms, I design assays utilizing the diversity of worm's bacterial food. First, I identify bacterial food of varying quality. Then, I find that *C.elegans* hunts for high quality food, and that previous experience of high

* This division applies to most, but not all animals. Sedentary animals, such as sponges or corals, passively wait for the food to come, so they "catch" rather than "seek".

quality food increases seeking activity. Finally, I show that it is the switching between two locomotory states, known as roaming and dwelling (Fujiwara et al., 2002) that allows worms to find high quality food. By analyzing mutants, such as *ttx-3* and *osm-6*, I show that food-seeking behavior depends on the balance between these states of locomotion.

2. Currents that shape pharyngeal action potential.

2.1. Background: *Caenorhabditis elegans* pharynx.

Caenorhabditis elegans eats bacteria and its feeding organ is called the pharynx (Fig. 1). It is a tubular muscle controlled by its own set of neurons. The anatomy of the pharynx has been reconstructed from serial section electron micrographs (Albertson and Thomson, 1976). The pharynx has been utilized as a versatile system to study how genes control excitability and behavior. Leon Avery has done screens to find mutants defective in feeding, called *eat* mutants. These screens have yielded a number of interesting and novel genes (Anselmo and Avery, 2004; Avery, 1993a; Avery and Horvitz, 1989; Davis et al., 1995; Raizen et al., 1995; Starich et al., 1996). In addition, the neuronal circuitry involved in regulation of pharyngeal contractions has been functionally mapped by laser ablation (Avery and Horvitz, 1989) and electrophysiology (Raizen and Avery, 1994). During pharyngeal contractions (each contraction / relaxation cycle is called a pump), soil bacteria are sucked in, trapped, ground and transported to the intestine, while the liquid is spit out (Doncaster, 1962; Seymour et al., 1983). Fig. 1D shows a time-lapse video of this process.

The pharynx contains 20 muscle cells, 7 marginal cells, 9 epithelial cells, 4 gland cells and 20 neurons. In the pharyngeal nervous system, two types of paired motor neurons are most relevant to my work: MC and M3. MC neurons synapse on mc2 marginal cells (Albertson and Thomson, 1976) and probably pm4 muscle cells (McKay, 2004 #80) . MC is a pharyngeal pacemaker: it excites the pharyngeal muscle via the nicotinic acetylcholine

receptor that includes non-alpha subunits EAT-2 and EAT-18 (McKay et al., 2004; Raizen et al., 1995), making it pump rapidly. EAT-2 is a very specialized protein: the translational fusion of it with the GFP localizes to a single synapse in the worm, the one that MC makes on the pharyngeal muscle. The pharyngeal muscle also has an MC-independent way of exciting itself; so that worms in which MC function is abolished by a laser ablation or mutations are still viable, although the pharyngeal pumping rate is reduced from 200 per minute to about 50. Even after the whole pharyngeal nervous system is killed, pumping still continues, although at a greatly reduced rate (Avery and Horvitz, 1989). Another pharyngeal neuron, M3, contributes to the repolarization by causing IPSPs during contraction (Raizen and Avery, 1994); it signals to the pharyngeal muscle via a glutamate-gated chloride channel AVR-15 (Dent et al., 1997).

Currently, there are two techniques for recording electrical activity in the pharynx. The first one is called an electropharyngeogram (Raizen and Avery, 1994). It is an extracellular recording of capacitive transients that flow in and out of the mouth of a worm; it records the derivative of the voltage across the pharyngeal membrane. Despite the fact that it is indirect, it turned out to be extremely useful due to relative simplicity and, more importantly, due to its ability to detect neuronal input. EPSPs and IPSPs, resulting from neuronal input, are seen in the electropharyngeogram as sharp current spikes. Another technique is a classical sharp electrode current clamp (Davis, 1995), which monitors the voltage directly. With it, action potentials and EPSPs can be observed (Fig. 1C).

Using genetics, laser ablations, these two electrophysiological techniques, and Ca imaging, several ion channels have been shown to function in the pharynx (Fig 1B.). These

studies led to the following model. The MC neuron releases acetylcholine that activates the EAT-2/EAT-18 receptor, causing an EPSP. This, in turn, activates the EGL-19 L-type Ca channel (Lee et al., 1997). Ca entry through EGL-19 further depolarizes the pharynx and causes contraction. During contraction, M3 fires IPSPs (Raizen and Avery, 1994), presumably causing small notch hyperpolarizations. At some point, possibly triggered by an M3 IPSPs, potassium channel EXP-2 recovers from inactivation, causing full rapid repolarization (Davis et al., 1999). Although the evidence for involvement of these proteins is solid, the currents that these channels conduct have never been directly recorded, because the whole cell voltage clamp technique has been unavailable. Voltage clamp allows direct measurement of membrane currents. Generally, *C.elegans* voltage clamp preparations are technically hard: special dissection and recording techniques are needed. Nevertheless, methods for voltage clamp recordings on *C.elegans* neurons (Goodman et al., 1998) and body wall muscle (Richmond and Jorgensen, 1999) have been established. Using these preparations, a variety of ligand- and voltage-gated channels have been studied (Francis et al., 2003; Jospin et al., 2002a; Jospin et al., 2002b; Mellem et al., 2002; Pierce-Shimomura et al., 2001). Previous attempts to adapt voltage clamp for the pharynx have not succeeded (Davis, 1999).

Genetics has its known limitations: the screens could miss some genes; mutation in other genes could be masked by other phenotypes or redundancy. If we were able to do voltage clamp on the pharynx, our knowledge of its function could be tested. In this chapter, I describe my attempt to achieve this goal. With the voltage clamp, I found that the model described above is generally correct with respect to EAT-2/EAT-18, EGL-19 and EXP-2, but

one player, a T-type Ca channel CCA-1, has been overlooked. Sequencewise, CCA-1 is the only T-type Ca channel α-subunit ortholog in the *C.elegans* genome, which makes it easy to study. However, it was not known whether it functions as a T-type channel, because attempts to study it even in a heterologous system have not succeeded. Also, it was not known where in the worm it functions. In this chapter, I show that CCA-1 activates in response to excitatory inputs from the MC neuron and accelerates the action potential upstroke. Part of this work was done in collaboration with Katherine Steger (Steger et al., 2004).

2.2. Voltage clamp for the *C.elegans* pharyngeal muscle.

The pharynx poses three main problems for voltage clamp experiments. First, the pharynx is not one electrically uniform cell; it is a structure of 60 cells of which 20 are muscle cells, connected by gap junctions. The second problem is a tough basement membrane covering the pharynx, which prevents formation of gigaseals. Finally, the pharynx is a powerful source of electricity: it has a low resistance and generates large currents.

Functionally and anatomically, the pharynx can be divided into three major compartments (listed from anterior to posterior): the corpus, the isthmus, and the terminal bulb (Fig. 2A). When a worm's head is cut off, the body wall muscles underlying the cuticle contract and the terminal bulb falls out, while the corpus remains covered (Fig. 2B). When I and others (Davis, 1999) attempted to voltage clamp the pharynx via the terminal bulb, the corpus apparently could not be clamped and fired action potentials in response to depolarizing voltage pulses. I found empirically that the pharynx could be clamped via the corpus, if a patch electrode seals on the pm4 muscle cell (Fig. 2A, area of patching is shaded). To make the corpus accessible to a patch electrode, I devised a microdissection procedure. Using two glass pipettes, the cuticle covering the pharynx is inverted and torn off (Fig. 2C). Then, the pharyngeal basement membrane is digested with enzymes, and the pharynx is attached to the glass slide (Fig. 2D). Why is it possible to voltage clamp the pharynx via one, but not the other compartment? It is likely that the corpus has lower resistance than the terminal bulb and is more powerful current source, which is suggested by

the fact that the relaxation transients of the terminal bulb recorded by electropharyngeogram are about 6 to 10 fold smaller than those of corpus (Raizen and Avery, 1994). In this case, currents that leak into the terminal bulb from the corpus will be large compared to the currents measured in the terminal bulb, whereas currents that leak into the corpus from the terminal bulb will be small compared to the currents measured in the corpus. When pharynxes were clamped via the corpus and other conditions were optimal (healthy pharynx, low series resistance), I did not see interference that looked like current injections from neighboring poorly clamped cells. Therefore, either the terminal bulb is clamped well from the corpus, so it cannot interfere, or, it is clamped poorly but it does not have the ability to interfere, because it is not as electrically active as corpus. I could not test how well the terminal bulb is clamped, because I could not measure its membrane potential with another electrode.

Mechanically, the pharynx is a very rigid structure – during contractions its inner lumen opens, while its outer shape does not change. Because the pharynx is attached to other tissues only at its very front and back ends, this mechanical rigidity is entirely conferred by the pharyngeal basement membrane. In order to be able to form gigaseals, I had to use rather harsh digestion with a mixture of collagenases, proteases and a chitinase. It is certainly possible that as a result of this digestion, the physiology of the pharynx changes, and I cannot test this because I cannot record from undigested pharynxes. One of the reasons why I think these changes are not too dramatic is because digested pharynxes still contract spontaneously and fire trains of action potentials in response to current injection (data not shown).

Electrical parameters of the wild type pharynx are as follows: input resistance 22.8 ±

5.2 MOhm, capacitance 362.6 ± 36.8 pF, equilibrium potential for the leakage current –53.6 ± 4.1 mV (n=29). Current densities are comparable to those in body wall muscle. For example, EGL-19 currents in the body wall have a peak density of 7 A/F (Jospin et al., 2002a). In the pharynx the maximal density of the high voltage-activated current (Which corresponds to EGL-19, see below) is about 12 A/F (Fig. 5A). For CCA-1 and especially EXP-2 currents, peak densities are much higher; up to 50 A/F (up to 18 nA in current amplitude). CCA-1 and EXP-2 currents function at the start and at the end of the action potential; thus, they must be large to rapidly charge the membrane capacitance. In comparison with EGL-19 currents recorded in the body wall muscle, which have peak amplitudes of 0.5 nA (Jospin et al., 2002a), pharyngeal currents are huge. This is not surprising, as the pharynx is an ensemble of many interconnected muscle cells, which activate in synchrony.

As expected for a large multicellular structure, good voltage clamp could not be achieved, so voltage escape is evident at the inward current activation threshold (Fig. 3). However, because of the availability of mutants, it was still possible to identify ion channels that conduct major currents. In theory, it is nearly infeasible to voltage clamp a cell with a resistance of 20 MOhm and currents of 10-20 nA via a single patch electrode with a series resistance of 10 MOhm (Sherman-Gold, 1993). I found empirically that if the amplifier gain is kept low (see methods), I could maximize clamp stability, although the speed of the clamp was sacrificed. Another trick I employ is using 5 ms voltage ramps instead of square pulses. If square pulses are applied, capacitive currents of more than 50 nA are injected, followed by the pharynx breaking down. In previous voltage clamp attempts, the main problem seemed to

be the connectivity between pharyngeal muscle cells, so that if one cell was clamped, others were poorly clamped and fired action potentials (Davis, 1999). Here, by using tricks and by clamping the pharynx via corpus, I overcame this problem, although the speed of the clamp is far from the accepted "gold standard".

Because the clamp is slow, this technique is hardly suitable for accurate kinetic analysis of the currents. But it allowed us to identify pharyngeal ion channels by the effect of mutations. CCA-1 and EXP-2 currents were identified by their complete absence in the respective null mutants, which was very obvious despite the imperfect clamp. The effect of EGL-19 hypomorphic mutation is less striking but significant and consistent with previous reports (see below).

In order to see whether or not I fully charge the pharynx in our voltage clamp, I compared its measured and calculated capacitance (which is the common way to do it). The pharynx capacitance, deduced from its membrane area, which includes outer surface and lumen membranes as well as some internal membranes of muscle and marginal cells, is at least 277 pF (see Methods). It is not known whether marginal cells of the pharynx are electrically active. They might be active because they appear in electron micrographs to receive neuronal input (Albertson and Thomson, 1976) and they are connected to the muscle cells via desmosomes. If marginal cells are not active, and, therefore, are not charged, the pharyngeal capacitance would be about 216 pF. Because the calculated capacitance is smaller than the measured capacitance (363 pF), I cannot say whether or not I fully charge the pharynx just based on this method, but this result is most consistent with the hypothesis that most of the capacitance is charged. Of course, this estimate is rough. On the one hand,

because I assumed that all fractional capacitances are in parallel and thus additive, it could be an overestimate. On the other hand, some membranes that lie within the pharynx, such as those lining cavities in the terminal bulb where gland cells reside or those of the terminal bulb marginal cells, were not included in this calculation due to their convoluted shape, and some internal membranes that were included are not flat and contain invaginations. These simplifications could result in underestimation of the capacitance.

The large CCA-1 and EXP-2 currents evidently function to rapidly charge membrane capacitance at the start and at the end of the action potential upstroke (see below). Thus, the physiologically relevant pharyngeal capacitance can be estimated. In current clamp recordings, the peak rate of the voltage change during upstroke reaches 15 V/s (Steger et al., 2004). The peak CCA-1 current amplitude is about 8 nA (Fig. 3A). Because for capacitive current $I = C\ dV/dt$, this active current can charge a capacitance of about 530 pF, which is not far from the measured capacitance of 363 pF. Therefore, both crude estimates of the pharyngeal capacitance, one based on its structure and the other on the size of active currents, are consistent with the experimentally measured capacitance. This suggests that most of the pharyngeal membrane is charged in my voltage clamp experiments.

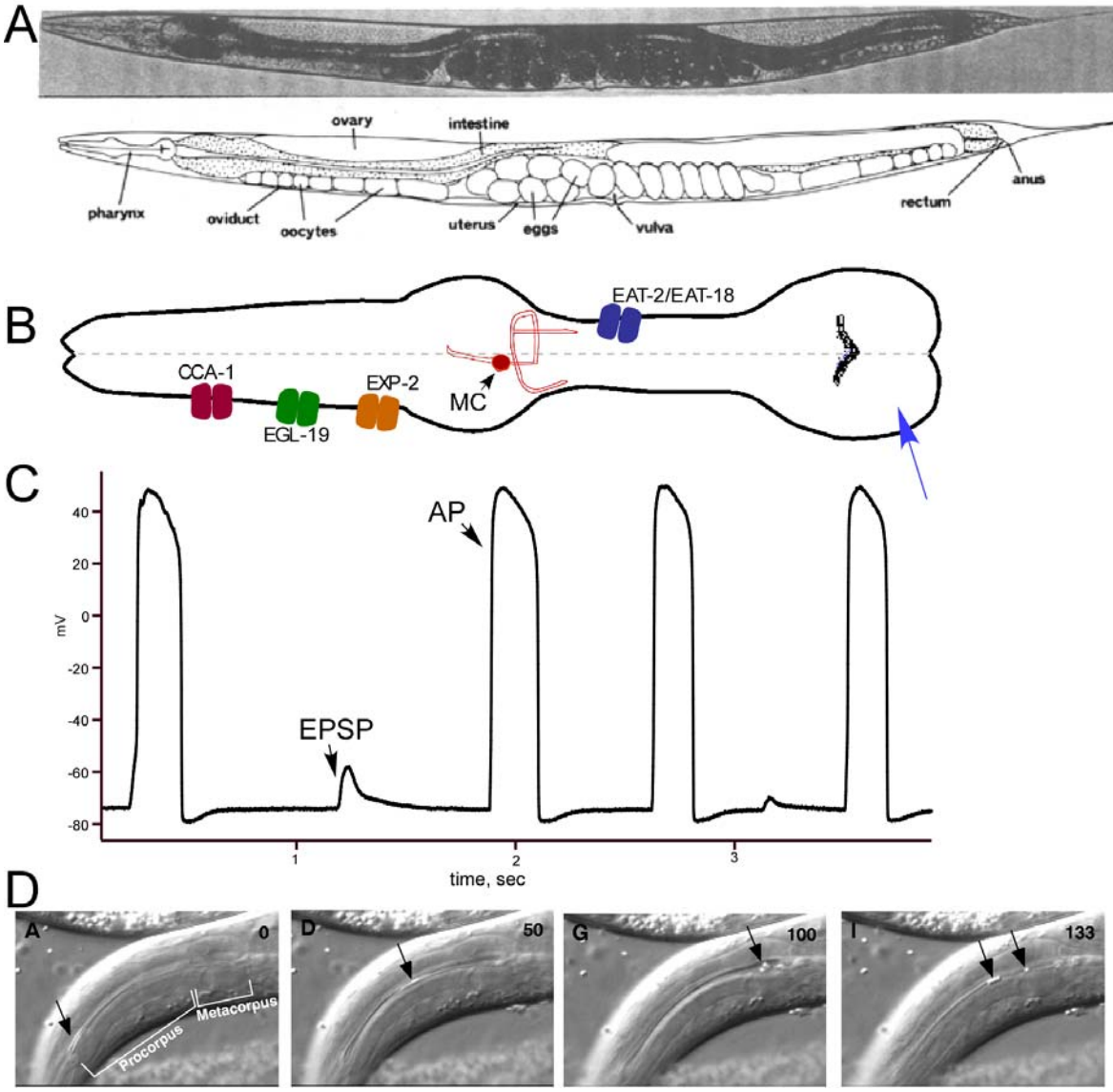

Figure 1. **The background on *C.elegans* pharynx. (A)** Worm general anatomy, showing the pharynx in the head. Anterior is to the left. Adapted from (Sulston and Horvitz, 1977). **(B)** Ion channels and neurons involved in the pharyngeal action potential. CCA-1 is a T-type Ca channel that functions to boost the action potential upstroke. EGL-19 is an L-type Ca channel that further depolarizes the membrane and is important for excitation-contraction coupling. EXP-2 is a potassium channel that drives the repolarization of the membrane. MC is a pacemaking neuron that excites the pharyngeal muscle via the EAT-2/EAT-18 nicotinic acetylcholine receptor. The blue arrow shows the location of the electrode insertion in the current clamp experiment shown in C. **(C)** A sample sharp electrode current clamp recording from the pharynx. A subthreshold excitatory postsynaptic potential (EPSP) and an action potential (AP) are labeled. These EPSPs usually result from MC activity. **(D)** Particle transport in the pharynx. The time sequence is from the left to the right; time in milliseconds is in the upper right corner of each frame; arrows show particles (0.8 μm latex beads) moving from the anterior to the posterior end of the pharynx as the contraction and relaxation proceeds. Data of Leon Avery, adapted from (Avery and Shtonda, 2003).

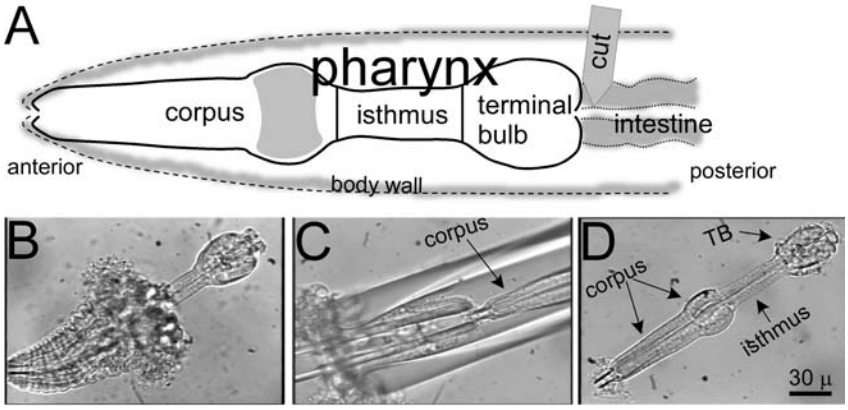

Figure 2. **The pharynx dissection procedure. (A)** Schematic of the *C.elegans* pharynx as it is positioned in the worm's head. To dissect the pharynx, the head is cut off right between the pharynx and the intestine. Three compartments of the pharynx are shown. The area of patch pipette attachment (shaded area of the corpus) roughly corresponds to the pm4 muscle cell of the pharynx. **(B)** Cut-off worm's head. **(C)** Body wall inversion using two pipettes. The smaller pipette (left) is pushed into the bigger one, inverting the body wall. **(D)** Skinned and digested pharynx, right before patching. TB: terminal bulb.

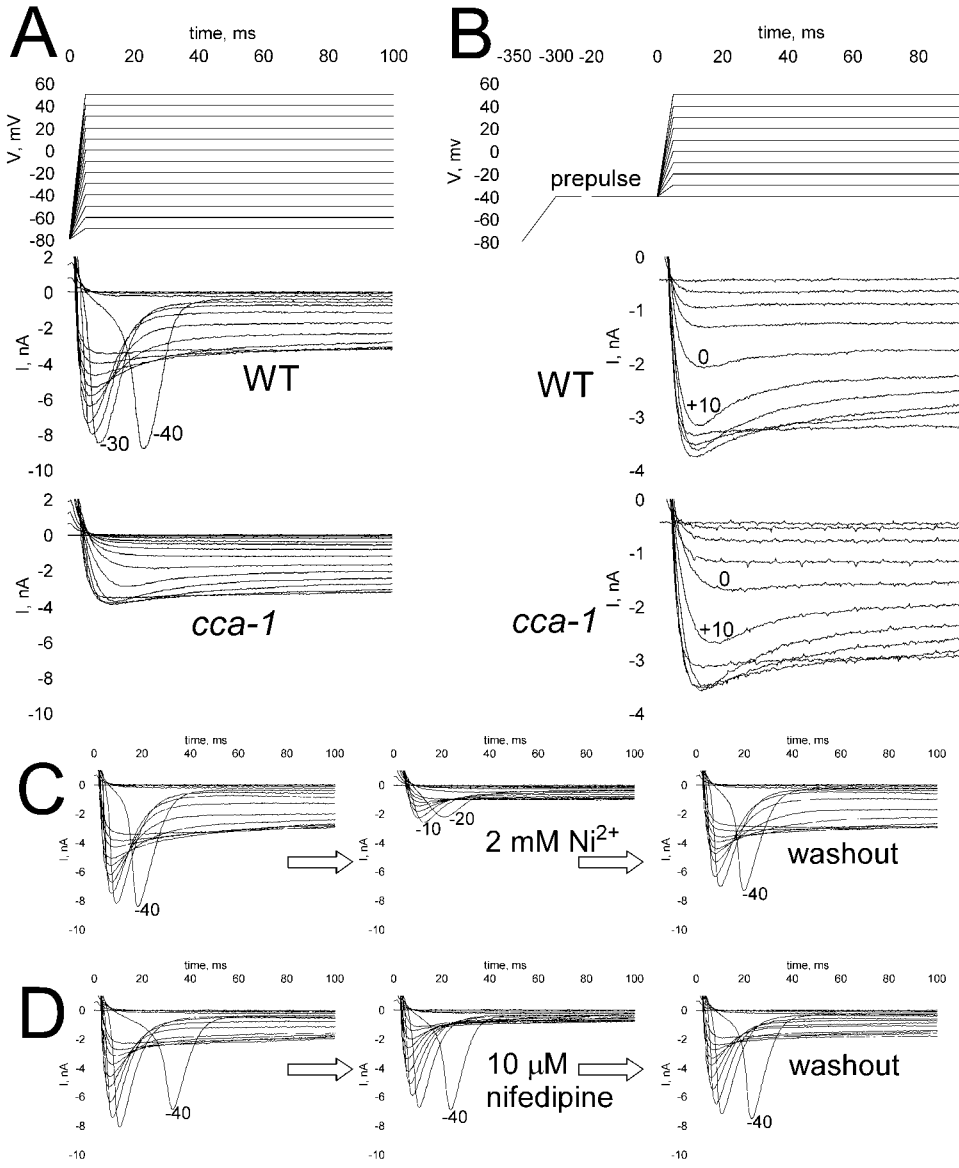

Figure 3. **Depolarization-activated inward currents in the pharynx. (A)** Total inward currents in the wild type and in the *cca-1* mutant. **(B)** High voltage-activated (HVA) currents in the WT and in *cca-1*. In these experiments low voltage-activated (LVA) current was inactivated with a 300 ms prepulse to –40 mV. **(C)** Ni^{2+} blocks both LVA and HVA currents. **(D)** Nifedipine blocks HVA, but not LVA current. Recordings in C and D are from wild-type pharynxes, and the pulse protocol is the same as in A. Numbers next to current traces indicate peak depolarization of the voltage pulse.

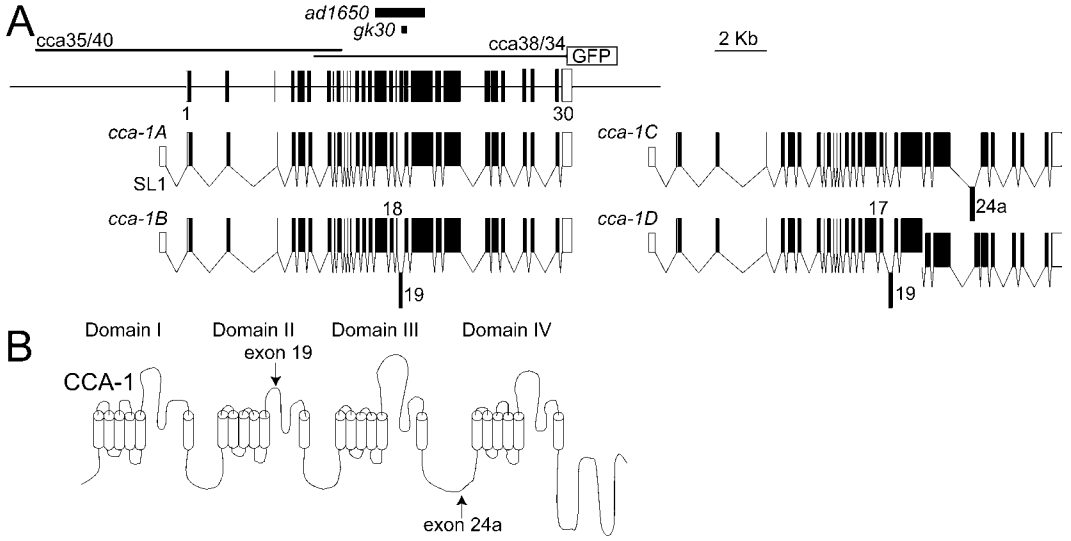

Figure 4. **Structure of the *cca-1* gene and CCA-1 calcium channel. (A)** Intron-exon structure of *cca-1*. Coding exons are represented by filled rectangles, non-coding exons by open rectangles. The *ad1650* and *gk30* deletions are indicated by bars. All cDNAs characterized were found to be *trans*-spliced at the 5' end to the SL1 leader RNA (SL1). The most-abundant transcript, *cca-1A*, is composed of all exons except exon 19. Splice variant *cca-1B* uses an alternate splice donor in exon 18, which is spliced to exon 19. The *cca-1D* transcript splices exon 17 directly to exon 19. The inclusion of exon 19 would add amino acid residues to the pore loop region of domain II, and may have significant effects on the activity of the channel. Splice variant *cca-1C* uses an alternative 5' splice donor for exon 24 which is predicted to result in the incorporation of an additional 15 amino acids in the III-IV loop. Sequences of the four splice variants have been submitted to GenBank under accession numbers AY313898 (*cca-1A*), AY313899 (*cca-1B*), AY313900 (*cca-1C*) and AY322480 (*cca-1D*). **(B)** Domain structure of CCA-1. Open cylinders indicate transmembrane domains, and the positions of the alternate exons found in splice variants B, C and D are shown. Figure and legend are adapted from (Steger et al., 2004). Data of Katherine Steger and Colin Thacker.

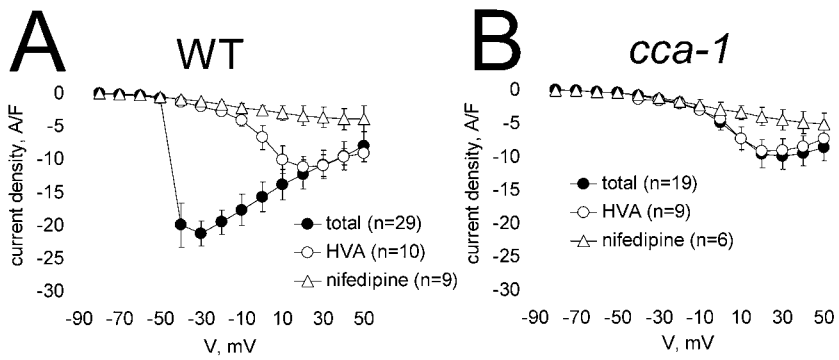

Figure 5. **Current-voltage relationships for inward currents in the wild type and *cca-1* pharynxes. (A)** Wild type. **(B)** *cca-1*. Voltage protocols for the total current and current in the presence of 10 μM nifedipine were the same as in Fig. 3A; HVA currents were measured with the same voltage protocol as in Fig. 3B. For nifedipine experiments, averaged current values at 50 to 60 ms of the pulse were used (after LVA current has inactivated); otherwise, peak amplitudes were used for I-V curves. Mean±SD.

Figure 6. **EGL-19 L-type Ca channel conducts HVA current in the pharynx. (A)** Total currents in *cca-1* and *cca-1; egl-19*. Voltage protocol is the same as in Fig. 3A. **(B)** HVA currents in wild type and *egl-19*. Voltage protocol is the same as in Fig. 3B. **(C)** Current-voltage dependencies of HVA currents in WT and *egl-19* (peak amplitudes); voltage protocol is the same as in Fig. 3B. **(D)** Activation time constants of HVA currents in WT and *egl-19*. * significantly different by t-test, $P < 0.01$. Mean±SD.

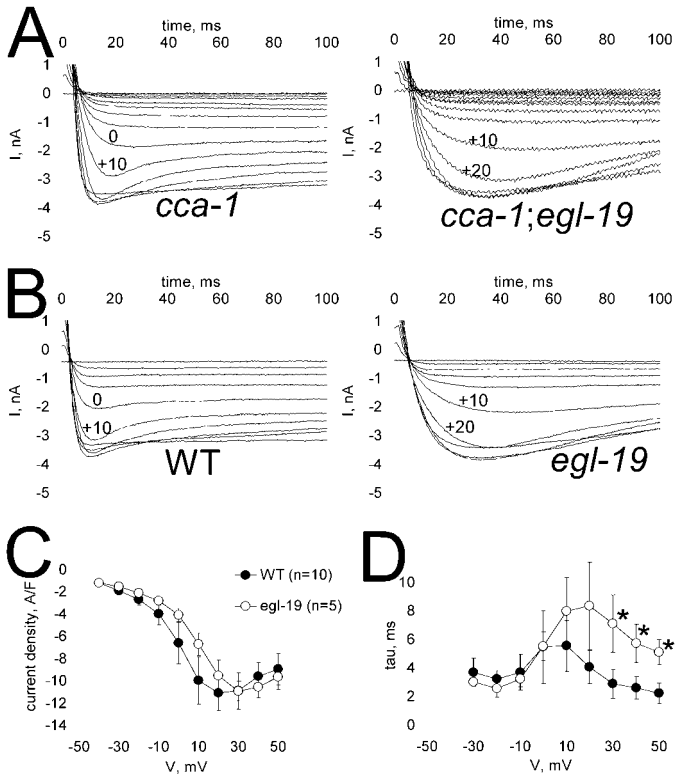

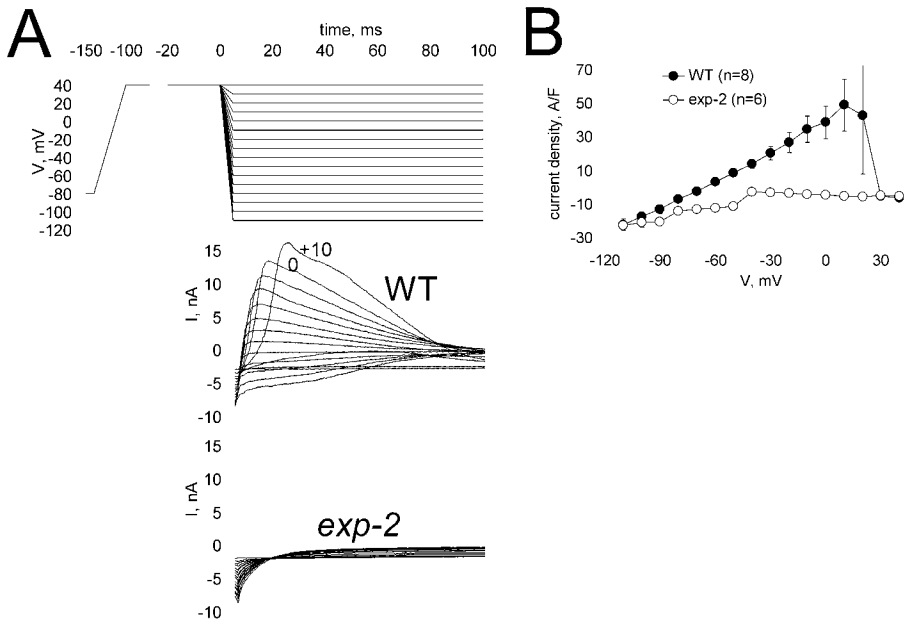

Figure 7. **EXP-2 conducts hyperpolarization-activated outward current. (A)** Sample recordings from the WT and *exp-2*. **(B)** Current-voltage relationships (peak amplitudes). Mean±SD.

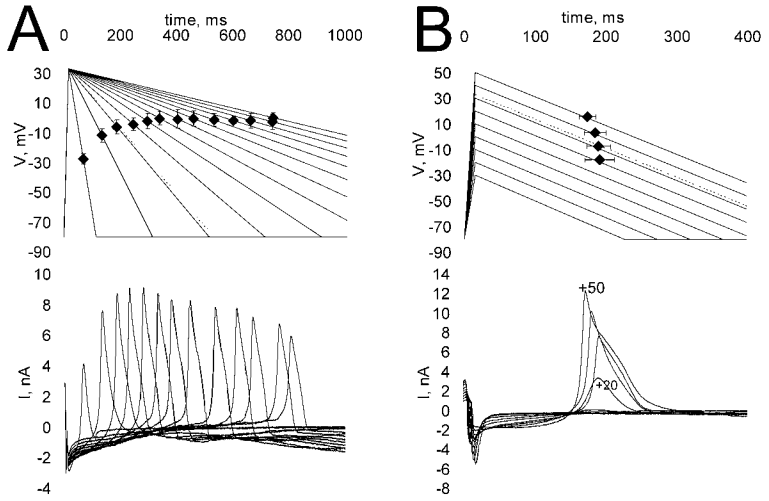

Figure 8. **The slope of the plateau phase determines the latency of the EXP-2 current.** Top panels are voltage commands; bottom panels are corresponding currents from one pharynx. **(A)** Outward currents in response to varying voltage ramps starting from the same depolarization to +33 mV. **(B)** Outward currents in response to varying peak depolarizations followed by the same negative ramp of –0.22 V/s. On command voltage traces, average timing of EXP-2 current transients is indicated with ♦ (n=4 pharynxes), and dotted lines show parameters of the wild type pharynx, as determined by current clamp recordings. To simplify pictures, standard deviations for the voltage only are shown in A, and for the timing only are shown in B. All recordings are from the wild type.

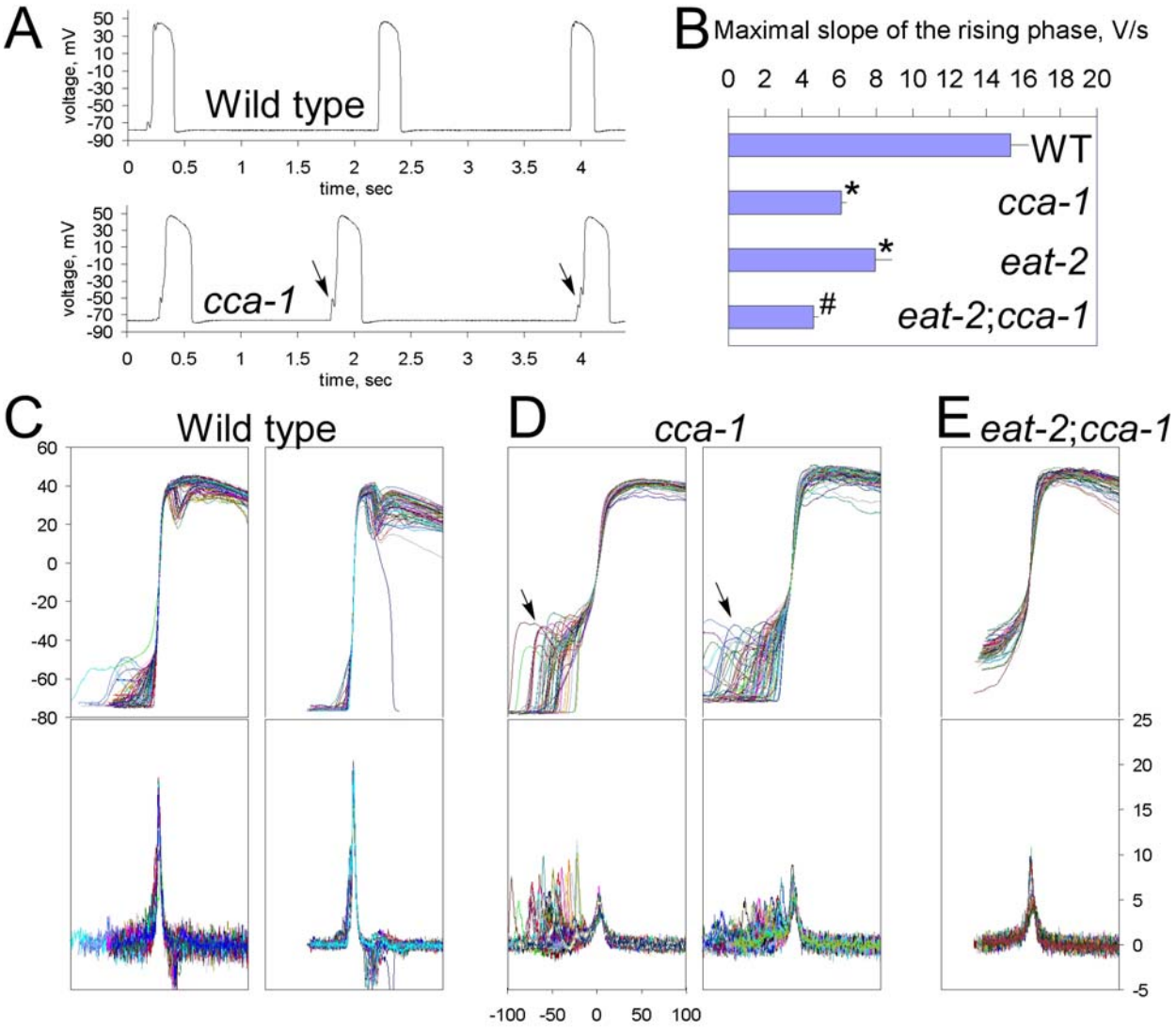

Figure 9. **CCA-1 boosts the pharyngeal muscle response to the excitatory inputs.** **(A)** Sample current clamp recordings from wild type and *cca-1* mutant pharynxes. While the depolarization phase of the wild type action potential usually rises steeply and steadily from resting potential to a peak, action potentials from *cca-1* mutant worms often display a notch in the depolarization phase (arrows). **(B)** Averaged maximal rising phase slopes for the wild type, *cca-1*, *eat-2* and *eat-2*; *cca-1*. Differentiated and aligned action potentials from each pharynx were averaged first; then peak slope values were measured from those averaged traces. Mean ± SEM; n=19 (WT), 16 (*cca-1*), 14 (*eat-2*), 11 (*eat-2*; *cca-1*). * significantly different from the wild type, # significantly different from all other strains ($p<0.005$ for all comparisons, t-test). **(C)** Upper panels: Superimposed action potentials (with rising phases aligned) from two representative wild type pharynxes. Lower panels: Time derivatives of the action potentials above. n=63 and 66 for left and right traces respectively. **(D)** Same as in (C) for two representative *cca-1(ad1650)* worms; n=51 and 74 for left and right panels respectively. While wild type action potentials generally display a smooth steep rising phase, the majority of action potentials from *cca-1* mutant worms contain an initial depolarization, followed by a flattened area or notch (arrows). **(E)** In the *eat-2*;*cca-1* double mutant, the upstroke is again smooth, suggesting that the small depolarizations seen in *cca-1* are due to MC activity. Note, however, that the membrane voltage at the very start of the action potential is elevated; this is because of adaptation and addressed further in Fig. 11.

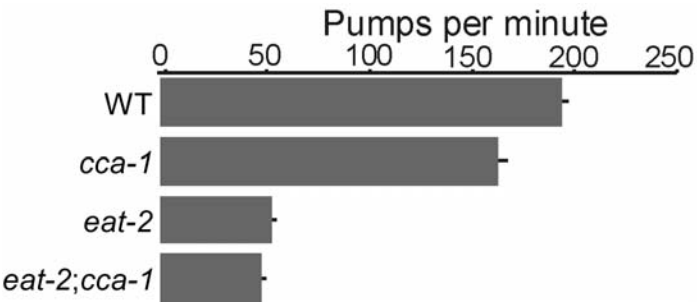

Figure 10. **Effect of *cca-1* and *eat-2* mutations on the pharyngeal pumping.** Pumping rates of adult worms were measured in the presence of *E. coli* HB101 food. Mean±SEM. Adapted from (Steger et al., 2004); data of Kate Steger.

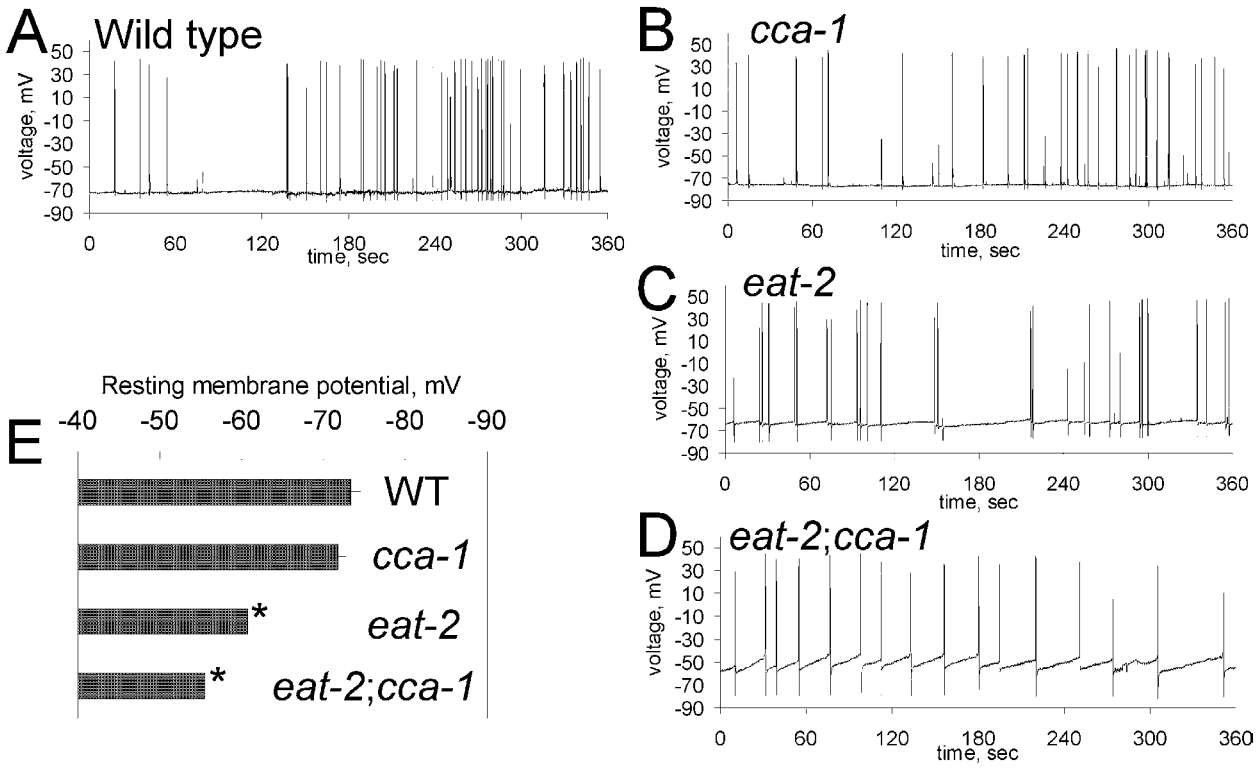

Figure 11. **Worms adapt to the loss of MC activity by raising the resting potential**. **(A)** through **(D)** 6 minute recording from the wild type and mutant worms (labeled). The resting membrane potential in *cca-1* is unchanged; however, the resting potential in *eat-2* and especially in the *eat-2*:*cca-1* double mutants is elevated and has a tendency to rise between action potentials. **(E)** Average resting membrane potential for above four strains. Mean ± SEM; n=12 (WT), 10 (*cca-1*), 15 (*eat-2*), 11 (*eat-2*; *cca-1*). * significantly different from both the wild type and *cca-1* ($p<0.005$, t-test).

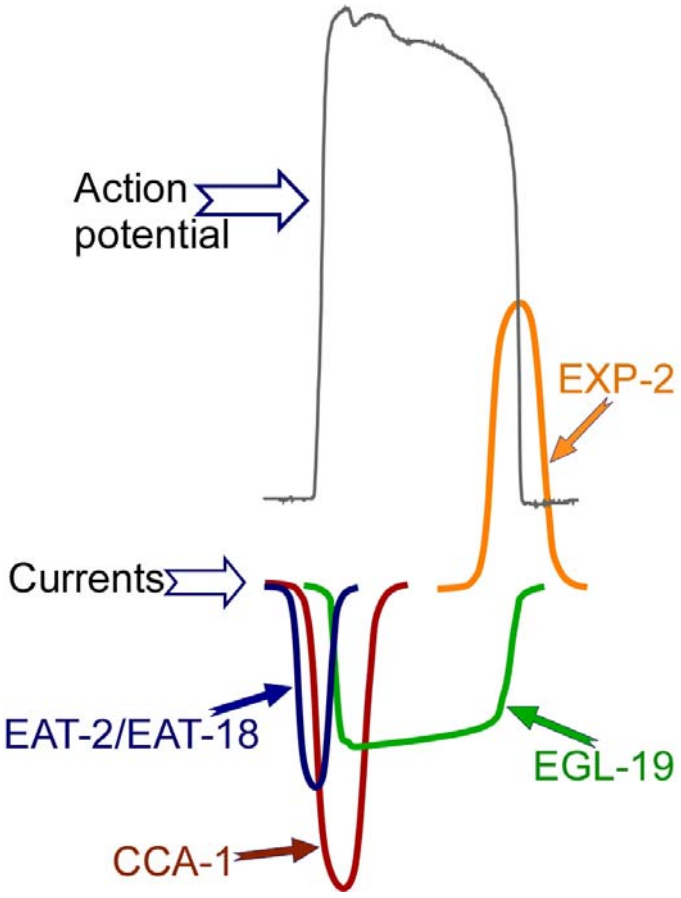

Figure 12. **Model of the pharyngeal action potential.** Motor neuron MC excites the pharynx via the EAT-2/EAT-18 nicotinic acetylcholine receptor, causing an inward cation current. This current depolarizes the membrane to about –30 mV, which triggers CCA-1 activation. CCA-1 gives rise to a large, quickly inactivating inward current, which drives rapid membrane depolarization. Starting from –10 mV, EGL-19 is activated. Ca^{2+} influx via EGL-19 activates muscle contraction and maintains depolarization during the plateau phase. As EGL-19 inactivates slowly, presumably in a Ca-dependent way, the membrane repolarizes; finally it reaches the threshold for the EXP-2 recovery from inactivation (deinactivation), about 0 mV. When this happens, EXP-2 generates a large outward K current, causing rapid membrane repolarization and termination of the action potential.

Currents are not drawn to scale. Currents resulting from M3 neurotransmission are omitted for clarity.

2.3. The T-type Ca channel CCA-1 boosts pharyngeal muscle response to excitatory inputs.

In response to step depolarizations from a holding potential of –80 mV, an inward current is activated (Fig. 3). In wild type pharynxes, there is a low-voltage activated (LVA), quickly inactivating component in this inward current, which looks like a conventional T-type Ca channel current (Hille, 2001). CCA-1 is a calcium channel alpha subunit in the *C.elegans* genome homologous to mammalian T-type Ca channel alpha subunits (Steger et al., 2004). In worms, a *cca-1::GFP* fusion protein is expressed in a variety of tissues, including the pharyngeal muscle. Pharynxes of the *cca-1(ad1650)* null mutant did not exhibit the LVA current (Fig. 3A). In order to isolate the non-LVA component of the inward current in the wild type, I used a prepulse voltage protocol. A 300 ms prepulse to –40 mV activates and inactivates the LVA current, revealing a high voltage-activated (HVA), slowly inactivating component (Fig. 3B). The HVA current is the same in the WT and in the *cca-1*. Consistent with the pharmacology of Ca channels, both HVA and LVA currents are blocked by a high (2mM) concentration of Ni^{2+} (Fig. 3C). Both T-type and HVA vertebrate channels are also sensitive to these concentrations of Ni^{2+}. Lower Ni^{2+} concentrations did not block inward currents. Among mammalian T-type α subunits, only α_{1H} is highly sensitive to low Ni^{2+} concentration; with IC_{50} = 13 μM (Lee et al., 1999a).HVA but not LVA current is partially blocked by the L-type Ca channel blocker nifedipine (Fig. 3D).

Fig 4. describes the CCA-1 gene structure and known deletion mutants; I only used

the *ad1650* allelle (Steger et al., 2004).

Current-voltage dependencies of LVA and HVA currents for the wild type (N2) and *cca-1* are shown in Fig. 5. The LVA current activates starting from –40 mV, reaching a maximum at –30. The HVA current starts to activate at about –10, reaching a maximum at about +20.

These results show that CCA-1 functions as a T-type Ca channel in the pharyngeal muscle. Also, they suggest that CCA-1 is a true worm T-type Ca channel ortholog with typical T-type kinetics, voltage dependence and pharmacology. In chapter 1.7 I further investigate CCA-1 function.

2.4. The L-type Ca channel EGL-19 regulates the plateau phase of the action potential.

In their high voltage activation and slow inactivation, HVA currents recorded from the pharynx look very similar to L-type Ca channel currents (Hille, 2001). They are also similar to L-type currents recorded in the *C.elegans* body wall muscle (Jospin et al., 2002a). Nifedipine, a dihydropyridine L-type Ca channel antagonist, blocks HVA current c. (In contrast to the body wall L-type current, which is blocked by 1 μM nifedipine, I only saw an effect starting from 5 μM). Other channels may also be affected by these rather high nifedipine concentrations, but in the pharynx it only affects HVA, not LVA current (Fig. 3D).

EGL-19, a *C.elegans* L-type Ca channel alpha subunit, has previously been implicated in pharyngeal physiology: hypomorphic mutations in the *egl-19* cause feeble pumping, whereas gain-of-function mutations cause extended terminal bulb contractions. In hypomorphic mutants the slope of the rising phase of the action potential is smaller than in the wild type (Lee et al., 1997). In the *egl-19(n582)* hypomorphic mutant (Trent et al., 1983) the activation of HVA current is clearly delayed. This is observed both in the *cca-1* background where LVA currents are conveniently absent (Fig. 6A) and in the wild type with a prepulse voltage protocol (Fig. 6B). Activation time constants in *n582* are significantly larger than in the wild type at pulses to 30, 40, and 50 mV (Fig. 6D). Consistent with the study of the same mutation in the body wall muscle (Jospin et al., 2002a), the current-voltage dependence in *n582* is shifted by about 10 mV to the right (Fig. 6C); however, in contrast to the body wall, the peak current amplitude is not decreased compared to the wild type. This

could be explained by a compensatory increase of mutant EGL-19 expression in the pharynx. (Compensatory changes in pharyngeal currents do occur, suggesting that pharyngeal excitability is tightly feedback-regulated; see chapter 1.7). Alternatively, the effect of *n582* on the pharyngeal EGL-19 could be different due to different non-alpha subunits. (Jospin et al., 2002a) recorded much lower time constants—as small as 0.5 ms for the wild type vs. 2 ms in our recordings. I think that this difference is due to the slow speed of my voltage clamp, which does not allow faster rise times to be measured. These kinetic measurements are therefore specific to this system; but one can nevertheless detect differences between the wild type and mutant L-type channel. The effect of the *n582* mutation on the HVA current rise time is also consistent with its effect on the speed of the action potential upstroke described by (Lee et al., 1997).

These results suggest that EGL-19 conducts a major component of the HVA current in the pharynx. Based on its voltage dependence and kinetics, the most likely role of EGL-19 is to maintain the action potential plateau phase.

A certain component of the depolarization-activated current is blocked by neither Ni^{2+}, nor nifedipine. This component shows almost no inactivation (Fig. 3C and 3D) and has very shallow voltage dependence (Fig. 5A and 5B). It is unlikely to be a residual L-type current because its voltage dependence is very shallow and totally different. It is also unlikely to be a T-type current because it is unchanged in *cca-1*. Most probably, this is a weakly voltage-dependent, leakage-like conductance.

2.5. K channel EXP-2 triggers rapid repolarization of the pharyngeal muscle.

EXP-2 is a potassium channel of the K_v family. However, when it is expressed in *Xenopus laevis* oocytes it behaves as an inward rectifier with properties similar to mammalian HERG, a potassium channel that functions in the heart (Fleischhauer et al., 2000). EXP-2 has been shown to regulate action potential duration in the *C.elegans* pharynx by initiating rapid repolarization at the end of the plateau phase of an action potential (Davis, 1999; Davis et al., 1999). Outward potassium current that arises upon hyperpolarization has also been described in the pharyngeal muscle of a parasitic nematode *Ascaris lumbricoides* (Byerly and Masuda, 1979). In the *exp-2* null mutant, action potentials in the pharynx are greatly extended; in the *exp-2* gain-of-function mutant, action potentials are shortened. However, the properties of the oocyte expressed EXP-2 are not well suited for its suggested role: being an inward rectifier, it conducts very little outward current at potentials higher than the equilibrium potential for potassium (about –80 mV in most cells). In the pharynx it must trigger a rapid repolarization at the end of the plateau phase, when the membrane potential is about 0.

Kinetic measurements on EXP-2 have shown that the inward rectification of this channel results from its ultrafast inactivation (Fleischhauer et al., 2000), similarly to mammalian HERG (Spector et al., 1996). The inactivation and the deinactivation (recovery from the inactivation) of EXP-2 are about 100 times faster than its activation. Because the inactivation is faster than the activation, EXP-2 does not conduct in response to the

depolarization. It also inwardly rectifies upon hyperpolarization to voltages higher than the equilibrium potential for K^+, because at those potentials inactivation is still faster than deinactivation. In oocytes, hyperpolarization-activated outward currents are small and transient (Fig. 4 in (Fleischhauer et al., 2000)). Because of that, it was not clear whether EXP-2 is well suited to terminate action potentials in the pharynx. Fleischhauer et al. hypothesized that it could still work this way because of the positive-feedback nature of the repolarization. I found that this explanation is not necessary to account for EXP-2 function in the pharynx, because in the pharynx, its native environment, EXP-2 is not an inward rectifier. It conducts large outward currents at potentials a lot higher than the E_{K+} (Fig. 7A). These currents are absent in the *exp-2(ad1426)* null mutant. (Note that an inward current in *exp-2(ad1426)* is most likely an EGL-19 tail current.) Starting from +20 mV and going more negative, the current-voltage dependence of EXP-2 is almost straight, with no signs of inward rectification (Fig. 7B). This is similar to the "negative spike" current in *Ascaris* pharynx, except in *Ascaris* this current arises starting from the hyperpolarization to -15 mV (Byerly and Masuda, 1979). The reversal potential of EXP-2 current is close to the predicted equilibrium potential for K^+ under these conditions (-82 mV). As expected, currents rise faster at more negative potentials, indicating strong voltage dependence of deinactivation.

These results suggest that properties of endogenous EXP-2 are similar yet different from those expressed in *Xenopus* oocytes. Similarly to the oocyte-expressed channel, pharyngeal EXP-2 does not conduct upon depolarization, thus the property of ultrafast inactivation upon depolarization observed in oocytes is maintained in the native system. But the recovery from inactivation that allows current to flow occurs at more positive potentials

in the native preparation, up to +20 mV (Fig. 7B). Thus, in contrast to the oocyte-expressed channel, pharyngeal EXP-2 does not inwardly rectify. Upon hyperpolarization, it conducts large outward currents at potentials much higher than E_{K+}. This allows it to trigger rapid repolarization when the membrane potential is about 0 mV during the plateau phase. In the pharynx, EXP-2 is a channel with unique properties, ideally suited to control action potential duration by initiating rapid repolarization.

2.6. The slope of the plateau phase determines action potential duration.

Timing of electrical activity in the pharynx is important for efficient food transport (Avery, 1993b; Avery and Shtonda, 2003). How is it regulated? We know that EXP-2 is critical for proper repolarization timing (Davis, 1999; Davis et al., 1999). During the action potential plateau phase, the membrane slowly repolarizes, presumably because of the slow EGL-19 inactivation. At some point, a sharp outward current spike is generated by EXP-2, causing rapid repolarization. I was interested in how the shape of an action potential, particularly of a plateau phase, affects the timing of the EXP-2 spike. Using current clamp recordings, I determined that in the wild type, the peak membrane potential during the upstroke was 33 ± 4 mV and the slope of the plateau phase was -0.22 ± 0.06 V/s (30 action potentials from 5 pharynxes, mean ±SD). Then, I voltage clamped pharynxes under two pulse protocols. To test the ramp effect, I depolarized pharynxes from the holding potential of –80mV to 33mV and then applied varying negative voltage ramps (Fig. 8A). To test the effect of the action potential amplitude, I depolarized pharynxes to different potentials and then applied the same ramp of –0.22 V/s (Fig. 8B). Under the varying ramp protocol, current transients appear starting from -30 mV at fast ramps and then at 0 mV (Fig 8B). These are EXP-2 currents, as they are absent in the *exp-2* null mutant (n=2, data not shown). Under the varying depolarization/constant ramp protocol, currents start at peak depolarizations to +20 mV, but, interestingly, with increasing depolarization, the potential at which the EXP-2 current transient develops increases by the same increment in such a manner that the time

when the current develops is almost unchanged (about 200 ms). These results suggest that EXP-2 is designed to generate a current spike once the membrane potential has dropped by a certain value, approximately 30 mV, from the peak depolarization. Thus, the timing of the repolarization onset is effectively regulated by the ramp of the action potential plateau phase; the action potential amplitude has very little effect once some minimum threshold has been reached (about +20 mV in our recordings). How could such regulation work? Most likely, it is explained by the voltage dependence of EXP-2 activation: at higher voltages, the activation occurs faster, so channels become available for the recovery from inactivation quicker. (Activation also affects the number of available channels, as seen from larger current amplitudes at higher depolarizations). In Fig. 8A, the voltage at which EXP-2 current develops is lower with very fast ramps, probably because under these conditions activation is limiting – even though EXP-2 deinactivates rapidly, there is no current until enough activation is achieved. When activation reaches saturation, the potential at which current develops does not change, it stays at about 0 mV. It is quite remarkable how nicely EXP-2 kinetic properties are tuned to control the action potential duration.

Finally, what regulates the slope of the plateau phase? Mutations in the region of *egl-19* known to be important for voltage-gated calcium channel inactivation cause dramatic elongation of pharyngeal action potentials (Lee et al., 1997), suggesting that EGL-19 inactivation is important for the slope. Extracellular Ca concentration affects action potential duration: in lower extracellular Ca^{2+}, duration is extended (Dent and Avery, 1993). Barium at 1 mM concentration causes extension of pharyngeal action potentials to over 1 s (Franks et al., 2002). Substitution of 6 mM Ca^{2+} with 6 mM Ba^{2+} slows the inactivation of the EGL-19

current in the body wall muscle (Jospin et al., 2002a). These observations are consistent with Ca-dependent inactivation of EGL-19. EGL-19 inactivation kinetics are critical for the shape of the plateau phase; thus, the amount of Ca entry is likely to be the key factor in regulating the plateau phase slope, and, by affecting the timing of EXP-2 current, the action potential duration. It is also possible that Ca-dependent potassium channels are involved in shaping the plateau phase, but their role has not been tested. At least one of these channels, *slo-1*, does not show expression in the pharyngeal muscle, although it is expressed and may play a role in pharyngeal neurons (Chiang and Avery, unpublished observations). Another important factor that regulates action potential duration is the inhibitory motor neuron M3 (Avery, 1993b); but in this work I did not address its role.

2.7. Interaction of two excitation mechanisms in the pharynx.

The voltage clamp data described above suggest that the T-type channel CCA-1 functions in the pharyngeal muscle. Using current clamp recordings from the pharyngeal terminal bulb, I looked at the effect of *cca-1* mutation on the shape of action potentials in the pharynx. The effect of *cca-1* is quite subtle at first sight (Fig. 9A), however, it is very evident when lots of action potentials are aligned by their rising phases and differentiated (Fig. 9C, wild type and 9D, *cca-1*). In *cca-1* the action potential upstroke is not as steep as in the wild type. In *cca-1*, inflections and notches are often noticeable in the rising phase; those are rare in the wild type. These inflections in the upstroke appear on differential traces as spikes to the left (negative time) of the main upstroke spike at 0 ms (Fig. 9C and D, bottom panels). When seen in the WT, they are usually slow and small, not exceeding –50 mV at peak, so they are not even visible on the differentiated traces. In the wild type, the upstroke is usually smooth, resulting in only one large spike in the differential trace at 0 ms.

What are these subthreshold events seen in the *cca-1* traces? Most likely, they are excitatory inputs (EPSPs) of the MC neuron to the pharyngeal muscle that fail to trigger action potentials rapidly. Interestingly, most of these EPSPs in *cca-1* peak at about –30 mV, exactly as needed to activate CCA-1. The motor neuron MC is thought to excite the pharynx via the nicotinic acetylcholine receptor, which includes the EAT-2 and EAT-18 non-alpha subunits; the alpha subunit of this receptor is not known yet (McKay et al., 2003; Raizen et al., 1995). Both *eat-2* and *eat-18* mutations result in the same phenotype as the laser ablation

of MC. *eat-2* is expressed in a single synapse in the worm: the synapse that the motor neuron MC makes on the pharyngeal muscle. As one would predict, subthreshold events in the upstroke observed in *cca-1* are gone in the *eat-2; cca-1* double mutant, so the upstroke is smooth again (Fig. 9E). *eat-18*; *cca-1* looked similar (n=4, data no shown). Therefore, inflections and notches in *cca-1* represent neurotransmission from the MC neuron that failed to evoke action potentials rapidly. In the *cca-1* mutant the maximal upstroke speed is decreased by about 2.5 times compared to the wild type (Fig. 9B). The maximal rise speed is further slightly decreased in *cca-1; eat-2* (Fig. 9B); however, the effect of *cca-1* and *eat-2* mutations is less than additive.

In the wild type, but rarely in *cca-1*, there is a negative notch in the first 30 ms of the plateau phase (compare Fig. 9C and D, upper panels). I saw this notch in 15 out of 19 wild type worms, but only in 1 out of 16 *cca-1* animals. Most likely, this notch occurs when CCA-1 is starting to inactivate, but EGL-19 is not yet fully activated. Very infrequently, it causes EXP-2 deinactivation and premature action potential termination (Fig. 9C, upper right panel).

These experiments confirm our voltage clamp recordings, suggesting that CCA-1 works at the start of the upstroke, boosting the response of the pharyngeal muscle to excitatory inputs of the MC motor neuron. However, they raise a question: how does the pharynx excite itself in the absence of both MC neurotransmission and CCA-1 in the *eat-2*; *cca-1* double mutant?

Very surprisingly, Kate Steger (Steger et al., 2004) has shown that the *eat-2*; *cca-1* double mutant in not sicker than *eat-2* alone, and the pharyngeal pumping rate is not decreased (Fig. 10). I suspected that in *eat-2; cca-1* other, redundant mechanisms of pharynx

excitation are activated. That turned out to be true: the pharynx adapts to the absence of MC neurotransmission (Fig. 11). First, in *eat-2* the resting membrane potential is elevated by 13 mV (Fig. 11E). In *eat-2; cca-1* the resting potential is elevated by about 18 mV (not significantly different from *eat-2*). Second, in *eat-2*, and, more strikingly, in *eat-2; cca-1*, membrane potential tends to spontaneously creep up (Fig. 11C and 11D) so that the threshold for EGL-19 activation can still be reached. These effects are very unlikely to be the direct effect of *eat-2* or *cca-1* mutations, considering what is known about these channels. Most likely, some leakage conductance is activated in order to compensate for the absence of excitatory input. A weakly voltage-dependent, Ni^{2+} and nifedipine insensitive conductance that I observed (Fig. 5), could be responsible for this.

Kate Steger has shown that synaptotagmin SNT-1 and vesicular acetylcholine transporter UNC-17 are required for compensation for the loss of either *eat-2* and *cca-1*: doubles of these with *eat-2* or *cca-1* are very starved and slow-pumping, which suggests involvement of cholinergic neurotransmission (Steger et al., 2004). Thus, this compensation mechanism is particularly sensitive to reduction in acetylcholine levels. But if all pharyngeal neurons are killed, the pharynx still pumps (Avery and Horvitz, 1989), so the source of acetylcholine could be extrapharyngeal. Acetylcholine can "tune" the membrane potential of the pharynx in a graded way ((Bessou et al., 1998) and my unpublished data). Leon Avery had an idea that muscarinic acetylcholine receptors GAR-1 and GAR-3 may be important, but the *eat-2; gar-1; gar-3* triple mutant is viable and not very sick (Kate Steger, personal communication). There are many nicotinic acetylcholine receptor genes in the *C.elegans*

genome (Bargmann, 1998), so now we are inclined to think that a non-EAT-2 nicotinic receptor is involved.

These results suggests there are redundant mechanisms to ensure pharynx excitation and that pharynx excitability is homeostatically regulated. It is intriguing to know how pharyngeal activity is sensed and which mechanisms are involved in this adaptation. Generally, the question of how excitable cells tune their excitability is of great interest (Marder et al., 1996; Turrigiano et al., 1995), and the pharynx may be a new model to study that.

2.8. Conclusions

In a project described in Chapter 2, I use voltage-clamp to identify three ionic currents in the *C.elegans* pharynx. Based on the properties of these currents and previous knowledge, I propose a model for the pharyngeal action potential (Fig. 12). Here currents that shape the action potential are shown. Motor neuron MC excites the pharynx via the EAT-2/EAT-18 nicotinic acetylcholine receptor, causing an inward cation current. This current depolarizes the membrane to about –30 mV, which triggers CCA-1 activation. (This is most clearly shown in intracellular recordings from the *cca-1* mutant, where the MC transients reach about –30 mV and then plateau, Fig 9D). CCA-1 gives rise to a large, quickly inactivating inward current, which drives rapid membrane depolarization. Starting from –10 mV, EGL-19 is activated. Ca^{2+} influx via EGL-19 activates muscle contraction and maintains depolarization during the plateau phase. As EGL-19 inactivates slowly, presumably in a Ca-dependent way, the membrane repolarizes; finally it reaches the threshold for the EXP-2 recovery from inactivation (deinactivation), about 0 mV (Fig. 8). Inhibitory neurotransmission from the M3 neuron via the AVR-15 channel speeds up this process. When this threshold is reached, EXP-2 deinactivates and generates a large outward K current, causing rapid membrane repolarization and termination of the action potential.

My voltage-clamp studies confirm roles previously proposed for EXP-2 (Davis, 1999; Davis et al., 1999) and EGL-19 (Lee et al., 1997). In addition, I present evidence that a T-type calcium channel encoded by *cca-1* acts in the action potential. In collaboration with

Kate Steger (Steger et al., 2004), I showed that CCA-1 aids in neurotransmission from MC to the pharyngeal muscle, and is necessary for the MC EPSP to rapidly and reliably trigger a muscle action potential. This is similar to the role of the T-type Ca channel in other systems. In mammalian sino-atrial node, T-type current triggers an action potential after the hypepolarization-activated inward current (I_f) brings the membrane potential to its activation threshold of about –50 mV (DiFrancesco, 1993; Hagiwara et al., 1988). Starting from –20 mV, L-type currents are activated. Similarly to the heart pacemaking tissue, T-type and L-type Ca channels function in concert in the *C. elegans* pharyngeal muscle.

In mammalian neurons, T-type channels have been implicated in the amplification of EPSPs (Gillessen and Alzheimer, 1997; Urban et al., 1998). In these studies, the role of the T-type channel has been dissected pharmacologically by Ni^{2+} sensitivity. However, it is not as clean as genetic dissection because of the several mammalian T-type channel α-subunits, only one is sensitive to low Ni^{2+} concentrations (Lee et al., 1999a). In worms, there is only one T-type channel gene, which makes it easier to dissect its role using the mutant.

The pharynx is likely the most powerful source of electricity in *C. elegans*. *C. elegans* neurons are extremely small and have a very high phenomenological input resistance; most probably, they conduct excitation passively and do not need regenerative action potentials (Goodman et al., 1998). In the body wall, spontaneous activity is slow; and the action potential upstroke is more than 50 ms long (Jospin et al., 2002a). The pharynx is different: the membrane depolarization and repolarization during the action potential are both very rapid, less than 10 ms long. No obvious homolog of the voltage-gated sodium channel that mediates rapid events in vertebrates has been found in the *C.elegans* genome (Bargmann,

1998). Its role is played instead by CCA-1 in the pharyngeal muscle. The CCA-1 current is huge—on the order of 10 nA, which evidently allows a very rapid charging of the membrane capacitance and drives a rapid action potential upstroke. Similarly to the role of CCA-1 in the upstroke, EXP-2 functions in the downstroke to rapidly terminate action potentials; EXP-2 currents reach 18 nA in amplitude. CCA-1 and EXP-2 are turbochargers that allow fast, precisely timed muscle contractions. Indeed, pharyngeal muscle motions are much faster than those of body wall muscle, especially the relaxation. Why is the pharynx so different? The answer probably lies in the structure and in the function of the pharynx. First, the pharynx is large, which is critical for the food intake, so a powerful excitation mechanism is required. Second, the contraction and relaxation timing of different pharyngeal compartments has to be precisely coordinated in order to achieve efficient food concentration and transport (Avery and Shtonda, 2003).

My results also suggest that the pharynx possesses redundant mechanisms of excitation, which ensure its proper function and a wide range of adaptation. The rate of pharyngeal contractions is tightly regulated by various factors, such as developmental stage and mechanical stimuli (Keane and Avery, 2003), food availability (Avery and Horvitz, 1990) and food quality (Steger, 2003). Even extreme perturbations, such as laser ablation of the whole pharyngeal nervous system or getting rid of both MC and CCA-1 excitation mechanisms do not completely abolish pharyngeal function. In the latter case, the pharynx adapts by raising its resting membrane potential and by upregulating the leakage current. As a result, the resting membrane potential tends to spontaneously increase, so that the threshold for EGL-19 activation can still be reached. According to (Hille, 2001), “pacemaking is a

quasi-equilibrium process driven by the miniscule imbalance of much larger component currents", and this is how the pharynx operates.

In this study, I have treated the pharynx as a single functional unit. This is not totally appropriate: the timing and nature of electrical activity is different in different pharyngeal compartments, and precise control of these differences is critical for efficient food transport (Avery and Shtonda, 2003). For example, the relaxation of anterior isthmus has to slightly lag the corpus relaxation. Corpus and terminal bulb movements are rapid, whereas posterior isthmus contractions are slow and peristaltic and do not occur in synchrony with other compartments. Undoubtedly, differences in ion channel expression and regulation underlie some differences in the function of pharyngeal compartments. I predict, for example, that in the posterior isthmus electrical activity is graded and CCA-1 and EXP-2 currents are absent; the isthmus may function similarly to body wall muscle.

2.9. Methods.

Worm culture and strains: Worms were grown on NGMSR plates seeded with *E.coli* strain HB101 at 20 ^{o}C. NGMSR is NGM medium (Sulston and Hodgkin, 1988) containing nystatin and streptomycin to prevent the growth of contamination (Davis et al., 1995). The strains used were: wild type Bristol strain (N2), MT1212 *egl-19(n582) IV* (Lee et al., 1997; Trent et al., 1983), DA1426 *exp-2(sa26 ad1426) V* (Davis, 1999; Davis et al., 1999), DA465 *eat-2(ad465) II* (McKay et al., 2004; Raizen et al., 1995), DA1666 *eat-2(ad465) II; cca-1(ad1650) X* and DA1694 *egl-19(n582) IV; cca-1(ad1650) X*.

Recording and dissection chambers: For dissection and voltage clamp recordings, disposable chambers were made (Appendix, Fig. 1F). A square piece of parafilm with a 10 mm circle embossed with a Sharpie pen cap was placed on a clean 50 × 30 mm cover slip (Fisher Scientific, Pittsburgh, PA). It was covered with another cover slip, moistened by breathing on it to prevent sticking. This assembly was placed on a dry heating block at 70-90 ^{o}C, thumb pressed for 3 seconds, and air-cooled. The upper slide was pried away with a razor blade and removed; the parafilm stuck firmly to the bottom slide. Chambers were stored like this to keep the glass clean. The parafilm circle was excised right before use, leaving a circle of clean glass surrounded by parafilm. The chamber held up to 150 μL of solution.

Dissection procedure: 2 – 2.5 day-old early gravid adult animals were used for

experiments. They were transferred to a 100 μL drop of low Ca Dent's solution (see "Solutions and Chemicals" for all solutions) on a cooled dissection chamber. (A flat tissue culture flask filled with ice-cold water was used for cooling.) Under a dissection microscope, worms' heads were cut off with a hand-held 25-gauge syringe needle (Fig. 1B). The corpses were removed with 50 μL of buffer, then 50 μL of digestion mix 1 was added. The slide was placed on an Axiovert 35 inverted microscope (Zeiss, Germany). 10-15 pharynxes were processed in each batch.

Under 400x magnification, the cuticle covering the anterior half of the pharynx was removed using two glass pipettes (Fig. 1C). These dissection pipettes were made of 1.2/ 0.68 mm borosilicate glass (A-M systems, Carlsborg, WA) by breaking micropipettes pulled on a P-2000 needle puller (Sutter Instruments, Novato, CA), followed by heat polishing. The larger pipette was heat polished to 32-36 μm opening size, the smaller one to 6-7 μm. Pipettes were mounted in holders on UMM-3FC mechanical manipulators (You Ltd., Japan), aligned on one axis and positioned at an angle as small as possible to the microscope stage, to allow insertion of the smaller pipette into the larger one. To control suction, syringes were connected to pipettes.

While the pharynxes were digesting in mix 1, body wall removal (skinning) was performed as shown in Fig. 1C. The terminal bulb of the pharynx was sucked in into the larger pipette. Then, the smaller pipette was attached to the front end of the pharynx and strong suction was applied to the small pipette by locking the piston of the 30 mL syringe as far out as it would go. The small pipette was then advanced into the big one, inverting the cuticle and the body wall covering the pharynx. At this point, the pressure in the small pipette

was switched to atmospheric. By moving the small pipette back and fourth, the cuticle was torn off the pharynx; in cases when the inverted cuticle stayed attached I cut it off later with a hand-held 25-gauge syringe needle. Finally the pharynx was expelled from the big pipette. Cuticles and dead pharynxes were removed in 50 μL of solution, and 50 μL of digestion mix 2 was added. After 15-20 min digestion at room temperature, pharynxes were transferred with a pipette to a 100 μL drop of Dent's solution on a clean recording chamber.

Using the same small pipette that was used for skinning, pharynxes were positioned in the center of the chamber and attached to the glass by gently pressing them with the pipette. Dissection pipettes were removed to allow patch pipette access. After 2-3 min perfusion with the Dent's solution, recordings were started. All recordings were done at room temperature (22-25 ^{o}C).

Voltage clamp recordings: An Axoclamp 2B amplifier (Axon Instruments, Union City, CA) equipped with the HS-2A 0.1LU recording headstage was used in the cSEVC (continuous single electrode voltage clamp) recording mode. The headstage was mounted on an MHW-4 (Narishige, Japan) one-axis water hydraulic manipulator, which was fixed on a UMM-3FC manipulator (Appendix, Fig. 1). The amplifier was interfaced with a Pentium 3 Windows NT computer via a PCI-6035E E-Series DAQ-200 board (National Instruments, Austin, TX) and controlled by custom-designed software developed in the Labview 6 environment (National Instruments) (Appendix, Fig. 2). Amplifier settings were as follows: gain 3 nA/mV, phase lag 0.07 ms, multiplier 100, output bandwidth 3 kHz. Sampling rate was 4 kHz. Patch pipettes were produced from 1 / 0.58 mm borosilicate capillaries (A-M

systems) on a P-2000 puller and heat-polished; they had resistances of 5.5 – 7 MOhm when filled with intracellular solution. After break-in to the whole-cell configuration by suction or mild buzzing, series resistance was 10-15 MOhm. Series resistance compensation ("BRIDGE" knob in the cSEVC mode) and capacitance compensation were used as stability allowed. Preparations with initial R_{series} > 15 MOhm could not be clamped. The bath solution was perfused by gravity flow at approx. 0.1 mL/min during recordings. The holding potential was –80mV. During pulse protocols, I used 5 ms voltage ramps in informative voltage steps, or 40 ms ramps for non-informative steps instead of instantaneous (square) voltage steps. This trick greatly increased the survival of the pharynxes and overall success rate; square pulses to above 0 mV usually killed pharynxes.

In addition to inward currents (Fig. 2), in some experiments, depolarizing pulses evoked an outward current similar to a delayed rectifier K_v current (data not shown). This outward current was highly variable, from non-existent to very noticeable. In these experiments I observed strong contractions in response to depolarizing pulses. I tend to distrust these experiments, because I believe that in these experiments intracellular Ca^{2+} was poorly buffered, causing non-physiological changes during recording. Such preparations were discarded. I only chose preparations in which $[Ca^{2+}]_i$ was apparently well buffered, as judged by the complete absence or hardly noticeable muscle contraction in response to the depolarization.

I observed that in preparations with high delayed rectifier K_v current, EXP-2 hyperpolarization-activated current was greatly decreased or absent. This suggests that EXP-2 itself might change its properties in response to rise in Ca: for example, it might be

degraded by Ca-dependent proteases, causing cleaving off a region responsible for the ultrafast inactivation. This would convert EXP-2 into a conventional K_v channel.

Current clamp recordings: Current clamp recordings were performed using the Axoclamp 2B with the HS-2A 0.1LU headstage as described by (Davis et al., 1999), except that recording chambers and extracellular solution were the same as used for voltage clamp experiments and pipette solution was 3 M potassium acetate, 10 mM KCl. Micropipettes were pulled from 1/ 0.58 mm borosilicate capillaries (A-M Systems) on the P-2000 puller; they had resistance of 50 to 100 MOhm when filled with the pipette solution. Data were acquired using custom-designed Labview software (Raizen and Avery, 1994) at a sampling rate of 2 kHz. Another Labview program was used to algorithmically extract, align, differentiate and average action potentials from recorded voltage traces (Appendix, Fig. 3). For analysis, regions of recorded traces were chosen in which the resting membrane potential had completely stabilized (normally 2-3 minutes after electrode insertion). The micropipette tip potential was measured after electrode removal and subtracted from the trace (the average tip potential drift during experiment was 4.25 ± 5.76 mV in positive or negative direction, n=48, mean ± SD). Action potentials were recognized when the following conditions were met in this order: 1) the analyzed point in the trace was within the specified baseline (between –90 and –50 mV for the wild type, adjusted for mutants with higher resting potential); 2) the analyzed point was followed within 200 ms by at least one point at voltage higher by 50 mV or more, and 3) the average rate of voltage change in the 50 ms following the analyzed point exceeded 0.5 V/s. The end of the action potential was determined as the

first point within the baseline where the voltage slope over the next 25 ms was positive. To align action potentials, I minimized the sum of squared time differences between the rising phase segment from –20 to 10 mV (this segment was chosen because it was the least variable) and a vertical line at 0 ms.

The resting membrane potential was extracted as all points in the analyzed region of the trace within the baseline for which the average rate of change of voltage over the next 100 ms was between –0.02 and +0.02 V/s. These points were averaged over a 1-3 minute interval to calculate the resting membrane potential for a given pharynx.

Data analysis: The linear current component (leak current) was measured using 6 test pulses of –20 mV and subtracted during recordings. Data were analyzed using Microsoft Excel and Labview. To measure activation time constants, current segments from 0 nA to the peak amplitude were fit to a single exponential with the Levenberg-Marquardt algorithm in Labview. Data are presented as mean ± standard deviation (SD) or standard error of the mean (SEM), as stated in figure legends. In all figures voltage commands and currents are time-locked.

Solutions and chemicals: Digestion mix 1 was prepared by mixing collagenases F and H (Sigma, Cat # C-7926 and C-8051) to adjust collagenase activity to 20 U/ml and protease activity to 45 U/ml in low Ca Dent's solution (same as Dent's solution, see below, except that the Ca^{2+} concentration was 10^{-5} M). Mix 2 contained (in U/ml, all from Sigma): 20 collagenase, 600 protease (adjusted by mixing collagenases F and H), 13 protease X (Cat

P-1512), 1300 trypsin (T-0303), 1 chitinase (C-6137) in low Ca Dent's solution. Modified Dent's solution (Dent and Avery, 1993) was used as an extracellular solution (in mM): 140 NaCl, 6 KCl, 1 $MgCl_2$, 3 $CaCl_2$, 10 Na-HEPES, pH 7.3, osmolarity adjusted to 345 mOsm/kg with xylitol. Intracellular solution contained (in mM): 130 K-gluconate, 10 NaCl, 5 K-EGTA, 0.5 $CaCl_2$, 1 $MgCl_2$, 10 K-HEPES, pH 7.3, osmolarity adjusted to 325 mOsm/kg with xylitol. Nifedipine was from Sigma.

Pharynx capacitance calculation: The physical dimensions of the pharynx of an adult worm were taken from table 1 in (Avery and Shtonda, 2003). The total length of the pharynx is 144.7μ. The perimeter of the interior lumen is 25μm in the corpus and 20μm in the isthmus and in the terminal bulb; the lengths of the corpus, isthmus and terminal bulb are 76.6, 35.8 and 32.3μ. Therefore, the area of the internal lumen is 76.6 x 25 + 35.8 x 20 + 32.3 x 20 = 3277μ^2. (I assumed the lumen section in the isthmus and terminal bulb to be the same.). Using a pharynx micrograph, I found the outer radius of the pharynx at 100 points along its length (R_1 to R_{100}). The area of the outer surface is a sum $\Sigma [\pi (R_i + R_{i+1}) \sqrt{((R_i - R_{i+1})^2 + L^2)}] = 8939\ \mu^2$ (from i=1 to i=99), where L is a step along the X axis (1.447μm).

Thus, the total surface membrane area is 12216 μ^2. In various studies, the specific membrane capacitance was measured in the range of 0.7 to 1.3 μF/cm^2 (Curtis and Cole, 1938; Gentet et al., 2000). Assuming the specific membrane capacitance of 1 μF/cm^2 (0.01 pF/μ^2), the surface capacitance is 122.2 pF. Three marginal cells run the length of the pharynx. Because marginal cells may contribute about 20% to the surface area (Fig. 5 an 6 in (Albertson and Thomson, 1976), the surface capacitance would be 97.7 pF if marginal cells

are electrically inactive and not charged.

Next, I estimated the contribution of some internal membranes to the total capacitance. In the corpus and isthmus, there is an invagination in each muscle cell. Assuming that the depth of these invaginations is equal to the radius of the pharynx (Fig. 5 an 6 in (Albertson and Thomson, 1976), the total area of invaginations is $6 \Sigma [(R_i + R_{i+1})L /2] = 5226 \mu^2$; they would contribute 52.3 pF of capacitance.

Each marginal cell has two lateral membranes that face pharyngeal muscle cells. The total area of lateral muscle cell and marginal cell membranes is $12 \Sigma [(M_i + M_{i+1})L /2] = 7231 \mu^2$ where $M_i = 0.7 R_i$ in the isthmus and $0.6 R_i$ in the corpus, as estimated from Fig. 5 an 6 in (Albertson and Thomson, 1976). These membranes would add 72.3 pF to the total capacitance, or 36.2 pF if marginal cell membranes are not charged.

In addition, I included membranes that connect different layers of muscle cells, as deduced from Fig. 21 in (Albertson and Thomson, 1976). These membranes would contribute at least 30 pF (their invaginations were not included).

Thus, the total membrane capacitance of the pharynx is at least 216.1 pF, or at least 276.7 pF if marginal cells are also electrically active. In this calculation I assumed capacitances of pharyngeal cells to be in parallel, so that they add up to produce the maximum possible total capacitance. This could result in overestimation: if some capacitances are in series, they would reduce the total capacitance, making the pharynx easier to charge. But, on the other hand, many of the invaginations were not included, which could result in an underestimate. Overall, this capacitance calculation should be considered very rough.

3. Food seeking and food preference behavior in *Caenorhabditis elegans.*

3.1. Background.

3.1.1. Feeding as a motivated behavior.

In mammalian behavioral paradigms food, along with water or addictive drugs is a powerful reward (also called *reinforcer* or *incentive*). This, of course, is due to the fact that, in contrast to plants, which photosynthesize, food is indispensable for animals. Much of animal behavior serves the purpose of finding food. These behaviors are *motivated* (also called *instrumental*, *goal-directed*, or *operant*) that is, an individual performs certain actions to achieve an outcome or get a reward. Unlike reflective behavior (when an animal responds to a stimulus) in motivated behavior the animal itself initiates the behavior. In case of feeding behavior, the animal's motivation is an internal state of hunger signaled by the nervous system and the reward is obviously the food. In native environments, an animal would search for food using in-built (*instinctive*) or learned strategies, or, more often, a combination of both. In lab paradigms, mammals can learn various tasks to get the food, of which pressing a lever is one of the commonly used for rodents (Skinner, 1938). With an ingenious use of animals' favorite food as a reinforcement, they can be made to perform various actions: dogs can learn to "dance", bears learn to ride a bicycle, and tigers learn to jump into a ring set on fire, which you may have observed in a circus.

Scientists have early separated the food-seeking, motivated component of mammalian feeding behavior and realized that mechanisms for sensing satiety and hunger that drive

animals to seek and ingest food when hungry and terminate feeding when satiated are conserved between humans and rodents (Skinner, 1938; Young, 1941). Indeed, it was found later that most of the nervous system components involved in these behaviors are localized to the brain stem and evolutionarily old areas of the forebrain such as the limbic system (Berridge, 1996; Berridge and Robinson, 2003; DiLeone et al., 2003; Saper et al., 2002; Schultz, 1998; Stellar and Stellar, 1985). In *C.elegans*, this motivational component has not been directly studied. One professor asked me: "What do you mean by food-seeking behavior in worms? They always seek for food." Although it was known that food regulates most worm behaviors, in the *C.elegans* field food has been mostly treated as a sensory stimulus, not as a reinforcer.

The common belief was that worms use taxes, such as odor-, chemo- and thermotaxis to find food, which is certainly true, and most research has focused on these, certainly interesting behaviors. The possibility that food also acts as reward that affects behavior after it is found and eaten has not been directly tested. In taxes, the worm follows environmental cues. In mammals, smell is also important for the food seeking and preference (Hullar et al., 2001; Lien et al., 1999)*. In mammals, there are in-built preferences for tastes, such as attraction to sweet or mildly salty and repulsion to bitter and sour taste. This is understandable, since sweet taste is a predictor of nutritious, sugar-rich food, while bitter taste is likely to be present in a spoiled, rotten food or in toxic plant alkaloids.

But after the food is eaten it provides a very important feedback: the feeling of satiety develops and an animal feels "happy". Thus, food also acts as a reward that provides positive or negative behavioral reinforcement. This feedback has a profound impact on mammalian

* In another example, my hamster that has escaped from its cage was found sleeping at the bottom of the trash bin.

behavior: an animal remembers the smell and appearance of food and the place where it is found, and other relevant environmental stimuli associated with this food. If, on the other hand, the food makes an animal sick, the odor and taste of this food will be perceived as repulsive in the future (Garcia et al., 1955; Garcia et al., 1968). The feedback from food, like any other feedback, is an error signal: it tells the animal whether it was a correct decision to follow that smell and taste and consume that food.

C.elegans navigational behaviors that enable worms to find food have been studied in detail, but it is not known whether worms get feedback from food. I thought that one of the approaches to look at the latter problem would be to vary the food and look at the changes in behavior. Specifically, I wanted to vary the biologically relevant property of food, its ability to support growth. Food that supports growth well should provide positive feedback, while food that supports growth poorly should provide no or negative feedback. I define the ability of food to support growth as the *food quality*. In a number of assays I have shown that the worms' behaviors changes as the food quality does. The main concern with these experiments is that as the food changes, not only the quality, but other properties, such as smell, water content, and chemical composition, also change. That is why *eat* mutants with compromised food consumption (Avery, 1993a), are indispensable controls for these experiments. Using an *eat* mutant instead of the wild type is the same thing as substituting a good food with a poor one; and if the feedback hypothesis is true, we expect to observe similar changes in behavior. Indeed, this is what I observed (see below).

In subsequent chapters I will try to show that I have identified behavioral paradigms in *C.elegans* that are related to the motivated food-seeking paradigms in other animals,

including mammals. One could probably ask why, instead of trying to adapt known mammalian paradigms to worms to study the question I am interested in, I came up with worm-specific paradigms and now attempt to interpret them from the point of view of what is known in other systems. The reason was mentioned above: the worms' natural environment is too different from the mammalian (rodent) and their native behavior is too poorly understood to use the first strategy. Instead, I tried to design paradigms based on what I thought is relevant and important for worms. As Leon Avery mentioned (personal communication), many of the paradigms to study learning in worms were attempts to "make them learn calculus", meaning that they are irrelevant in their natural environment and, as a result, *C.elegans* performs poorly in those paradigms. To design robust paradigms in which animals perform well, a relevant behavioral stimulus, something that an animal of interest really cares for, is needed. I thought that others had overlooked the natural variability of bacterial food as a behavioral stimulus. I hypothesized that this is something very important for *C.elegans*, and designed assays using food as a variable.

In contrast to behaviors triggered by external stimuli, motivated behaviors have no apparent external cause. These behaviors are also called operant or instrumental to emphasize the fact that the animal itself initiates and performs the behavior. According to Skinner (Skinner, 1938), in operant behavior "no correlated stimulus can be detected upon occasions when it is observed to occur. It is studied as an event appearing spontaneously … with a given frequency". While in reflective behaviors the magnitude or penetrance of the response to the stimulus is measured, in motivated behaviors, the incidence (frequency) is measured; the magnitude can be measured as well.

For example, a hungry rat that has learned that pressing a lever will deliver a food pellet will regularly press the lever to get food, and the frequency of this behavior is easily determined. No explicit stimulus causes a single lever-pressing event. When animal feels hungry, it initiates behavior. As it gets satiated, it will press less and less frequently and finally will stop and switch to other activities. Lever pressing is a learned behavior useful only in a particular lab environment. In other environments, the same animal would learn and utilize different strategies.

What motivates a rat or mouse to press the lever is something that we, humans, perceive as "hunger", which is an internal state. Since motivated behavior is initiated by the nervous system not in response to the stimulus, there should be some kind of the activity generator within the nervous system. Multiple environmental and internal stimuli as well as memories are integrated by the nervous system into a certain pattern of activity that signals an internal state of hunger, thirst, satiety, pleasure, etc. This drive then triggers behaviors based on the analysis of current environment and previous experience; the particular behavior may be different in different situations for different individuals. As Skinner (Skinner, 1938) explains, "the problem of drive arises because much of the behavior of an organism shows an apparent variability. A rat does not always respond to food placed before it, and a factor called its 'hunger'is invoked… The rat is said to eat only when it is hungry. It is because eating is not inevitable that we are led to hypothesize an internal state to which we may assign the variability. When there is no variability, no state is needed. Since the rat usually responds to a shock to its foot by flexing its leg, no 'flexing drive' comparable to hunger is felt to be required".

Since living creatures are shaped by evolution, every biological phenomenon requires an evolutionary explanation. In my opinion, a nervous system that signals an internal state has a selective advantage over a nervous system that does not signal an internal state and simply processes information: an animal that "feels" is genuinely interested in the result of its own behavior. For example, consider pain sensation. There could be reflective loops that initiate avoidance or withdrawal response once the stimulation of a certain modality reaches certain threshold, and such loops are known to exist. However, nociceptive stimulation is also accompanied by a subjective pain "feeling". It is this pain experience that makes us avoid painful stimuli. An animal or human has no idea how its own nervous system works, but it "feels" what its current need is. A drive, or state, is kind of a common denominator of multiple nervous activities, that tells an animal: "now, you are hungry, seek for food" or "now, seek for a mating partner" or "now, avoid pain". This "feeling" is hard to analyze experimentally in non-human animals because it is subjective. Generally, in vivo recording of the nervous system activity in behaving animals is needed. Patterns of neuronal activity, correlated to changes in behavior, may be interpreted as the correlates of the drive states. It is not clear, however, in any organism, including humans, how patterns of neuronal activity, even if they are known, result in subjective "perception". In a fantastic situation, when the activity of all neurons at a given moment during behavior is known, will it be possible to explain this?

Motivated behavior is regulated efficiently by feedback: an animal does things that alleviate initial drive. Ingestion of food by a hungry animal is an example. As the food is being eaten, signals from the gastrointestinal system and blood act on the brain to reduce the

feeling of hunger, causing slowing and termination of feeding. In rats, the amount of food eaten per unit of time follows a function $N = cx^n$, where n is ~0.7 (Skinner, 1938). The rate of feeding decreases as satiation approaches. The subjective perception of the taste of food also decreases with satiation—a phenomenon called alliesthesia (Cabanac, 1971). Essentially, food is not as rewarding for a satiated animal as it is for a hungry one. Somewhat similar phenomena have been observed in *C.elegans*: well-fed worms increase their feeding in response to food much more weakly than starved worms (Avery, 1990).

Pavlovian conditioning (Pavlov, 1927) is a form of associative learning. In one paradigm, a dog will start to salivate in response to a stimulus previously paired with the presentation of food. But this behavior also has a motivated component: this association is only possible when an animal has been deprived of food for a few hours (Anokhin, 1974). Only a hungry animal is motivated to learn that a flash of light is a food signal, which in this case turns out to be the best food-seeking strategy. This example illustrates that motivation has a powerful influence on behavior, even when it is not looked at directly in the assay.

There is almost no research on motivated behaviors in invertebrate systems, such as *Drosophila* and the worm. (More precisely, the concept of the motivation and drive has not been implicated in many known behavioral paradigms where it is certainly involved). My hope was to come up with paradigms of hunger-driven food-seeking behavior in *C.elegans*. In worms, there is probably a single described case of a motivated behavior: males leave the food lawn in search of a hermaphrodite (Ghosh et al., 2003; Lipton et al., 2004). Hermaphrodites do not seem to hunt for males because they produce their own sperm and do not need males to reproduce. Males, however, must mate to preserve their genes, so they

possess a strong sex drive. Interestingly, starved males leave food less frequently; indicating competition between sexual and food seeking drives in the worm's mind. This suggests that, despite the much lower processing power of the worm nervous system as compared to mammals, it may still signal and utilize drive states to weigh and integrate stimuli and to produce an outcome.

3.1.2. Regulation of food intake and food choice.

For most animals feeding behavior involves choosing between food sources. In making these choices, an animal must satisfy its energy needs and supply a number of limiting compounds such as vitamins and essential amino acids. Behaviors must have evolved to accomplish this.

Indeed, when offered a selection of food, rats eat a proportion of each food to provide essential elements for growth (Richter et al., 1938). When offered a choice of two food sources of similar composition, one of which is missing an essential component and therefore does not support normal growth, rats select food that contains all essential elements (Osborne and Mendel, 1918). Mammals show specific, separate "hungers" for particular nutrients, such as fat, carbohydrate, protein, calcium, sodium, and certain vitamins. The extent of each drive depends on prior dietary history, food deprivation, age, disease, and current metabolic needs (Young, 1941). For example, rats fed a diet lacking vitamin B develop an overwhelming appetite for it (Richter et al., 1937). Even when 12 other containers filled with different foods are available, vitamin B-deprived rats immediately find the bottle with the vitamin B

solution. “Efforts to remove the bottles were met with fierce resistance. The bottle was held tightly with both paws and even with the teeth.” In addition, vitamin B-deprived rats will prefer the food containing the vitamin to the food lacking it; if the vitamin is switched from one food to another, the choice also switches (Harris et al., 1933).

In another study, the effect of adrenal gland removal on the salt appetite in rats was studied (Richter, 1936). (Adrenal glands, among other things, secrete aldosterone, which stimulates sodium reuptake in kidneys). Rats fed a normal diet normally die within 10 to 15 days after operation due to the salt loss. However, if 1% NaCl solution is available separately, animals drink enough of it to compensate for the loss and survive the operation: salt consumption increases about 10 fold following the surgery.

Similarly, rats increase consumption of Ca lactate solution 3.9 fold after removal of parathyroid glands in order to survive (Richter and Eckert, 1937). Normally, 50% of animals die within 24 hours after surgery due to Ca^{2+} loss if no high-Ca source is available.

These and other experiments suggest that the intake of food and selection of the food source is homeostatically regulated. When the organism runs low in a certain nutrient, the “appetite” for this particular nutrient is created. This appetite drives a change in feeding behavior to increase consumption and restore the normal level of this nutrient.

Many other experiments, however, have shown that it is not only metabolic demand that regulates the food intake and food choice in mammals; there are many environmental, cognitive and social factors involved (Capaldi, 1996; Sclafani, 2001). One example is social transmission of the food choice. Rodents smell each other and are more likely to search for and consume the food that they have smelled on another animal, when other food choices are

available (Galef et al., 1984; Posadas-Andrews and Roper, 1983). This behavior is adaptive: the food that has been eaten by other animals of the population is probably available and safe to eat. It has also been shown that simply increasing the availability of food increases food consumption. In one experiment, rats were given either 3 cups containing protein, carbohydrate, and fat, or these 3 cups plus 3 additional cups of either carbohydrate or fat. Animals increased the consumption of the diet that was available in excess: the group with extra carbohydrate ate more carbohydrate and the group with extra fat ate more fat than the control group (Tordoff, 2002).

Therefore, factors other than the nutrient composition of food regulate feeding. Of these non-homeostatic factors, the most important is the sensory stimulation that food provides. For most mammals, and particularly rodents, it is smell and taste. For example, anosmic mutant mice fail to survive due to inability to suckle (Belluscio et al., 1998). Mice, rats, monkeys and humans show stereotypical reactions in response to taste placed in the mouth. In human infants, "sweet or mildly salty taste elicits a mild rhythmic smacking, slight protrusions of the tongue, a relaxed expression accompanied sometimes by a slight upturn of the corners of the mouth. A bitter, sour, or very salty taste elicits a grimace, a turning away, a gape or gagging movement, … and a pushing away with the hands" (Berridge, 1996; Steiner, 1979). In rats, sweet taste causes tongue protrusions and paw licking, whereas bitter taste elicits rearing, head shaking, and wiping the face with forelimbs (Grill and Norgren, 1978a). Our hard-wired hedonic reaction to the sweet taste is the basis for the flourishing industry of diet drinks, in which sugar is replaced with the non-nutritive sweet tasting sugar substitutes.

Affective responses to taste do not require cerebral cortex because they are also observed in anencephalic human infants (Steiner, 1973) and decerberate rats (Grill and Norgren, 1978b).

Experimental techniques are available to separate the role of homeostatic and non-homeostatic properties of food in feeding behavior. In an intragastric (IG) infusion paradigm an animal is fooled: whenever it drinks one fluid, its stomach is infused with the same or another fluid via an implanted catheter (Elizalde and Sclafani, 1990). Using this technique, it has been shown that nutritional and sensory properties of food interact in determining food preferences and intake (Sclafani, 2001). In one experiment, rats were allowed to drink either solution with a preferred taste, 0.2% saccharin, or a mildly unpreferred bitter solution, 0.03% sucrose octaacetate, while being IG infused with the same sugar solution, 32% maltodextrin, in both cases. Animals exposed to saccharin consumed more liquid than the other group and consequently were infused with more maltodextrin solution and gained more weight over a 4 week experiment (Sclafani et al., 1996). Other IG infusion experiments have demonstrated the importance of food nutritive content. When saccharin solution was paired with IG delivery of carbohydrate, rats consumed more of it as compared to when it was pared with IG infusion of water (Ramirez, 1996). Interestingly, this increased intake develops with time and extends for a day after pairing with carbohydrate has been terminated, indicating that the behavior is learned. When rats are given a choice of the same liquid from two tubes, drinking from one of which results in the IG infusion of sugar, while drinking from the other only results in water infusion, animals develop a strong (90%) preference for a tube pared with carbohydrate (Elizalde and Sclafani, 1990; Perez et al., 1999). This experiment works when animals are allowed to drink either pure water or a flavored solution. Therefore, mammals

can choose food solely based on its nutritive value, even when no taste cues are available. Pairing of the flavor with the IG infusion of fat also results in preference and overeating (Lucas et al., 1998).

Consequently, for rodents and humans, an excess of flavored calorie-dense food, rich in carbohydrate and fat ("supermarket diet"), is a particularly strong stimulant of feeding. Rats given unlimited access to such diet overeat and develop obesity (Sclafani, 1989). Overeating, combined with insufficient physical activity, is also a major cause of obesity in humans. Most likely, the mammalian nervous system has evolved to deal with food insufficiency, rather than food excess. It is highly improbable for an animal in the wild to experience an excess of a highly nutritive food for a long time, so homeostatic mechanisms often fail to protect mammals against overeating and obesity under continuous presence of a highly nutritive food.

3.1.3. Feeding behavior involves learning.

In most if not all animals, and especially in mammals with their powerful forebrain, learning serves to enhance and improve inborn behaviors. Feeding behavior is no exception.

In classical (Pavlovian) conditioning, an animal learns to associate the availability of food with an otherwise irrelevant environmental stimulus (Pavlov, 1927). In a place preference paradigm, an animal associates the presence of food with a particular location (Schechter and Calcagnetti, 1993), and of course the hippocampus with its place neurons is a critical substrate for the spatial learning (O'Keefe and Dostrovsky, 1971). Bees are known

not only to remember the route to the feeding location, but also transmit this information to other members of the colony.

Rats learn to prefer the flavor of nutritive food (flavor-nutrient association). This has been best shown by the intragastric infusions: delivery of nutrients directly to the stomach increases animal's preference for the flavor (Elizalde and Sclafani, 1990). Rats also learn to prefer another smell or taste paired with the already preferred one (flavor-flavor association) (Capaldi, 1996).

In instrumental or operant learning, an animal itself learns and performs an action to get the food. Lever pressing by a rat is an example (Skinner, 1938). A food-reinforced operant learning paradigm (biting behavior) has also been developed for the snail *Aplysia* (Brembs et al., 2002)

But if eating the food makes an animal sick the flavor paired with this food will be strongly avoided (aversion conditioning) (Garcia et al., 1955; Garcia et al., 1968). With rodents, this can be achieved by adding nausea-causing LiCl to the food. Interestingly, there is evidence that *C.elegans* can also learn to avoid the smell of pathogenic bacteria (Zhang et al., 2004).

To summarize, food acts as reinforcement in various learning paradigms. It has been shown that sensory, non-homeostatic, and nutritive, homeostatic properties of food interact in its reward action. The extremely rewarding nature of highly flavored, calorie-dense "supermarket" diet is one of the major causes of overeating and obesity. It is well known that feeding habits are hard to change; brief deprivation of the favorite food results in rebound: "food craving", "carbohydrate craving", and binge-eating (Capaldi, 1996). In fact,

neuropeptide signaling mechanisms that mediate food and drug addiction are thought to overlap (DiLeone et al., 2003).

3.1.4. Food-related behaviors in *C.elegans*.

Almost all *C.elegans* behaviors are affected by food, as usually measured by the presence versus absence of standard worm food, *Escherichia coli* strain OP50. *C.elegans* is attracted to odors and soluble chemicals secreted by bacteria (Andrew and Nicholas, 1976; Grewal and Wright, 1992), although the precise nature of the bacterial attractants has not been determined.

The presence of food activates pharyngeal contractions (Avery and Horvitz, 1990) and egg-laying behavior (Chalfie and White, 1988) . Bacterial food is needed for expression of social behavior, although just the odor of live bacteria is sufficient to promote clustering (de Bono et al., 2002). Food availability regulates the rate of locomotion (Croll, 1975; Sawin et al., 2000) and turn and reversal frequency during locomotion (Tsalik and Hobert, 2003).

Thermotaxis in worms is their ability to migrate to the temperature of cultivation. It is a form of associative learning and is completely food-dependent (Hedgecock and Russell, 1975). Upon removal from food, animals migrate to the cultivation temperature and move along the isotherm (isothermal tracking). The neural network involved in this behavior has been partially unveiled (Mori and Ohshima, 1995).

C.elegans aerotaxis behavior (preference for certain oxygen concentration) has been investigated (Gray et al., 2004b). In a gradient of O_2 from 0 to 21% worms concentrate at the

intermediate concentration of 5-10% in the absence of food. In the presence of food, this distribution is very shallow. In was found that the oxygen concentration in bacterial milieu is decreased compared to the atmospheric level, presumably because of bacterial metabolic activity. O_2 concentration is 12.8% on the border and 17% in the center of the bacterial lawn (the border tends to be thicker). It is possible that aerotaxis is also an associative learning paradigm: after having been cultivated in the presence of food at a decreased O_2 concentration, animals migrate to this O_2 concentration in search for the food; but if food is available, they no longer care about oxygen.

If worms are transferred from bacterial food onto an empty plate containing a point source of an attractant, they will migrate to the odor, such as benzaldehyde, or chemical, such as NaCl. But after prolonged exposure, worms will adapt to the chemoattractant and will no longer respond to it, or the positive response will switch to avoidance (Colbert and Bargmann, 1995; Colbert et al., 1997; L'Etoile et al., 2002). Interestingly, the presence of food inhibits this adaptation (Nuttley et al., 2002; Saeki et al., 2001). In addition, after adaptation has occurred, brief exposure to food revives chemoattraction. These findings suggested that sensory adaptation in *C.elegans* is in fact a form of associative learning: the chemical is associated with the presence or with the absence of food, and the response to this chemical changes appropriately from attraction to avoidance.

One of the differences between the feeding behavior of worms and mammals lies in the relation of feeding behavior to other behaviors. Most mammals do not feed continuously. Periods of feeding are interrupted by other activities such as sleep, play, aggression, etc. Worms, except for developmentally required interruptions during molting, *always* eat if food

is available. The reproduction rate of worms is so high that in order to support it, non-stop feeding is required (*r* strategy vs. *k* strategy). Even brief food deprivation is a red flag. Therefore, one would predict that the internal motivation for food seeking in worms is very high; they are always "hungry". In mammals, neuropeptides secreted by the digestive system, impulses arriving from gustatory receptors, and possibly other mechanisms signal satiety to terminate feeding. Is there anything indicating the state of satiety in worms by the same criteria? Work of Kate Steger suggests that there is: *C.elegans* regulates its rate of feeding (pharyngeal pumping) depending of how well-fed it is (Steger, 2003). On high quality food, such as *Comamonas* or *E.coli* HB101, the pharyngeal pumping rate drops to about 150-180 pumps per minute, while on low quality food such as *E.coli* DA837 or *B.megaterium* it reaches 250 pumps per minute. Although this regulation is not as dramatic as in mammals in the sense that worms do not interrupt feeding, they do seem to modulate the rate of feeding. This is evidence in support of feedback regulation of feeding by a "hunger state".

Food emits multiple stimuli: it has smell, taste, and feel, and, when consumed, it quenches hunger. In mammalian behavioral research, the distinction between sensory and homeostatic impact of food was stressed early (Young, 1941). In worm research, however, the homeostatic component has not been directly studied; food has largely been treated as a sensory stimulus. No research was done in worms linking the biological value of food, its nutritional value and ability to support growth, with behavior. In mammals, one of the techniques used to separate sensory and homeostatic action is intragastric bypass infusion (Elizalde and Sclafani, 1990). How one would proceed with worms? It is infeasible to fill the worm intestine with something different from what is being eaten. My approach was to

utilize the bacterial food variability, which I thought was a biologically relevant parameter, to dissect the worm's food preference and food-seeking behavior.

3.1.5. The hypothesis.

This project started with several simple considerations: 1) starved worms are hyperactive; 2) very starved worms, such as the ones in which the critical pharyngeal neuron M4 has been ablated, sometimes crawl off the plate; 3) when there is non-*E.coli* bacterial contamination on the plate, worms often choose either *E.coli* or the contaminant; 4) soil bacteria are likely variable and, finally 5) possibly not all of the soil bacteria species can support *C.elegans* growth well. These considerations have led to the hypothesis that *C.elegans* must have evolved the following behavior: an ability to evaluate food quality and then make a choice of either staying in this food or leaving and searching for the better food.

3.2. Bacterial food as a variable.

As Anokhin (Anokhin, 1974) noted, “the reinforcing strength of an unconditioned alimentary (food—B.S.) stimulus becomes greater with its increasing ability to satisfy the animal, i.e., to relieve the initial need”. A similar thought is also expressed in the Thorndike’s “law of effect” (Thorndike, 1965, reprint of 1911 ed.): “Of several responses made to the same situation, those which are accompanied or closely followed by satisfaction to the animal will, other things being equal, be more firmly connected with the situation, so that, when it recurs, they be more likely to recur… The greater the satisfaction or discomfort, the greater the strengthening or weakening of the bond”. Thus, if food is a reinforcer for *C.elegans*, one of the predictions is that better food is a better reinforcer. We expect to see changes in behavior when a poor food is changed to a good one and vice versa. Kate Steger (Steger, 2003) has shown that the rate of feeding is regulated by food quality, and I wanted to look at food seeking and food choice behaviors.

To do that, a tool, that is, a set of bacterial foods, is needed. Unlike mammals, for which the nutritional requirements of food necessary for normal metabolism and growth are well studied, it is not well known what the worm’s requirements for food are. *Escherichia coli*, a mammalian intestinal symbiotic bacterium, has been used to grow *C.elegans* in the laboratory (Sulston and Hodgkin, 1988) and it seemed to work well. For obvious reasons, *E.coli* is unlikely to be the natural *C.elegans* food, although occasional encounters are certainly possible. It has been shown that bacteria other than *E.coli* support the growth of

C.briggsae, a species closely related to *C.elegans* (Briggs, 1946). *C.elegans* can also be grown in axenic media without bacteria (Nicholas et al., 1959; Nicholas and M.G., 1957), although worms are not as healthy in these media as in the presence of bacteria.

From Leon Avery's studies on the mechanisms of feeding (Avery, 1993a), we know about *eat* mutants with defective function of the feeding organ, the pharynx. *eat* mutants, in addition to the pharyngeal phenotype, usually show additional ones: smaller size, pale body, small brood size and delayed growth. These phenotypes are thought to result from insufficient food consumption, although there are other things that also cause them, such as defects in adipogenesis (McKay et al., 2003). For *C.elegans* survival as a species, normal growth and reproduction are critical, and from observation of *eat* mutants we know that normal feeding is needed for this. On the other hand, a variety of bacterial species live in soil, and some of them might not be nutritious foods. Thus, behaviors should have evolved that allow worms find the high quality, nutritious foods that provide all elements for normal growth.

So I screened bacteria isolated from soil for their ability to support growth. (The other strategy would be to test known bacteria, but back then I thought it would be harder since I did not have any basis for picking candidates. Now I realize that it would be interesting to systematically test bacteria of different nutrient composition, since microbial biochemistry is very well studied.) I was particularly interested in those bacteria that poorly support growth of the wild type *C.elegans*, since all known *E.coli* strains support growth at the maximum or close-to-maximum rate. In these experiments, after identification of bacterial species, I got a range of about 16 different foods (Fig. 13), of which 5 species were selected for subsequent

experiments (Fig. 14). Most bacteria supported the growth of the wild type *C.elegans* well, like *E.coli.* These good foods are taxonomically unrelated: *Pseudomonas*, *Comamonas* and *Acinetobacter* are Gram negative aerobes, *Pantoea* and *Escherichia* are Gram negative facultative anaerobes, *Bacillus* and *Paenibacillus* are Gram positive, spore forming bacteria. I only found three *Bacillus* species that were markedly bad foods for the wild type *C.elegans*: *B. cereus*, *B. megaterium*, and one unidentified *Bacillus* species.

Some bacteria, such as *Enterococcus faecalis, Streptococcus pneumoniae*, and *Staphylococcus aureus* (Garsin et al., 2001), *Serratia marcescens* (Pujol et al., 2001), and fungi, such as *Drechmeria coniospora* (Jansson, 1994) are pathogenic for *C.elegans*. Therefore, it is important to be able to distinguish a growth delay that results from toxicity of bacteria from a growth delay resulting from inadequate diet. Here, *eat* mutants help. If bacteria are pathogenic, using an *eat* mutant with a strictly pharyngeal phenotype should result in no or mild further growth delay, because feeding is not limiting growth. If, however, bacteria are poor food, using an *eat* mutant instead of the wild type should grossly exacerbate the growth defect, because *eat* mutants are already compromised in feeding. Three *eat* mutants of very different nature, *eat-2* (McKay et al., 2004; Raizen et al., 1995), *eat-4* (Lee et al., 1999b) and *eat-5* (Starich et al., 1996) all grow worse than the wild type on foods that are mediocre for the wild type. And, as one would predict, the difference is particularly large for *B.megaterium*, which is an extremely bad food for the wild type (Fig 13 and 14). One could argue that *eat* mutants may cause defects outside the pharynx that weaken the worm's immunity. This is certainly possible, but unlikely for *eat*-5 and especially *eat-2* which is expressed in a single cell in the worm, and localizes to a single synapse that the motor neuron

MC makes on pharyngeal muscle (McKay et al., 2004). The growth defects of *eat-2* and *eat-5* on *E.coli* strain DA837 were known previously.

In addition, I observed the worm's morphology and behavior on poor food. On *Bacillus megaterium*, worms showed normal locomotion and did not show gross behavioral or anatomical abnormalities.

Leon Avery had a specific prediction: big bacteria will be poor quality food, while small bacteria will be good foods. Indeed, the two worst foods, *B.cereus* and *B.megaterium* are both noticeably larger than other bacteria, while the best food, Comamonas, is tiny (Fig.13) (Avery and Shtonda, 2003). One exception to this rule is *eat-5* on *E.coli* DA837. There is no difference in size between *E.coli* strains HB101 and DA837, yet the former is good food, while the latter is very bad for *eat-5*. DA837 is also mediocre food for other *eat*s. At present, we do not fully understand what causes that. Most likely, the difference between *E.coli* strains HB101 and DA837 is in water content: when grown on an NGM plate, DA837 tends to be chunky, while HB101 is gooey. For *C.elegans* to feed, lubrication between particles is needed, and this is even more critical for *eats*, since they are already limited in feeding.

Leon Avery has also made another interesting observation, which is a disproportional growth of the pharynx during development. In the newborn L1 larva, the pharynx is 71 μm long, which is about 30% of the body length. In adults, the pharynx is 145 μm, which is 14.4% of the body length (Avery and Shtonda, 2003). The pharynx grows slower than the rest of the animal. This suggests that worms are born with the pharynx as big as possible, because the size of bacterial food is limiting for feeding of young animals. In the adult, the

inner diameter of the pharynx varies within 3.9-4.9 μm along the length of the pharynx, which should allow them to swallow even the biggest bacteria. In L1 larvae, the inner lumen varies within 1-1.8 μm, meaning that newborn worms may have problems swallowing the biggest bacterial cells. Leon's model for food transport in the pharynx (Avery and Shtonda, 2003) predicts that small particles are transported more efficiently. To put his calculations in a perceptible form, the particle can only move to the back of the pharynx if the lumen of the pharynx is bigger than the particle. For small particles, this condition will hold true for a longer time during the cycle of pharyngeal contraction/relaxation than for bigger ones, and that is why the transport of small bacteria is more efficient.

To summarize, it is likely that differences in the growth rate of *C.elegans* on different bacteria are due to mechanical differences between the bacteria due to size or water content. It is also likely that these differences are most limiting for worms with small pharynxes, especially for newly hatched L1s. In fact, the latter claim is supported by my and other Avery lab members' unpublished data. We repeatedly observed that on poor food, worms spend very long time in the L1 stage. But once they overcome this limiting step, their growth is almost normal. Unfortunately, this is not reflected in the Fig. 13 and 14, since I measured the total time of growth to the adult stage.

All experiments described in chapters to come were done on L1s, newly hatched worms, for two main reasons. First, in most cases worms have to be naïve, that is, they should not have experienced any food in their life. It is not known and I have no way to predict how experience of one food will affect behavior on the same or another food. The

second reason has been just described: it is the L1 larval stage when the food is likely to be most limiting for growth and, consequently, most important for behavior.

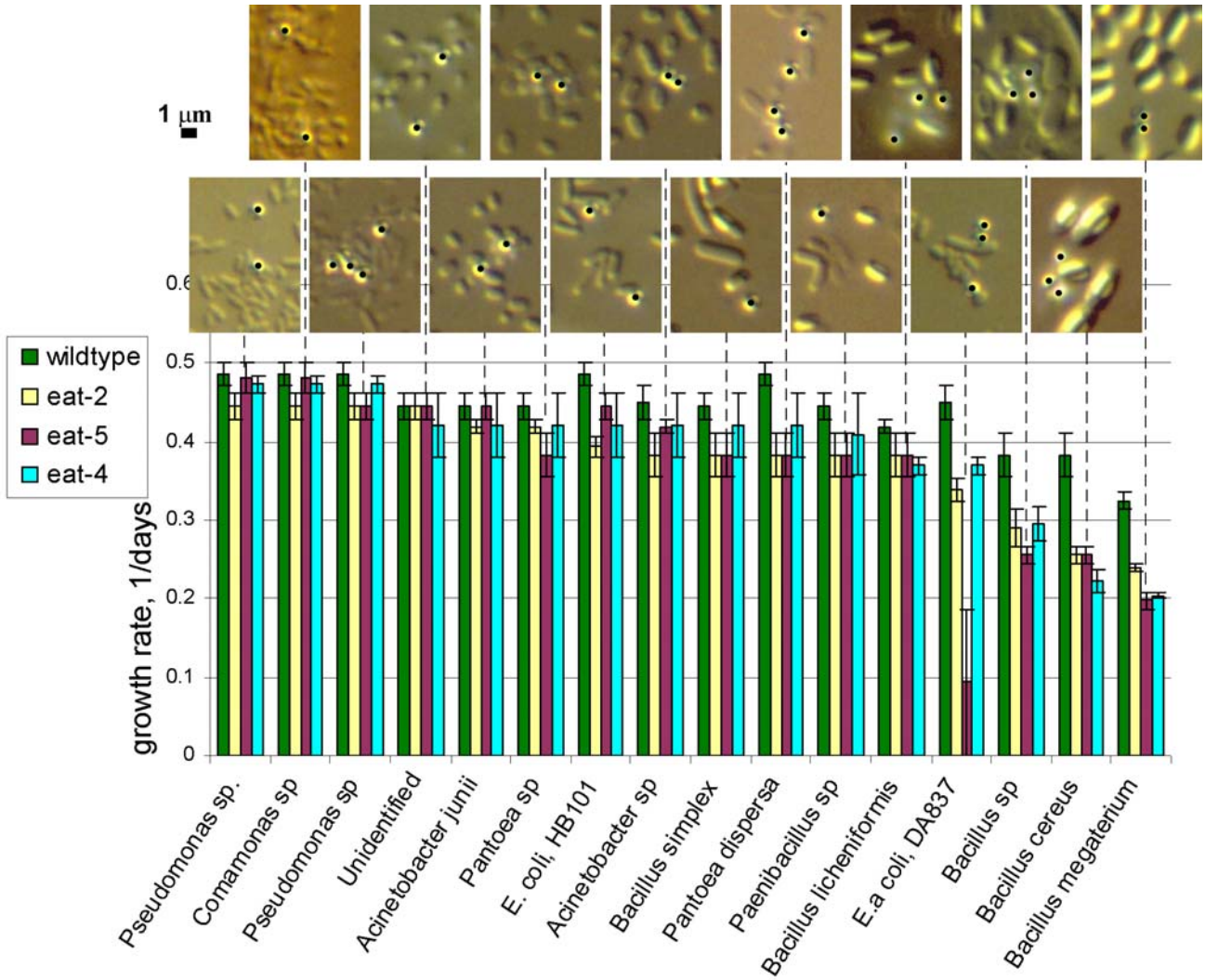

Figure 13. **Varying ability of different bacterial species to support *C.elegans* growth.** Growth rates (the inverse of the time from hatching to adulthood) of the wild type *C.elegans* (N2) and three feeding-deficient *eat* mutants were determined on 14 environmental bacteria isolated from soil and two *Escherichia coli* strains, HB101 and DA837. Small bacteria appear to be better food than large species, with the exception of *E.coli* DA837, which tends to form clumps. This is a single experiment done on 3 plates. Error bars represent the inverse of the time between two observations of the plates: a final observation, when the worms were scored as adults, and another observation preceding the final one. Bacteria were photographed by Leon Avery, growth rates measured by the author. 0.8 μm latex beads, labeled with black dots, were added to the bacterial samples for photography as a size standard. Modified from (Avery and Shtonda, 2003).

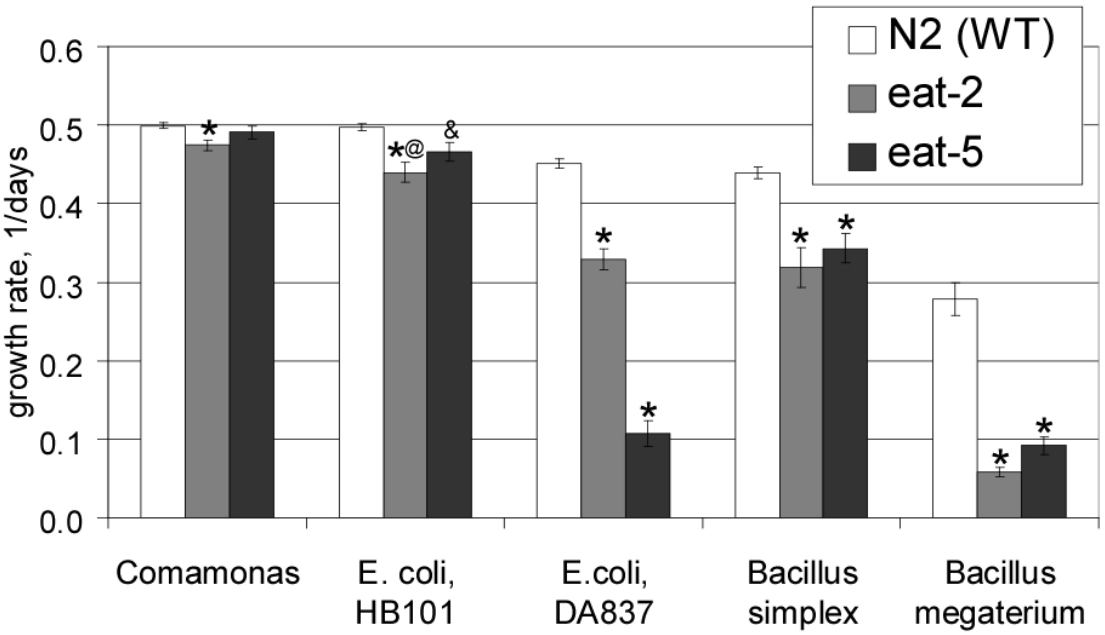

Figure 14. **Varying ability of different bacterial species to support *C.elegans* growth—a refined experiment.** Five bacterial species were selected from the experiment of Fig. 13 for more careful growth measurements. Here, a spontaneous sporulation-deficient variety of *Bacillus megaterium* was used, which was found to be worse food than the original *Bacillus megaterium* isolate. The original *B. megaterium* isolate produces sporulation mutants at rather high incidence, so the bacterial culture is heterogeneous. I used the sporulation mutant in this and all the rest of experiments because it grows to a homogeneous bacterial lawn. Each bar is the average of five data points, each of which is a different experiment done on different day; each experiment was done on two plates. In cases of large variability between individual worms (*eat-5* on DA837, *eat-2* on *Bacillus megaterium*, and *eat-5* on *Bacillus megaterium*) the growth rates were measured on single worms, one per plate (41,45, 43 worms respectively). Mean ± SEM. * $p < 0.001$, significantly different from the WT on the same bacteria. @ $p = 0.022$, different from *eat-2* on *Comamonas sp*. & $p = 0.036$, barely different from WT on HB101. All statistical testing by Student's T-test.

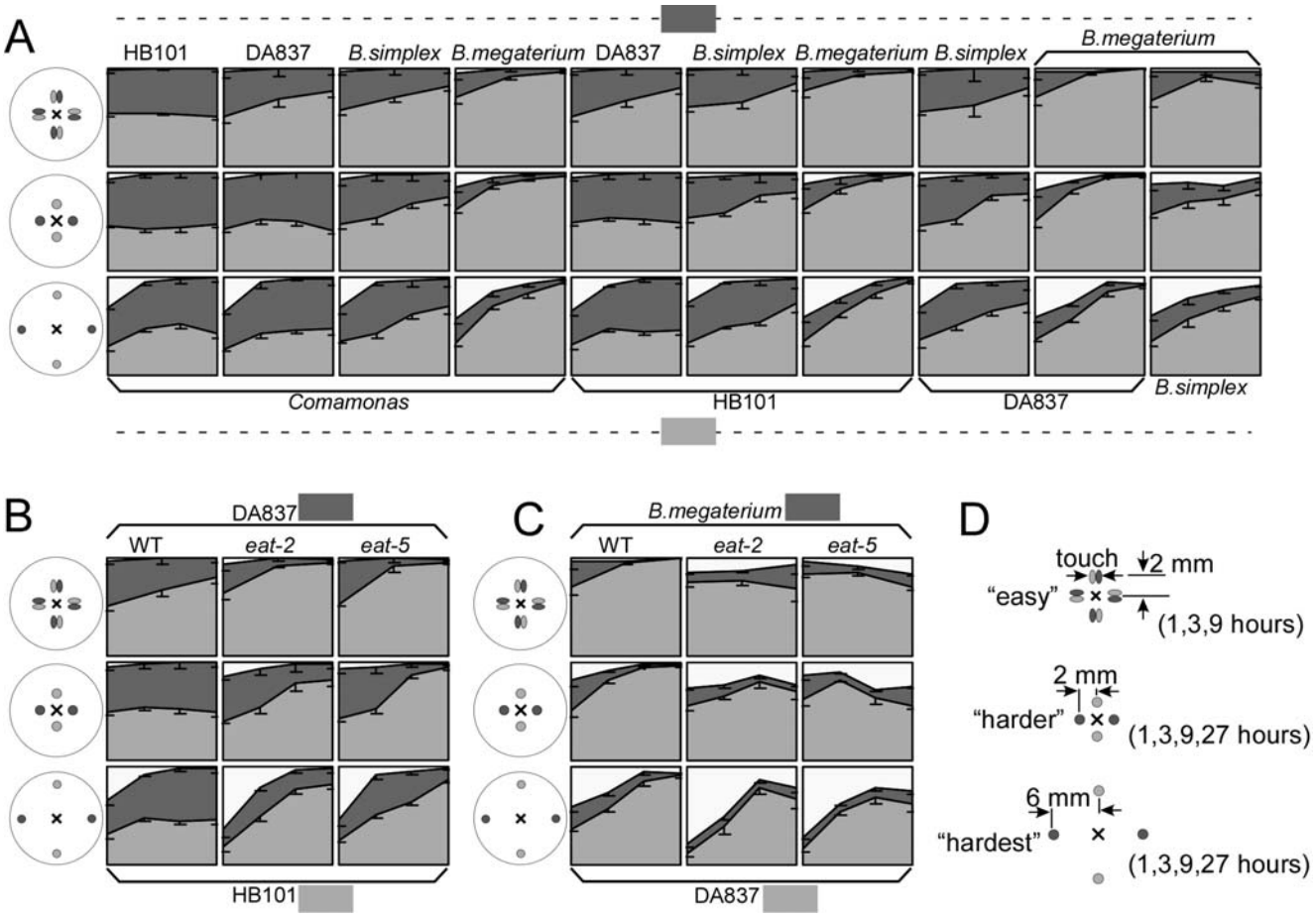

Figure 15. **Food choice behavior of L1 larvae. (A)** Wild-type food choice. There are 3 arrangements of bacterial food, detailed in D. Each square represents a time course of the food choice between two bacterial species. At given time points the number of worms in each food and outside of any bacteria was counted. Light gray and dark gray areas depict the fraction of worms in each food; bacteria are labeled correspondingly beneath and above the panels. White area shows worms found outside of bacteria. In almost all cases where food choice develops, it is in favor of the bacteria that better support growth. An exception is a rather weak preference for DA837 over *Bacillus simplex*, which does not seem to correlate well with the growth rate. **(B)** Food choice of *eat* mutants, *eat-2* and *eat-5* between two *Escherichia coli* strains, HB101 and DA837. In all arrangements of bacteria, the food choice of *eat* mutants for the better food HB101 is more robust than that of the wild type, consistent with DA837 being far worse food for both *eat* mutants. **(C)** Food choice of *eat* mutants between DA837 and *Bacillus megaterium*. While the wild type shows clear preference for DA837, the choice of *eat* mutants is not as strong, and does not show a distinct trend in the "easy" and the "harder" arrangements, consistent with both DA837 and *B.megaterium* being bad foods for *eat* mutants.**(D)** Three arrangements of bacteria used in food choice experiments. In the "easy" arrangement, colonies of different food touch each other (upper row), in the "harder" arrangement they are separate and 2 mm from the center of the plate (middle row), and in the "hardest" arrangement they are separate and 6 mm from the center (bottom row). At time point 0, worms were placed in the center of the plate at equal distance from the bacterial colonies (shown with "x"). The time points at which worms were killed and counted are shown on the right. N=5 (each data point is a plate, on which a distribution of 70-150 worms was measured); mean ± SEM.

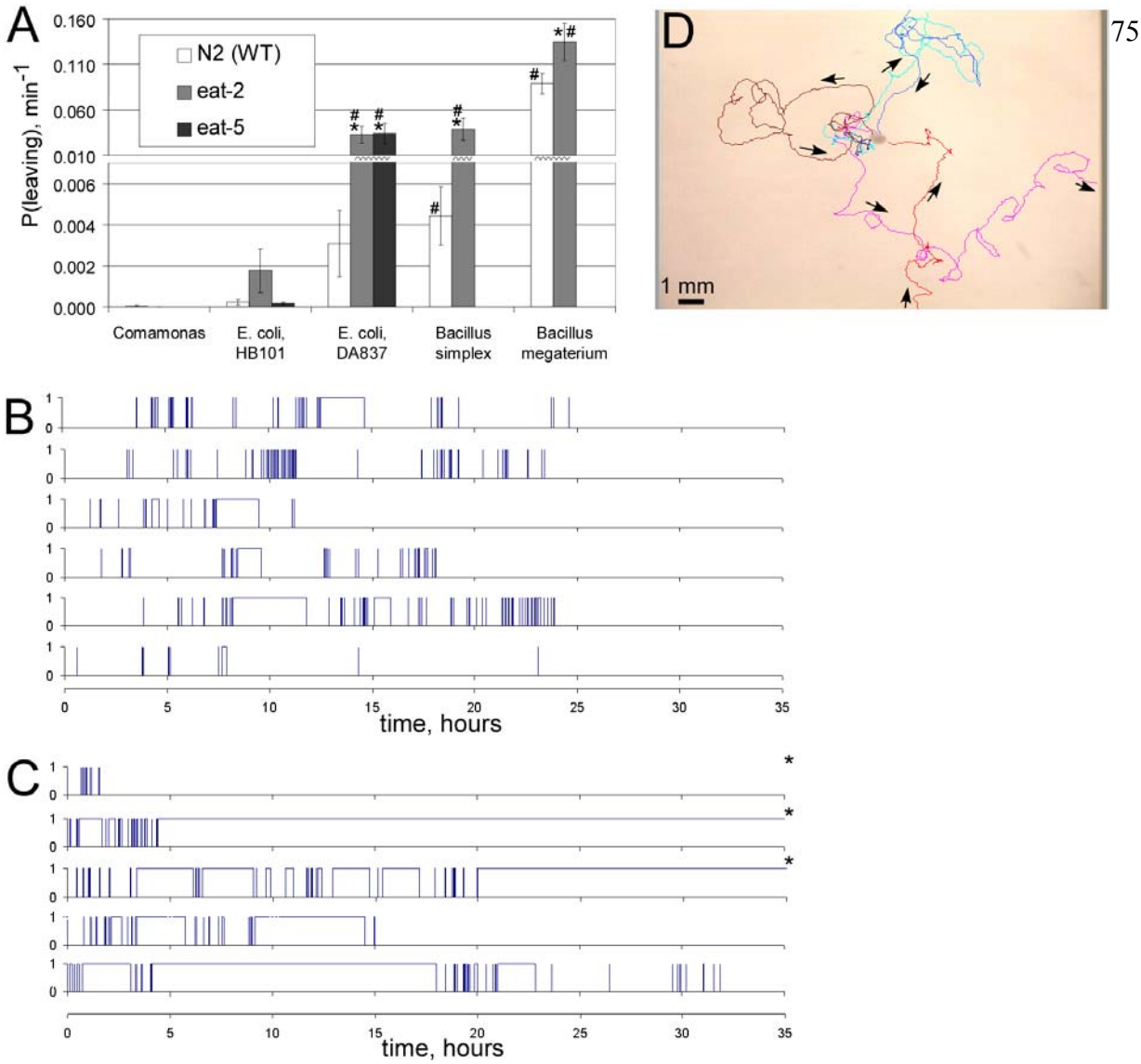

Figure 16. **Leaving behavior of L1 larvae. (A)** Leaving frequency of the wild type and two *eat* mutants, *eat-2* and *eat-5* (on *E.coli* foods only), in a population leaving assay. Worms were placed near the small chunk of bacteria and allowed to enter it; the time when the first worm entered the colony was time 0. The plot shows average leaving frequency between 1 and 2 hours after the start. On poor quality food, leaving is more active. On bad food, leaving behavior of *eat-2* and *eat-5* is more active than that of the wild type. N = 8; mean±SEM. * $p < 0.05$, different from the WT on the same bacteria. # $p<0.02$, different from P(leaving) of the same worm strain on good food, HB101 and *Comamonas*. All comparisons are by *t*-test. **(B)** Leaving behavior of 6 individual worms, *eat-2* on a small colony of DA837. A late stage egg was placed near the colony. Time 0 is when the hatched larva first entered the colony. On the Y axis, 0 corresponds to time spent in bacteria, 1 corresponds to time spent outside bacteria. **(C)** Leaving behavior of 5 individual wild type worms on *Bacillus megaterium.* Three out of five worms at some point left the colony and never returned within 40 hours (*) **(D)** Sample leaving trajectories of an individual worm, wild type on *Bacillus megaterium*. The width of the field of view is 18 mm in this experiment.

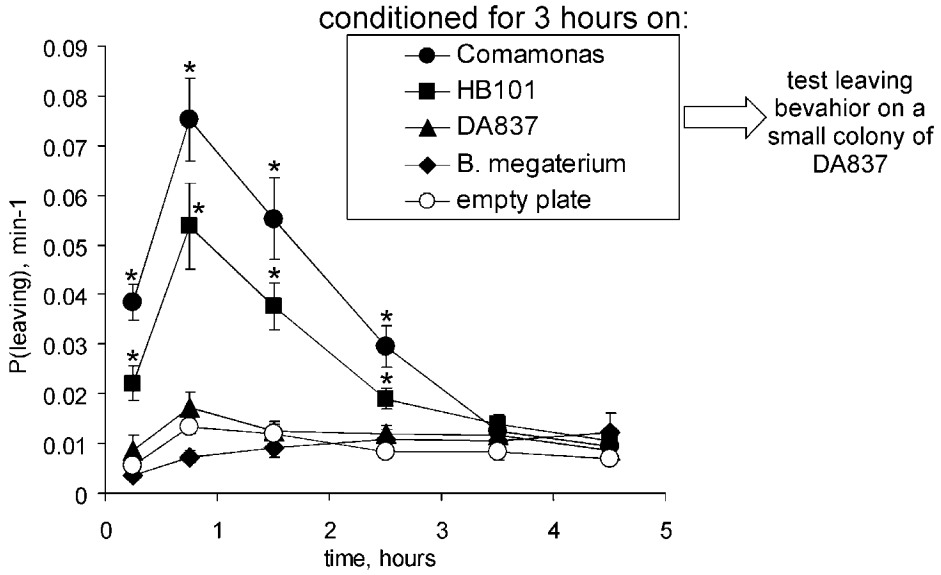

Figure 17. **Effect of food experience on leaving behavior.** Naïve *eat-2* L1 larvae were conditioned in one of the five indicated conditions for 3 hours. They were then washed and transferred to another plate for a leaving assay. The time when the first worm entered the colony is time point 0. The X axis shows the time intervals within which leaving probability was determined: 0 to 30 min, 30 min to 1 hour, 1 to 2 hours, and then in one hour increments. After exposure to high quality food, *Comamonas* or HB101, leaving behavior is increased as compared to conditioning on the same, worse food or without food (empty plate). Mean±SEM. * $p < 0.02$ by T-test, different from worms conditioned in any of the other conditions.

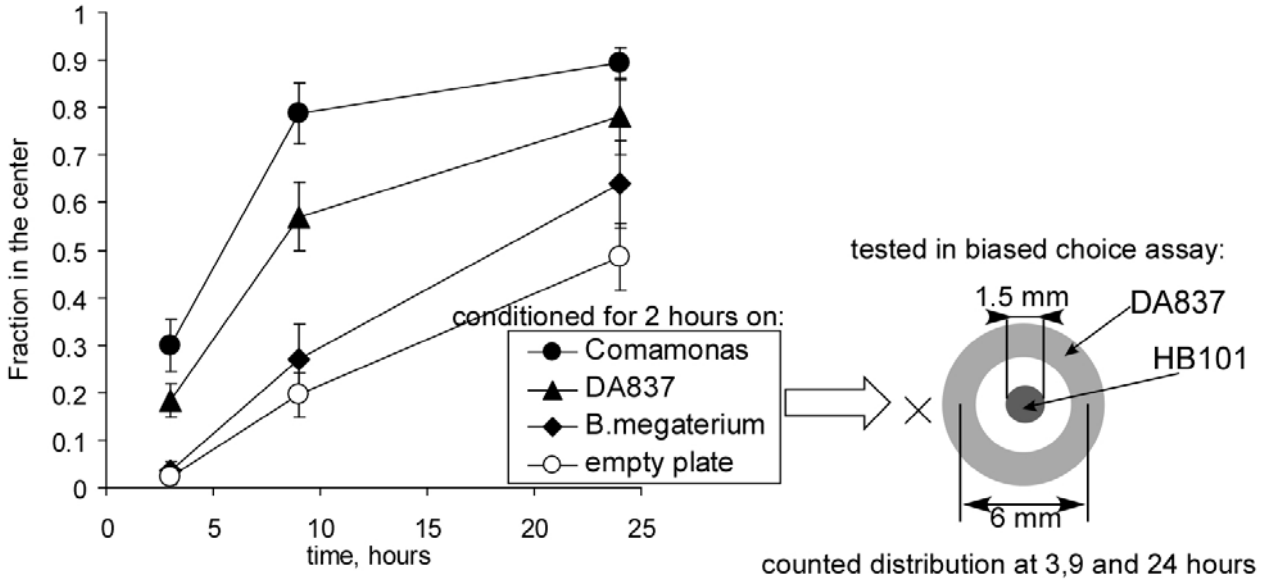

Figure 18. **Effect of experience on the food choice in biased (circle) choice assay.** Wild type larvae were exposed to one of the listed conditions for 2 hours and then tested in a choice assay with a circle of DA837 surrounding a central colony of HB101. At the start, all worms have to enter the circle, but with time, a fraction of worms cross the circle and locate the good food in the center (Y axis). Worms that have experienced the high quality food, *Comamonas*, show the most robust food choice, similarly to the effect of experiencing good food on leaving behavior. In this assay, however, worms conditioned on food mediocre for the wild type, DA837 and even bad food, *B.megaterium*, perform better that the ones conditioned without food. Mean±SD; n = 20 (10 plates with 2 circle assays on each). At all time points groups conditioned on food are different from the empty plate control ($P<0.01$, Student's *t*-test).

On the right is a schematic of the arrangement of bacteria in the biased choice assay. At time point 0, worms were placed outside of the circle, as shown by the "X". At indicated times, worms were killed by chloroform vapors and their distribution was counted.

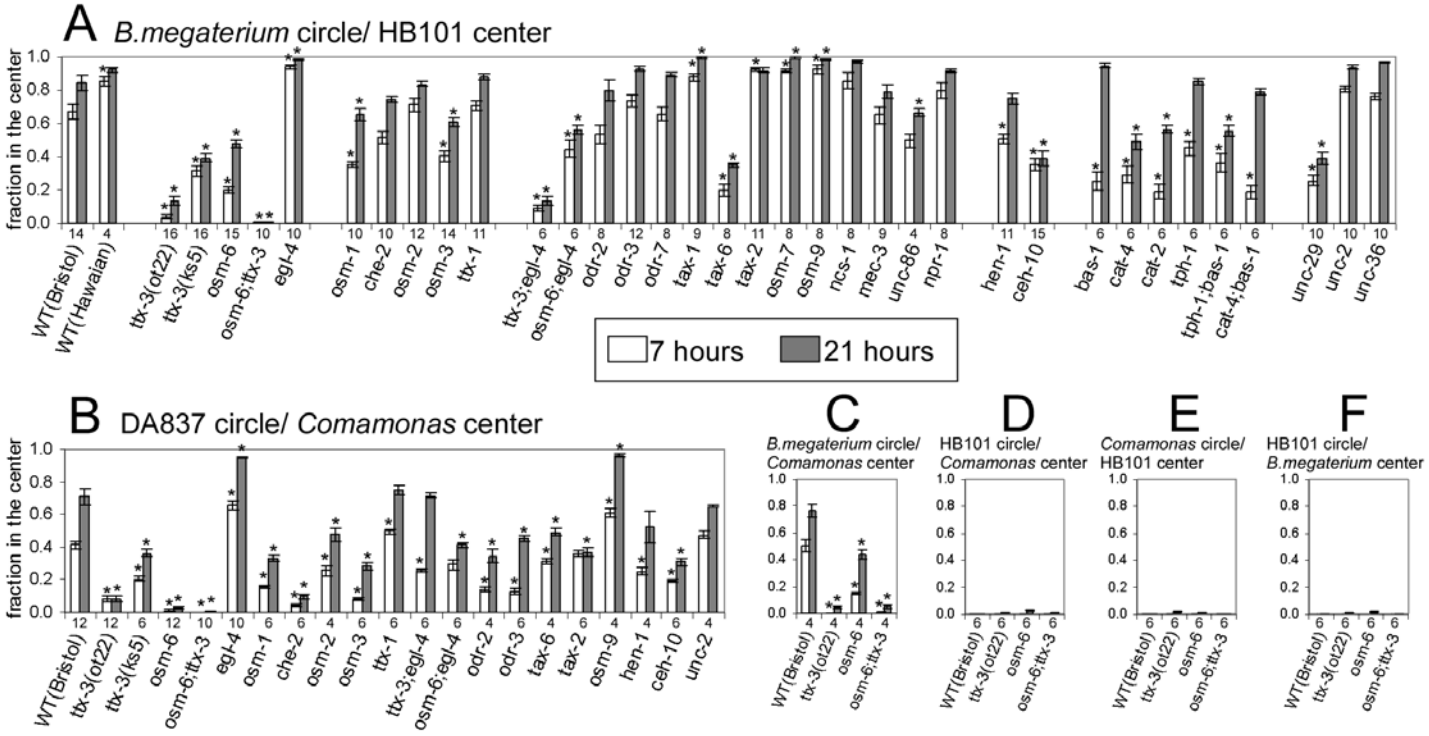

Figure 19 **Circle (biased) food preference assay. (A)** Choice between bad food, *B.megaterium*, shaped in a circle, and good food, *E.coli* HB101, located in the center of that circle. A number of candidate mutants were tested. The arrangement of two types of bacteria, one surrounding another (Fig.18), is such that all worms have to first enter the circle, thus their food choice is biased. With time, however, a fraction of worms re-distributes to the center. Mutants are described in Table 1 of the Appendix. The distribution of worms was counted after 7 and 21 hours. **(B)** Biased choice assay with DA837 circle and *Comamonas* center. By 21 hours, about 75% of the wild type worms are found in the center. **(C)** Same assay with *B.megaterium* circle and *Comamonas* center. Robust preference is still obvious. **(D)** and **(E)** When either of the good foods, HB101 or *Comamonas*, is located in the circle and another good food is in the center, almost all worms stay in the circle, which is the food they encountered first. **(F)** If a circle of good food, HB101, surrounds the colony of bad food, *B.megaterium*, worms stay in the circle of good food.

All results are shown as mean ± SEM. Numbers beneath the bars indicate N, with every data point being a single circle assay; two assays were done on each plate. *Different from the wild type, P<0.01 (Student's *t*-test).

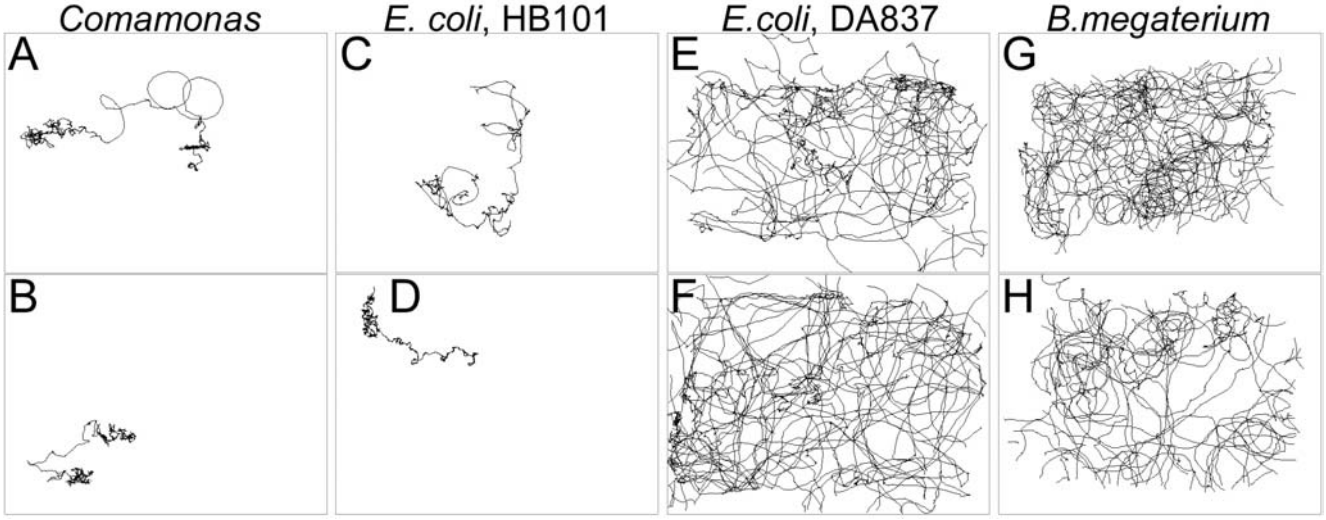

Figure 20. **Sample trajectories of wild type L1 larvae on different bacterial food sources. (A)**, **(B)**: on *Comamonas*, **(C)**, **(D)**: on *E.coli* HB101, **(E)**, **(F)**: on *E.coli* DA837 and **(G)**, **(H)**: on *Bacillus megaterium.* A single larva was placed on a roughly rectangular bacterial lawn, and its movement trajectory during the subsequent 10 hours was recorded. The width of the field of view is approximately 10.3 mm; the bacterial lawn fits into the video field. The trajectory on *B.megaterium* is fragmented due to poor contrast; this problem is most severe at the edges where bacteria tend to be the thickest.

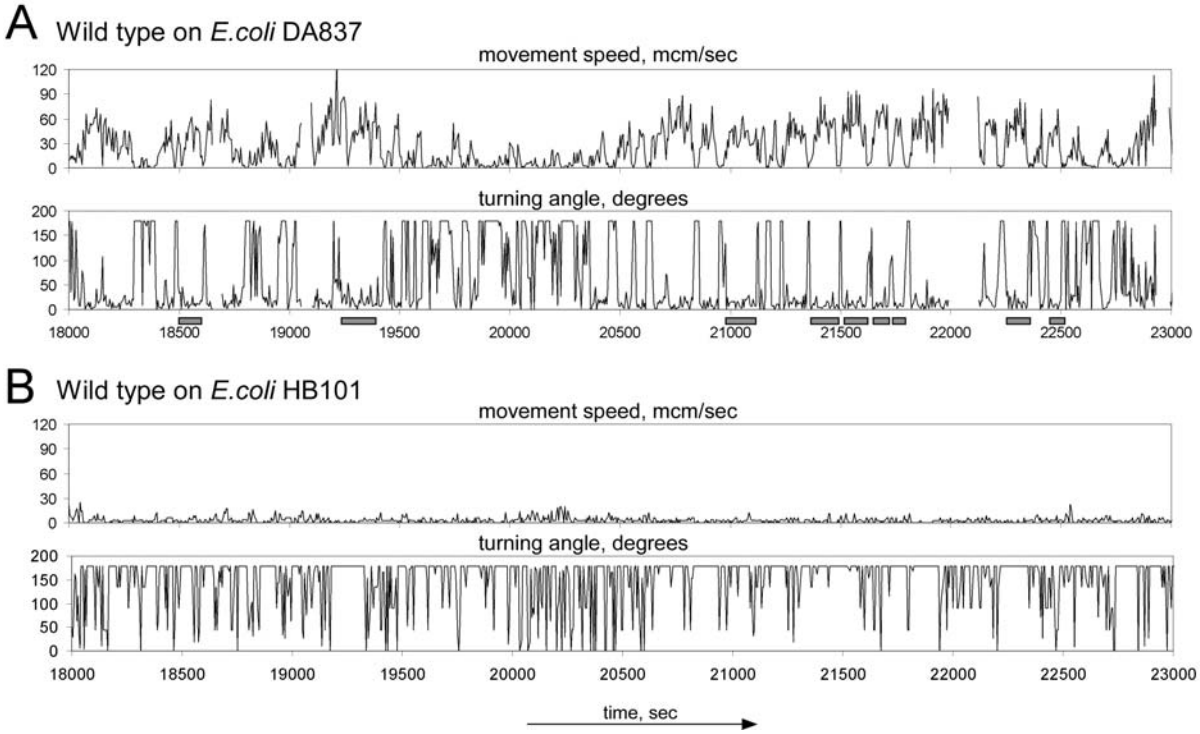

Figure 21. **Sample locomotion speed and turning angle traces. (A)** Sample speed of locomotion and turning angle (direction of movement change) traces of the wild type on *E.coli* DA837. Gray bars indicate periods of rapid straight movement, called running or roaming, when the turning angle stays low and the speed is high (not all running periods in this recording are marked this way). **(B)** Same as A on HB101. Running periods are common on mediocre food, DA837, but very rare on good food, HB101. All traces are time-locked; a 5000 second segment is shown.

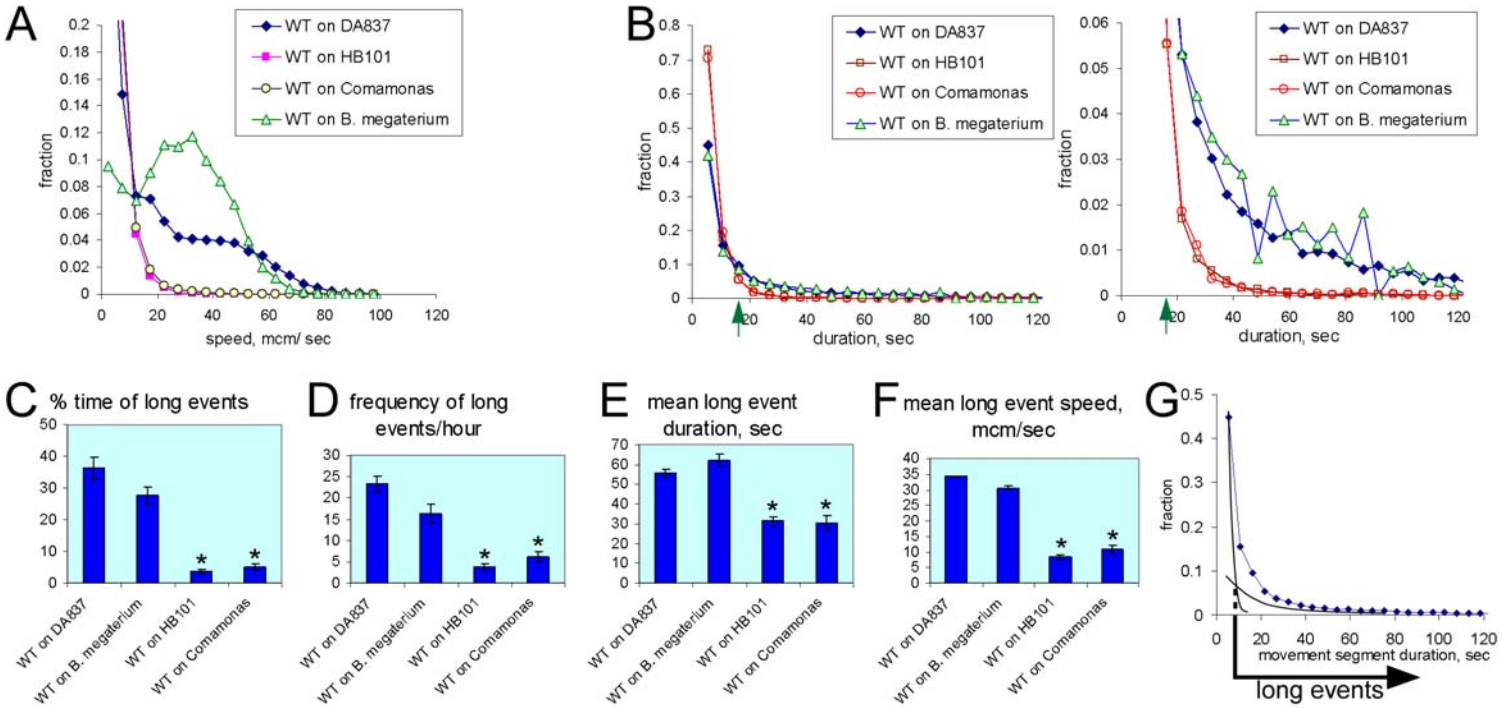

Figure 22. **Analysis of the wild type locomotion on different food sources. (A)** Speed of movement histogram of the wild type on different food sources. **(B)** Duration of movement histogram. The green arrow indicates the movement duration threshold obtained by the fitting method (panel G) for the wild type on DA837. This threshold was used in subsequent analysis. On the right, the same histogram is shown with the Y-axis expanded. **(C)** The fraction of time spent in long movements, relative to the total time of the recording. **(D)** Frequency of long movements on different foods **(E)** Average duration of long movements. **(F)** The average speed of locomotion during the long movements. **(G)** Schematic of the thresholding technique (Pierce-Shimomura et al., 1999). The duration of movement histogram is fit with the sum of two exponentials. The point of their intersection is the threshold duration. Movements above this threshold are counted as long movements, or "runs" and are thought to represent roaming mode of locomotion. For analysis, traces from 2 to 10 hours starting from placing an L1 larva on bacterial lawn were used. *Ddifferent from both mediocre foods (DA837 and *B.megaterium*), $P < 0.02$ (Student's *t*-test).

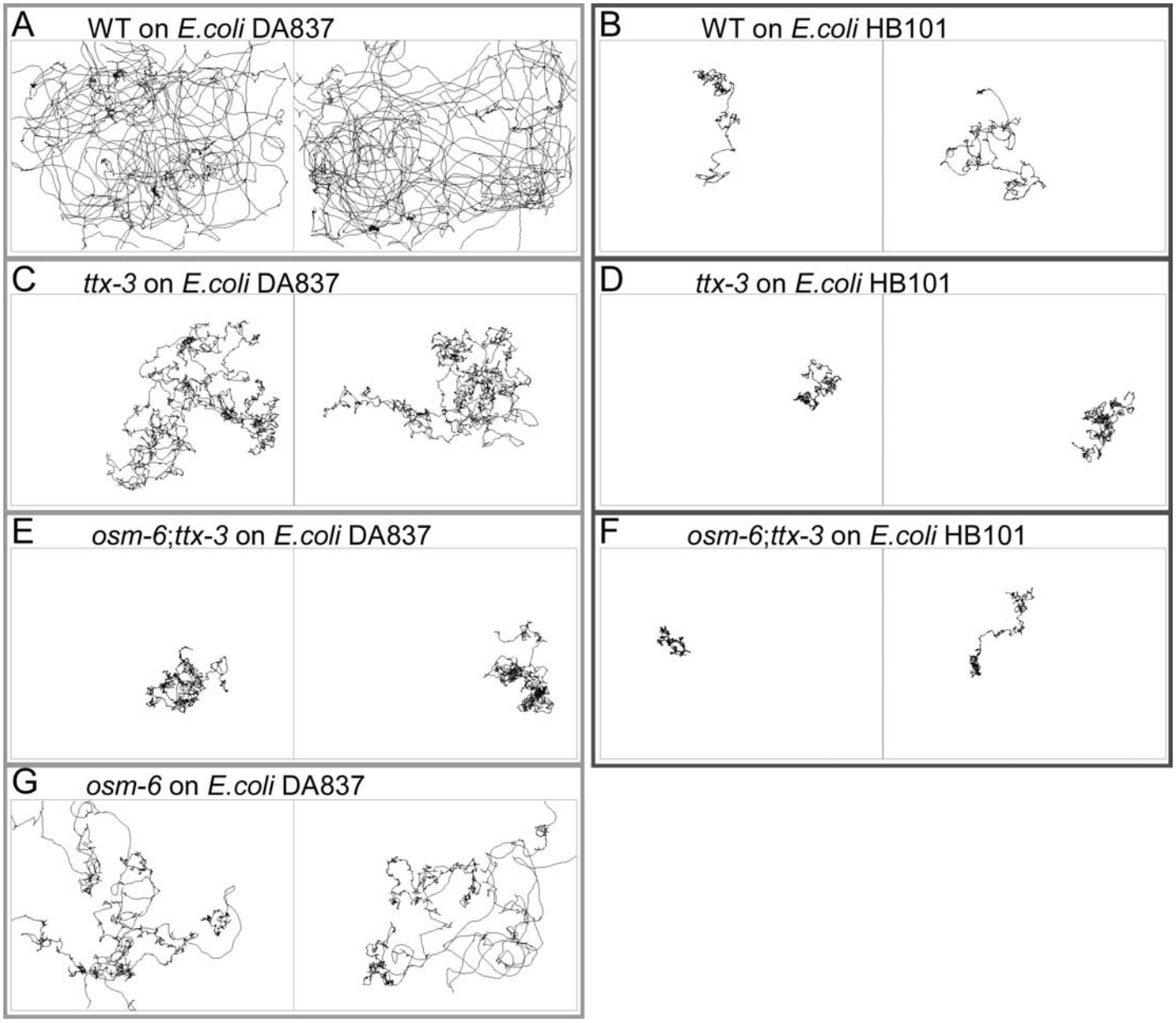

Figure 23. **Trajectories of the wild type, *ttx-3*, *osm-6*, and *osm-6*; *ttx-3* mutants on two *Escherichia coli* foods, DA837 and HB101.** Experimental conditions are the same as in Fig. 20. Mutants and bacterial food are as labeled; 2 representative worms are shown for each combination. Traces were recorded for 10 hours. **(A)** and **(B)** The wild type shows a robust food-dependent regulation of locomotion. **(C)** and **(D)** *ttx-3* mutant trajectories do not span the whole lawn on DA837; there are far fewer long straight roaming events. On good food HB101, the trajectory is more compact than on DA837, so although food-dependent regulation is still present, it is not as strong as in the wild type. **(E)** and **(F)** The *osm-6*; *ttx-3* double mutant is very deficient in food choice (Fig. 19), and, consistent with that, its locomotion is only weakly affected by food type. On both foods, trajectories are very compact; almost no straight long movements are observed. **(G)** *osm-6* mutant on DA837. Roaming events are not initiated as frequently as in the wild type.

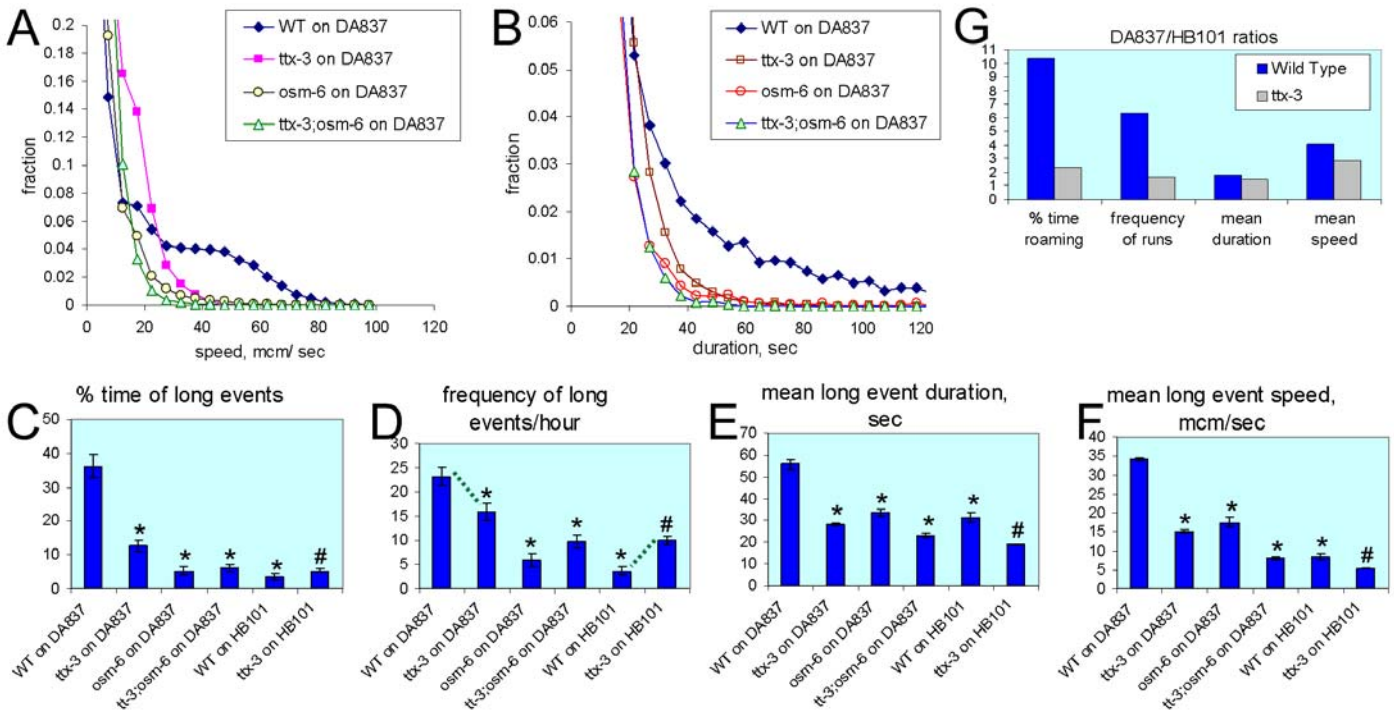

Figure 24. **Locomotion analysis of *ttx-3*, *osm-6*, and *osm-6*; *ttx-3* mutants. (A)** Movement speed histogram of the wild type and mutants. **(B)** Duration of movement histogram for the same strains. In *ttx-3*, *osm-6*, and *osm-6; ttx-3* the population of long movements is greatly diminished. **(C)** The fraction of total time spent in long movements. In mutants, the fraction of the time spent roaming on DA837 is greatly decreased compared to the wild type. **(D)** Frequency of long movements. Note that in *ttx-3*, not only is the frequency of long events lower on DA837, it is also higher on HB101 than in the wild type on the same food. Dashed lines show this. **(E)** Average duration of long movements. In *ttx-3* it is decreased by about 2 fold. **(F)** The average speed of locomotion during long movements. **(G)** Ratios of the long event parameters on the mediocre food DA837 to the good food, HB101. The food quality-dependent regulation of roaming is shallower in *ttx-3* compared to the wild type.

The movement duration threshold derived from the wild type on DA837 (same as in Fig. 22) was used for C through F. *Different from the WT on DA837, $P < 0.02$ by Student's *t* test. #Different from the WT on HB101, $P<0.02$.

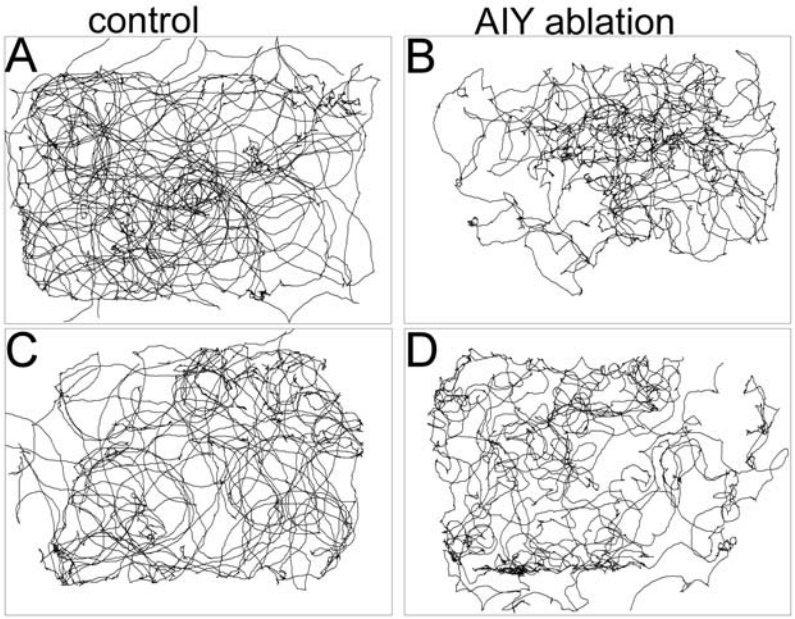

Figure 25. **Trajectories of AIY ablated and control larvae on *E.coli* DA837. (A)** and **(C)**: mock operated controls. **(B)** and **(D)**: AIY ablated animals. Trajectories of AIY- worms have fewer straight long movements than controls. Ablations were done on L1 larvae within 1 hour after hatching. After a 2-hour recovery, the worm's behavior on DA837 was recorded. The recordings are about 10 hours long.

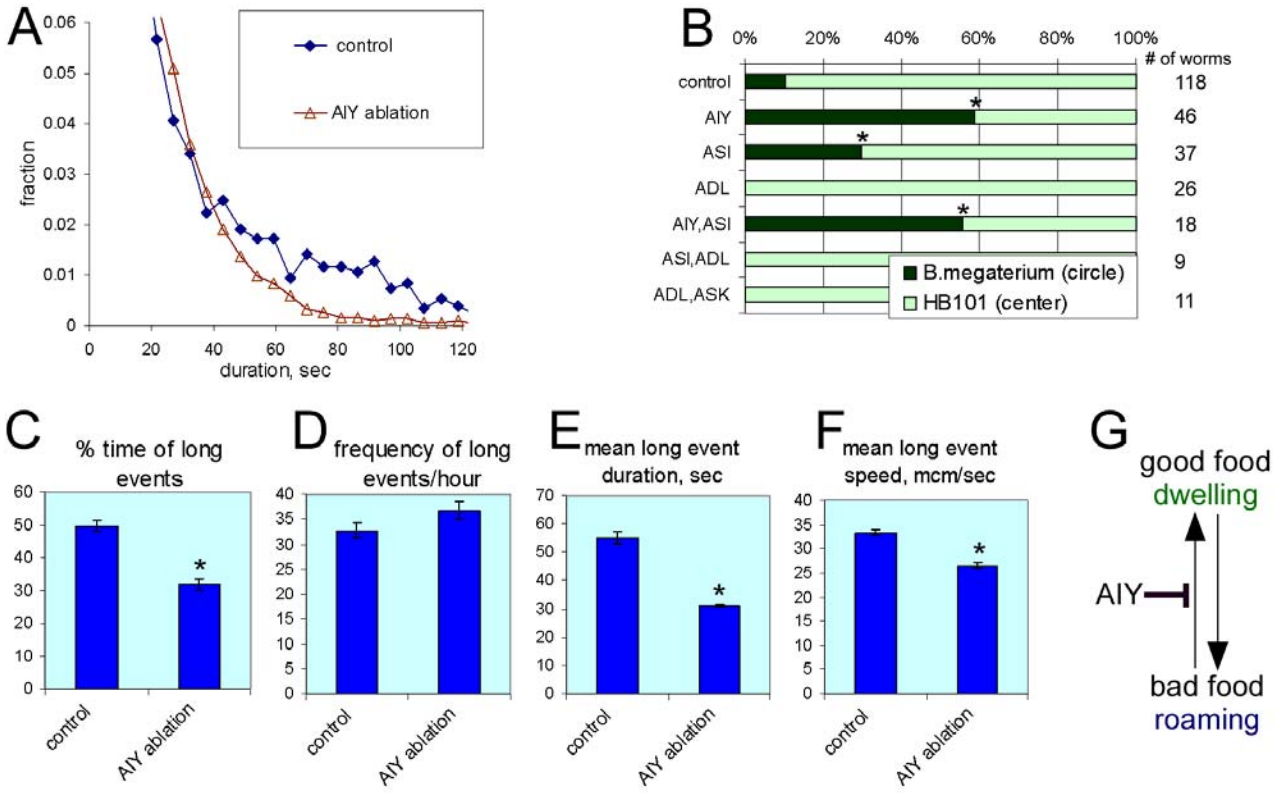

Figure 26. **Locomotion analysis of AIY ablated worms on *E.coli* DA837. (A)** Movement duration histogram for animals after AIY and mock ablation. **(B)** Behavior in a circle food preference assay after laser ablation of some amphid neurons. *Different from the mock-ablated controls, $P < 0.005$ chi-squared test of independence. Distribution was determined 20 hours after the start of the experiment. **(C)** The fraction of total time spent in long movements. **(D)** Frequency of long movements. **(E)** Average duration of long movements. **(F)** The average speed of locomotion during long movements. The movement duration threshold used for C through F was derived from analysis of the mock operated animals. *Different from control, $P < 0.02$, ` test. **(G)** A model for the role of AIY in the control of food-dependent locomotion. Ablation of the AIY neurons results in decreased duration of "runs". Thus, AIY may inhibit the switch from the roaming to the dwelling mode of locomotion.

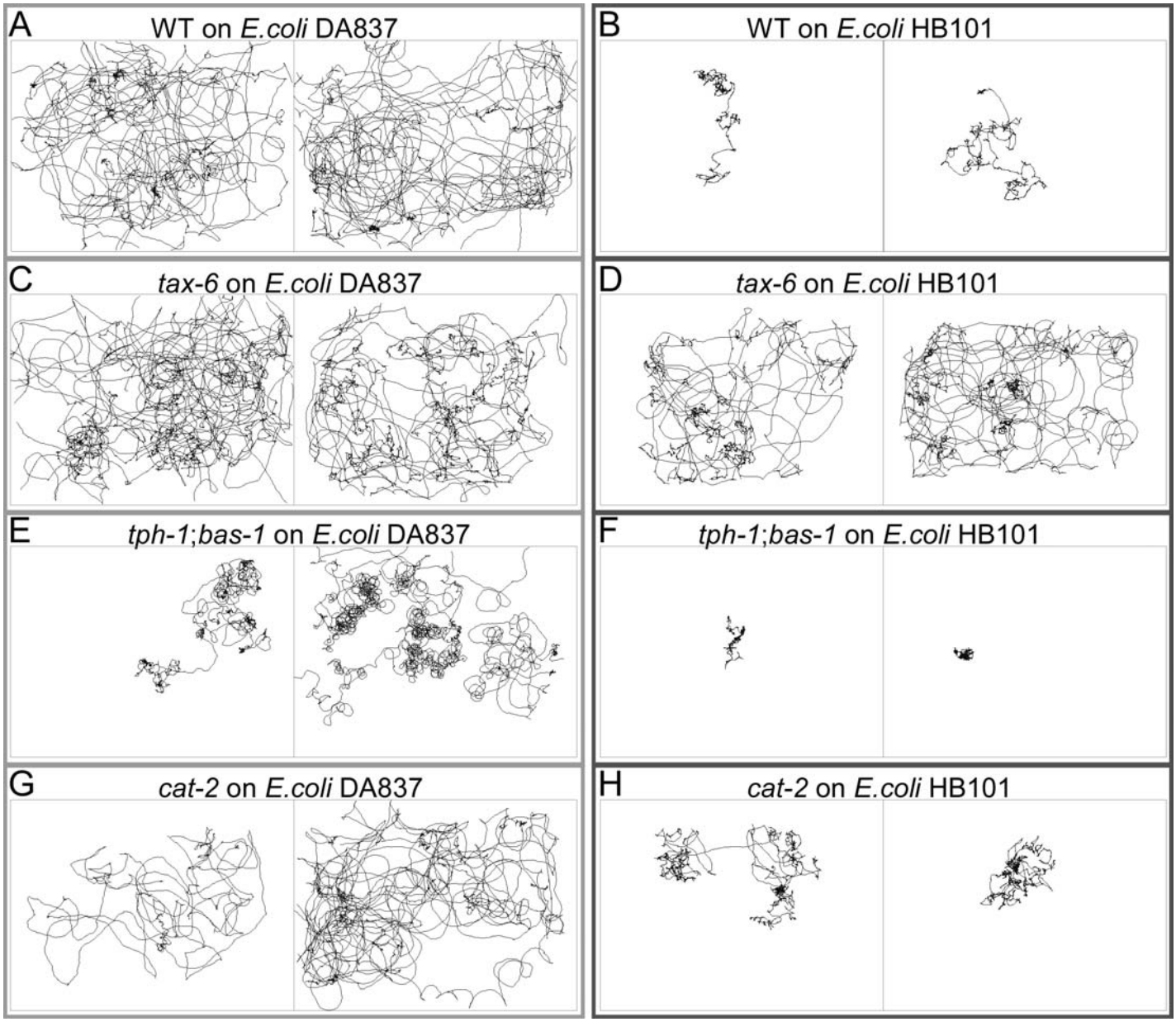

Figure 27. **Trajectories of the wild type, *tax-6*, *tph-1;bas-1*; and *cat-2* mutants on two *Escherichia coli* foods, DA837 and HB101.** Experimental conditions are the same as in Fig. 20. Mutants and bacterial food are as labeled; 2 representative worms are shown for each combination. Traces were recorded for 10 hours. **(A)** and **(B)** The wild type shows a robust food-dependent regulation of locomotion. **(C)** and **(D)** In *tax-6* mutants roaming on good food, HB101, is elevated. **(E)** and **(F)** The *tph-1;bas-1* double mutant shows a food-dependent regulation of locomotion, but the movement is somewhat uncoordinated, animals tend to move in circles. This may explain a food-preference defect of *tph-1;bas-1* (Fig. 19). **(G)** and **(H)** *cat-2* mutant exhibits nearly normal food-dependent regulation of locomotion. Roaming on DA837 might be slightly less active than in the WT.

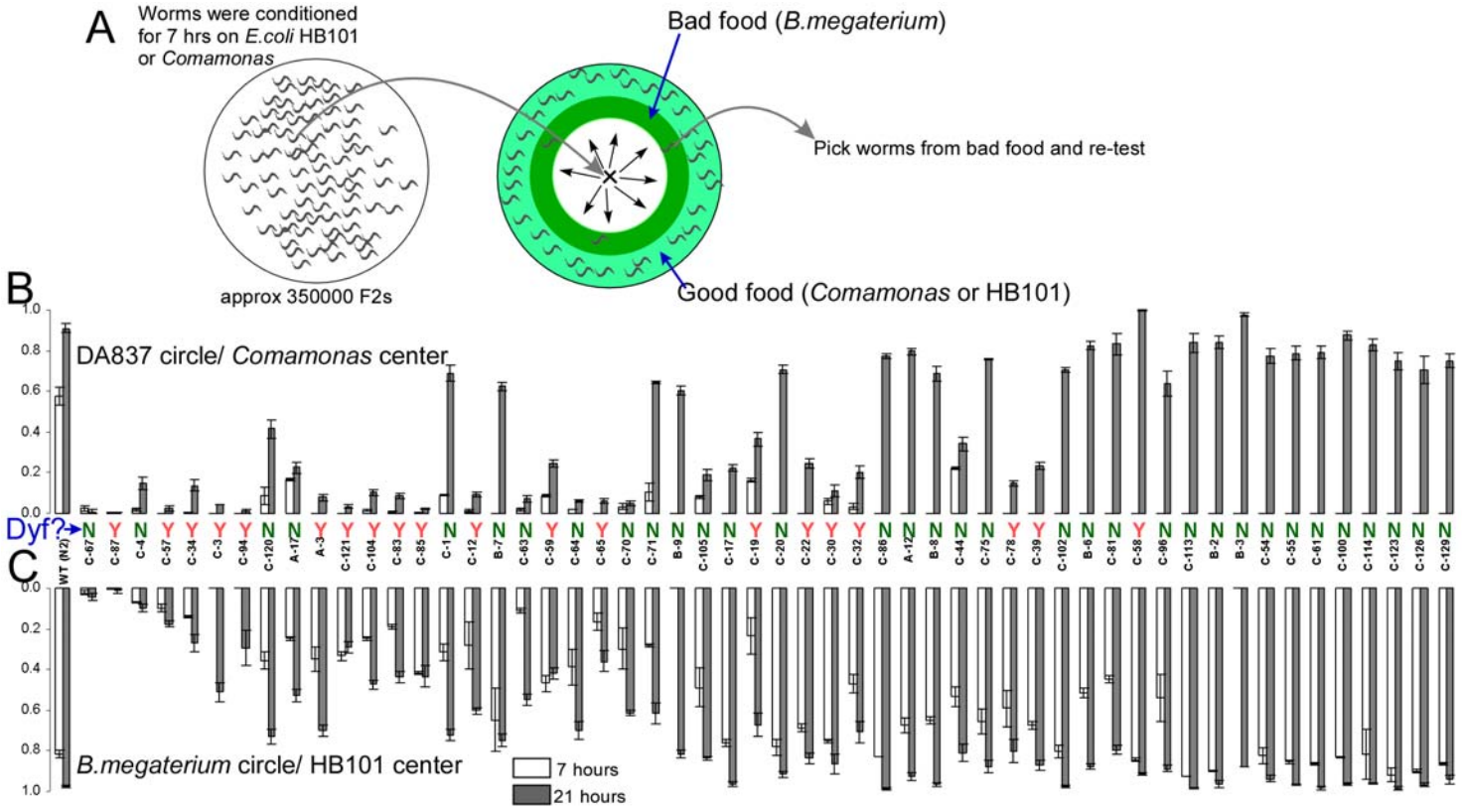

Figure 28. **An attempt to screen for worms defective in food choice. (A)** Schematics of the screen. Wild type (N2) worms were mutagenized with EMS. Approximately 350000 F2s, a progeny of 3600000 F1s, were conditioned on high quality food for 7 hours, and tested for the food choice on a plate with bacterial food arranged as shown. Worms that fail to select good food in this assay were collected, pooled and run though this selection again in some experiments. 1-3 rounds of selection were done. Finally, candidate mutant strains were established. **(B)** and **(C)** Re-testing of the candidate mutants in bFPA assay with DA837circle/*Comamonas* center (B) and *B.megaterium* circle/ HB101 center (C). Setup of an experiment in the same as in fig. 19. To check if sensory amphid neurons have gross anatomical defects in the mutants, DiO staining was performed. Failure to absorb the DiO fluorescent dye is a Dyf phenotype, and this is shown between panels B and C. "Y" and "N" above each mutant strain name indicated complete failure to stain (Dyf) and at least some amphid staining, respectively.

3.3. Food preference behavior.

As described in the introduction, one of the important roles of neural circuits involved in feeding behavior is to enable an animal to select the best food in the environment. Mammals do exhibit food choice, which is modulated by current metabolic needs, sensory stimulation and nutrients that the food provides, previous experience, and social factors. When other variables are kept equal, mammals choose the food that is more nutritive and better fits metabolic needs of normal growth (Osborne and Mendel, 1918; Ramirez, 1996), suggesting that the food provides feedback that drives behavior.

With the set of foods varying in their ability to support *C.elegans* growth, I tested whether worms exhibit food choice behavior. In the experiment shown in Fig. 15A, wild type worms were given a choice between two types of bacteria. Every effort was made to keep other variables equal: the colonies were equally accessible to the worms and of similar size. One variable that cannot be controlled is soluble and volatile compounds secreted by bacteria. It is known that different bacteria vary in their "chemoattractiveness" to *C.elegans* (Andrew and Nicholas, 1976; Grewal and Wright, 1992), so if chemo- and odor attraction is the main determinant of the food choice, we expect to see food preferences that do not correlate with the food quality. The result, however, is the opposite: in 9 out of 10 tested pairs worms choose the better food, the one that better supports growth. The exception is a weak preference for *E.coli* DA837 in the DA837/*B.simplex* pair. On the growth rate chart, these strains are the same for the wild type (Fig. 14). In other cases when there is no

difference in growth rate on 2 different bacteria, the choice is hardly detectable (such as *Comamonas* vs. HB101). And, it is fair to say that in all cases when there is a difference in the food quality, worms choose the food that better supports growth. For example, for wild type worms *B.megaterium* is the worst food, and the preference against *B.megaterium* is particularly strong, whatever the other food is.

I used three varieties of food arrangement in this assay (Fig. 15D). By varying the distance between foods, the sensitivity of the assay can be adjusted. Making the choice between foods should be easier is less effort is needed, that is, if two foods are located close to each other. Indeed, in the "easy" configuration, when two foods are located very close to each other (so close that it is enough for an animal to stick out its head to get into another colony) the choice is stronger: for example, there is a weak preference for *Comamonas* and HB101 when the other choice is *E.coli* DA837 (Fig. 15A). In the "harder" and "hardest" arrangements, no choice is seen between these foods, which lie close in the growth rate range for the wild type.

One of the interesting observations from these experiments is that food preference shows a time trend, suggesting that worms need to try the food to make a decision. This is similar to observations on rats, which show that animals taste both foods before making a choice, and the preference also exhibits a trend (Young, 1933; Young, 1941). Young (Young, 1933) has proposed that preference "curves show a learning to like or learning to dislike dependent not upon immediate sensory cues but rather upon some bodily after-effect". If an innate preference for the smell of particular bacteria were the main guidance cue in food choice, we would expect animals to migrate to the better-smelling bacteria from

the start. The fraction of worms outside of bacteria would decrease, but the ratio of worm numbers in one food to another would not change with time. That this ratio changes suggests that animals that have initially entered less preferred food at some point switch – they leave that colony and go to the other one. Except for male leaving behavior (Ghosh et al., 2003; Lipton et al., 2004), it was not known that worms can leave bacteria.

A most instructive result is the food choice of *eat* mutants, of which *eat-2* and *eat-5* were tested. Given a choice of two *E.coli* strains, DA837 and HB101, both of these mutants show a much stronger food preference than the wild type (Fig. 15B). For example, in the "harder" and "hardest" arrangements, the wild type does not show a preference, while both *eat* mutants do show a robust, about 90% preference. It is very unlikely that *C.elegans* has evolved an ability to discriminate between human-engineered *E.coli* strains by their smell. Even if this were true, it would not explain why mutants show a stronger preference for the high quality food than the wild type. Of course, it is theoretically possible that both of these mutations have the same effect on chemoattraction to bacteria, but very unlikely. The most viable explanation for this observation is that food consumption provides feedback that drives food choice. In *eat*s, the food consumption is changed and so is the food choice. They are feeding-limited and their behavior is adjusted so that they efficiently locate the high quality food.

Given a choice of mediocre (*E.coli* DA837) and bad (*B.megaterium*) foods, the behavior of *eats* is also different for the wild type, but in the other direction: their preference for DA837 in this pair is slightly less robust than the wild type's (Fig. 15C). The preference time course is shallower. This result is also consistent with the explanation that feeding

provides feedback. For the wild type, DA837 is the food that supports close-to-a-maximum growth rate, and *B.megaterium* is clearly very bad food. For *eats*, DA837 is mediocre or bad, especially for *eat-5*, and *B.megaterium* is very bad. Animals are confused by having to make a choice between bad and very bad, so the choice is not as robust. Note that with this pair of foods, the fraction of *eats* outside the bacteria stays very high throughout the experiment: a significant fraction of worms keeps searching; while with the wild type, it drops to almost 0 by 9 hours

One observation that seems counterintuitive is that *eat-5*, for which the growth rate is about the same on *E.coli* DA837 and *B.megaterium*, still chooses DA837 (Fig. 15C). One explanation would be that in addition to being hard-to-eat, *B.megaterium* is also repulsive. This is contradicted by the observation that in many pairs, equal numbers of worms enter *B.megaterium* and another food (this is most pronounced in the "hardest" arrangement of foods, when the choice develops slower and not yet visible after 1 hour). So I favor a different explanation.

B.megaterium is probably hard-to-eat because the cells are big, so it does not even get into the pharynx well. In *eat-5*, the terminal bulb (the last compartment of the pharynx, see Fig. 2) contractions are slow and not in synchrony with the rest of the pharynx (Starich et al., 1996). That *eat-5* is so slow growing on DA837 suggests that DA837 is specifically incompatible with the slow and/or asynchronous terminal bulb. *eat-2* also pumps slowly, but the pharynx is synchronous. Therefore, it is likely that DA837 gets to the pharynx in *eat-5*, but does not get through the terminal bulb to the intestine well. For *eat-5*, DA837 and *B.megaterium* are similarly bad foods because they both do not get to the intestine well, but

the difference between them is that DA837 probably gets into the pharynx, while *B.megaterium* does not. So, both of these foods very poorly support *eat-5* growth, but DA837 provides better stimulation within the pharynx. It is known that the pharynx itself detects food: pharyngeal NSM neurons are required for the slowing response upon entering the bacterial lawn (Sawin et al., 2000).That is why *eat-5* still chooses DA837.

It is likely that at least two food-sensing mechanisms are interacting here: one at the level of the pharynx, another one at the level of the intestine. There is evidence that multiple mechanisms are involved in the regulation of behavior in response to food: for example, expression of about 100 genes is changed by at least 4 fold after 6-hour food deprivation (Jim McKay, personal communication).

These experiments have demonstrated that C.*elegans* can assess the food and choose the higher quality food in the environment. They have also shown that assessment of food required feeding, that is, most likely the food acts postingestively to regulate this behavior. Therefore, the action of food in this paradigm, as Young has proposed (Young, 1933) is "dependent not upon immediate sensory cues but rather upon some bodily after-effect".

3.4. Leaving behavior.

One of the immediate implications of the food choice experiments described above is that the worms leave poor quality food. This turns out to be true (Fig.16). Between 1 and 2 hours after first entering a bacterial colony, the wild type larvae leave *B.megaterium* with a probability of about 9% per minute. Leaving DA837 and *B.simplex* is much less active: 0.3 and 0.4 % min^{-1}, and leaving good foods, *Comamonas* and HB101, is undetectable. Consistent with the food choice experiments, leaving of *eat* mutants is more active: about 3.5% on DA837 and *B.simplex* and 13.5% on B.megaterium. This again suggests that feedback via food consumption drives food seeking behavior.

This leaving behavior is a stochastic all-or-none phenomenon (Fig. 16B, C). There is no stimulus causing every single event, and there are no directional gradients on the test plate. The pattern of leaving activity, observed in individual animals over a long time is interesting: most leaving events are very short and last just a few minutes, but very infrequently, worms undertake a long adventure that lasts for 2-5 hours. (In fact, in some experiments, a worm leaves food and never returns; it probably crawls off the plate and dries, see Fig. 16C). After 25 hours, leaving activity of *eat-2* on DA837 suddenly ceases.

Previously, it was thought that once *C.elegans* finds food, it stays there and eats until death or until the source is exhausted. Leaving experiments show another level of regulation: after the food is found, the animal may decide to stay in the food or leave, and this decision is based on the assessment whether the food is good or bad. Leaving behavior is a compromise:

on the one hand, it is a risk to lose the food that has already been found and get into adverse environment, on the other hand, there is a chance of finding even better food. Clearly, a mechanism must exist that controls this equilibrium between "taking risks" and "being cautious". And, as Fig. 16A and particularly the effect of *eat* mutations suggests, this equilibrium is regulated by feedback via food consumption.

Leaving behavior is similar to motivated food-seeking behaviors in other animals, such as, for example, lever pressing behavior in rats or biting in Aplysia: 1) It is stochastic; 2) It is inhibited by food consumption. Worms given good food leave less than the ones given poor food, similarly to the satiated rat doing less lever pressing than the food-deprived one. By the logic of Skinner (Skinner, 1938), who thought that "a rat does not always respond to food placed before it, and a factor called its 'hunger' is invoked", we can propose the existence of an internal state in *C.elegans*, analogous to the "hunger state" in mammals, that regulates this behavior. There are also differences between the worm leaving and rat lever-pressing behaviors: 1) the former is probably hard-wired and the latter is learned and 2) the latter may also be a goal seeking behavior, that is, a rat anticipates the reward. The first difference lies in the experimental setup—it is certainly possible to design a paradigm that tests the hard-wired rat behavior and it *might* be possible to design a worm paradigm that tests learned food-seeking behavior. The second difference is probably impossible to experimentally address with worms since anticipation is subjective; it is even hard to address in non-human mammals.

In my leaving assay, worms essentially change their natural attraction to bacteria, which allows them to find and enter the food colony in the first place, to avoidance, escape

behavior. Or, the exploratory drive temporarily takes over the attraction to initiate leaving. The described worm paradigm most similar to this phenomenon is probably an adaptation to a volatile or soluble attractant. Upon extended exposure to the odor (typically, 1 hour or more) in the absence of food, the odortaxis to this odor dwindles (Colbert and Bargmann, 1995; Colbert and Bargmann, 1997). Likewise, attraction to a soluble chemical switches to avoidance after 3-4 hour exposure (Saeki et al., 2001) in the absence of food. In view of my results, the adaptation phenomenon has a clear biological meaning: it is a weakening of a hunger-motivated food-seeking behavior because of the lack of reinforcement. The authors of two studies (Nuttley et al., 2002; Saeki et al., 2001) have already obtained evidence in support of this. (Nuttley et al., 2002) have proposed that "this learning may reflect a food-seeking behavior, where animals approach a source of benzaldehyde in search of food but leave the area if none is found". They have shown that in the presence of food, chemoattraction is suppressed (if I already found food, why bother?). Similarly, aerotaxis fades in the presence of food (Gray et al., 2004b). And, if animals are conditioned to the odor or taste *in the presence* of food, no adaptation occurs. More than that, if worms are adapted to the stimulus in the absence of food, but then briefly exposed to food, chemoattraction robustly revives (Nuttley et al., 2002; Saeki et al., 2001). Similarly, faded drug seeking behavior is greatly enhanced by the brief drug exposure—a well known phenomenon called reinstatement (Jaffe et al., 1989).

These considerations give rise to the following easily testable predictions: 1) worms *will* adapt (desensitize) to the odor/taste of *any* bacterial food in the absence of food, 2)

worms *will* adapt to the odor/taste of the poor food even in the presence of this food and 3) worms *will not* adapt to the odor/taste of good food in the presence of good food.

Also, it is interesting to test whether, during leaving events, worms actually avoid the smell or taste of the food they leave, and whether they are more sensitized and tend to follow the smell of novel bacteria they have not experienced previously. This can be done by pre-establishing a linear gradient of smell or taste of the corresponding bacteria, and testing whether worms tend to leave in the direction of this gradient or against it. The avoidance hypothesis can also be tested by ablating ASH and ADL neurons, known to be involved in avoidance response.

Certainly, a mechanism must exist to suppress the worms' hard-wired attraction to a stimulus unless it is supported by a reward; as well as to strengthen it when the reward is provided. The taxis behavior is quite useless by itself, unless there is a way to tell the animal whether it is *successful*, i.e., unless there is an error signal. The feedback that food provides is such a signal, and we have seen that in the case of worms, it is the ability of food to support growth, the food quality. With the set of foods that vary in the reinforcement they provide and with clever use of *C.elegans* genetics, this mechanism can potentially be dissected.

3.5. Effect of experience on leaving and food preference behaviors.

Here, I tested the effect of prior food experience on two behaviors: leaving behavior and food choice behavior.

Only hungry mammals, ones motivated to get food, show behaviors such as Pavlovian association of food with an unconditioned stimulus or food-seeking behavior. After eating a meal, food loses its attractiveness for hours*. If we extrapolate mammalian paradigms to worms, we would expect that well-fed worms would search for food less actively until they are starved and become motivated again. This is hard to test with worms, since there is no independent way of telling when the worm is hungry**. Only the behavioral output can be measured.

The effect of prior food experience on leaving behavior is shown in Fig. 17. The result is striking: worms that have experienced high quality food, such as *E.coli* HB101 or *Comamonas*, leave the mediocre food *E.coli* DA837 much more actively as compared to worms conditioned on the same food DA837, bad food *B.megaterium* or an empty plate. Here, *eat-2* is used instead of the wild type, because the wild type leaving frequency on DA837 is too low to be measured accurately (Fig. 16).

Let's assume that when the food is switched (time point 0), worms that have

*This is not a general rule for all mammals, however. Squirrels, for example will hide excessive food for the future. It is remarkable that in a satiated squirrel the food triggers a behavior completely different than in a hungry animal.

**With mammals, there is no such way either, unless they are humans. Mammalian paradigms measure hunger by food seeking and consumption. This is partially justified because of the periodic nature of feeding in mammals, but inapplicable to worms which feed continuously.

experienced good food are more “satiated”, or less “hungry”. If this experiment were done on mammals, we would expect that a satiated rat would search for the food less actively until gets hungry again. But worms, unlike mammals, feed continuously throughout life to support a 3-day life cycle and high rate of reproduction. It is likely that for worms, brief food deprivation or brief decline in food quality is a red flag. In view of this consideration, my result makes sense: within less than an hour, worms activate exploratory behavior, because a switch from good to bad food is an alert signal, possibly even before energy stores are exhausted. If a worm is taken off food, there is about half an hour period of area-restricted search, followed by active “running” (Hills et al., 2004). It is important for *C.elegans* to detect rapidly that the high quality food is gone and start exploring the environment. As Fig. 17 shows, experience of good food makes worm more “risk-loving”, more willing to explore environment.

A trivial explanation for this result is that well-fed worms are simply healthier and hence explore the environment more actively than unfed ones, which strive to save energy. This, however, cannot stand, since I have shown in Fig.16 that in fact under the *continuous* presence of good food, leaving is suppressed. Clearly, it is the *switch* from good to bad food that causes a dramatic increase in exploratory behavior.

At least two other explanations are possible. The first (and the simplest) explanation invokes two signals for sensing the food intake: one fast and one slow. The fast one is for detecting momentary feeding status: food intake, amount of food in the intestine, or nutrient influx from the intestine. The slow one signals replenishment of energy stores (e.g., fat stores). For example, eating well may release hormones that signal satiety, as happens in

mammals. If the fast signal is high, exploratory behavior is suppressed regardless of what the slow one is. If both signals are low, the exploratory behavior is activated. If the fast one is low, while the slow one is high, which corresponds to the sudden food-deprivation of a well-satiated animal, exploratory behavior is activated even further.

The second explanation is an extension of the first one, except that the slow signal (the satiety signal) is imprinted in the nervous system; it is a memory. This second explanation is supported by two considerations. First, it is known that worms can associate food with temperature and chemical stimuli, and this requires a neural circuit. Second is the time course of the effect: the enhancement of leaving is not high at the very beginning, but reaches a maximum after 0.5-1 hours. This indicates that time is needed to assess new conditions, followed by some kind of comparison. It is unlikely that this can be accomplished without the use of neurons.

It would also be interesting to test if after the exploratory response fades, exposure to the odor of a previously experienced good food causes a revival of leaving behavior, similarly to the reinstatement of the drug seeking behavior after brief drug exposure (Jaffe et al., 1989). This would prove that even after the enhanced leaving response is gone, worms still remember the smell of good food they have experienced in the past, therefore, it would provide evidence in support for the second, “learning” mechanism.

Next, I tested whether this increase in exploratory behavior after a switch from good-to-bad food actually helps worms to locate good food faster in the environment. (For worms which develop in 2 days, every hour is precious.) This experiment is shown in Fig. 18. The food choice assay here is different from the one described above (Fig.15). In the assay used

in Fig.15 the two foods are equally accessible, so that the range is from 0.5 (worms distribute equally) to 0 or 1 (all worms are in one type of food). In the food choice assay shown in Fig. 18, good food is surrounded by a circle of mediocre food, so that all worms have to enter the circle first. The fraction of worms that locate the central colony of good food is counted, so that the range of this assay is from 0 (no worms reach the center) to 1 (all worms reach the center). I call this assay a "biased" choice assay, since all animals are forced to experience one food first. This assay is also technically easier (see methods). It does not allow measurement of an unbiased discrimination between foods, but I have already shown in Fig.15 that the choice is made for the high quality food, so that's not necessary as long we have a control or wild type strain to compare with other conditions or mutants. This biased assay is similar to the "stimulus integration assay" (Ishihara et al., 2002), where an attractive stimulus is surrounded by circle of repellent.

I conditioned naïve L1s for 2 hours on good food (*Comamonas*), mediocre food (DA837), bad food (*B.megaterium*), or an empty plate, then tested food choice on a circle of DA837 surrounding an HB101 colony. This experiment was done with wild type *C.elegans*. The result is generally consistent with the effect on leaving behavior: the better the food during conditioning, the faster the animals locate good food during the test. At 9 hours, only about 20% of worms that have experienced an empty plate reach the center, whereas 80% of worms that have experienced *Comamonas* reach the HB101 center by this time. This four-fold improvement over nine hours is a huge competitive advantage on the worm time scale. Note that the high quality food during the test (HB101) is different from the good food used in conditioning (*Comamonas*), so it is not that the worms necessarily seek the same food, by

following the odor, for example. What happens is that their general exploratory activity is increased, so *any other* good food can be found faster.

In humans, powerful diet preferences can form, especially for nutritious fat- and carbohydrate-rich foods, such as chocolate, ice cream, desserts, pizza, etc. (Capaldi, 1996). This is one of the phenotypes associated with obesity and it is one of the reasons why it is very hard for many people to lose weight. In addition, preference for calorie-rich foods increases after dieting and weight loss, which is somewhat analogous to the increased food-seeking behavior when the food is switched from good to bad in *C.elegans*. Of course, the time scale of these effects has to be normalized to the life span. These behaviors are adaptive in the wild, where good food is usually scarce and precious: animals that "know" that high quality food is available in the environment, seek for it more actively. But in a human environment (only in the developed countries though), where the high quality food is always easily available, they contribute to obesity. My results suggest that at least on the phenotypic level, the phenomenon of "addiction" to good food might be conserved between worms and humans.

3.6. Identifying mutants deficient in food preference behavior.

With a circle (biased) food preference assay, I tested the food choice of a variety of *C.elegans* mutants. If a circle of mediocre food surrounds the central colony of good food, 70-90% of wild type worms are found in good food after 21 hours. This works for all tested combinations: *B.megaterium* circle/HB101 center (Fig. 19A), DA837 circle/*Comamonas* center (Fig.19B), *B.megaterium* circle/*Comamonas* center (Fig. 19C), DA837 circle/HB101 center (data not shown). In both combinations of the two good foods HB101 and *Comamonas,* almost all worms stay in the circle, which is the food they encounter first (Fig. 19D and E). If a circle of good food (HB101) surrounds bad food (*B.megaterium*), all worms also stay in the circle (Fig. 19F). These results are consistent with the unbiased choice of worms (Fig. 15), where worms choose better food. The difference here is that in this assay, we only look at worms that switch from bad food to good.

Both wild type Bristol *C.elegans* strain and a different wild isolate from Hawaii show food choice in this assay (Fig.19A). (The most obvious behavioral difference between Bristol and Hawaiian strains is that the former is a solitary feeder, whereas the latter is a social feeder (de Bono and Bargmann, 1998).) I also tested several mutants, including various sensory mutants (*ttx-3, osm-6, osm-1, osm-2, osm-3, che-2, ttx-1, odr-2, odr-3, odr-7, tax-1, tax-6, tax-2, osm-7, osm-9, mec-3*), other mutants affecting the nervous system (*ncs-1, npr-1, hen-1, egl-4, ceh-10, unc-86*), a number of uncoordinated ones (*unc-2, unc-29, unc-36*), mutants in biogenic amine metabolism (*bas-1, cat-4, cat-2, tph-1*) and some double

combinations. Information on the mutants is given in Table 1 of the Appendix. A few interesting observations arise.

The assay turned out to be rather sensitive: a majority of mutants tested show detectable differences in food preference from the wild type. There is even slight, but statistically significant difference between the two wild *C.elegans* isolates. Consequently, I will mostly limit myself to mutants with the largest defects that show up on two pairs of food: *B.megaterium* circle/HB101 center (Fig. 19A) and DA837 circle/*Comamonas* center (Fig.19B). The latter assay is supposed to be more sensitive even to the weak behavioral phenotypes, because DA837 and *Comamonas* lie close in the food quality range for the wild type. The difference in growth rate between *B.megaterium* and HB101 is very large, and an unbiased choice between these bacteria is very robust (Fig.15), so it should take more of a behavioral perturbation to make worms incapable of discriminating between these foods.

Among mutants affecting sensory function, *ttx-3*, *osm-6*, *osm-1*, *osm-3*, and *tax-6* show defects in food preference in both food combinations, with *ttx-3* and *osm-6* being the strongest.

TTX-3 is a LIM homeodomain transcription factor required for the differentiation of the AIY, which are involved in thermotaxis (Altun-Gultekin et al., 2001; Hobert et al., 1997). Wild type worms migrate to the cultivation temperature, while *ttx-3* migrates to lower temperatures (cryophilic), and this phenotype is reproduced by AIY laser ablation (Mori and Ohshima, 1995). *ttx-3* mutants are normal in odortaxis at supra-threshold odorant concentrations, but defective at near-threshold concentrations. Also, *ttx-3* shows increased tonic frequency of reversals during locomotion at higher (20^{o}C and above) temperature and

fails to downregulate the reversal frequency in response to water-soluble or volatile stimulants at all temperatures (Tsalik and Hobert, 2003).

It is unlikely that a thermosensory defect of *ttx-3* is the cause of the food preference deficiency. Other mutants deficient in thermotaxis, such as *ttx-1*, *tax-2*, or *ncs-1*, are normal in food preference on the *B.megaterium*/HB101 pair. *tax-6* mutants, on the other hand, are defective it thermotaxis and in food preference, but they also shows other sensory defects (Kuhara et al., 2002). Generally, there does not appear to be a strict correlation between thermosensation and food preference. It is more likely that other functions affected by *ttx-3* and *tax-6* mutations cause food preference defects.

osm-1, *osm-3* and *osm-6* mutants were identified by their inability to avoid high osmotic strength (Culotti and Russell, 1978). Other alleles of these genes were identified in a screen for mutants in which amphid neurons do not take up fluorescent dye (Dyf phenotype), indicating defects in sensory process development or anatomy (Starich et al., 1995). These mutants are also defective in chemotaxis, but normal in thermotaxis. The defect in osmotic avoidance of *osm-1*, *osm-3* and *osm-6* is unlikely to explain the food preference defect, because *osm-7* and *osm-9* are also defective in osmotic avoidance, but they are normal in food preference (in fact, they show accelerated food choice). *osm-7* and *osm-9* mutants are not Dyf, suggesting that at least the anatomy of amphid sensory neurons is normal. There is another phenotype common to *dyf* mutants: altered equilibrium between two locomotion states (Fujiwara et al., 2002). On food, wild type worms switch between two modes of locomotion, known as roaming—rapid straight movement, and dwelling—slow movement

with frequent reversals. *dyf* mutants such as o*sm-1*, *osm-3* and *osm-6* spent much more time in the dwelling mode than the wild type.

This phenotype of *osm-6* is somewhat similar to the increased reversal frequency of *ttx-3* and to the inability of *ttx-3* to decrease reversal frequency in response to chemical cues (Tsalik and Hobert, 2003). Subsequently, this will become the main focus of my work.

In contrast to most other mutants, the *tax-6* defect is stronger on the *B.megaterium*/HB101 pair than on DA837/*Comamonas*. TAX-6 is a *C.elegans* calcineurin. *tax-6* mutant shows multiple neural defects: worms are thermophilic (migrate to temperatures higher than the cultivation temperature), partially defective in taxis to odorants sensed by the AWA and AWC neurons, and hypersensitive to ASH-sensed osmotic stimuli, and they show an increased rate of sensory adaptation to AWC-sensed odorants (Kuhara et al., 2002). The thermophilic phenotype of *tax-6* is likely caused by the hyperactivation of AFD thermosensory neurons. It is thought that TAX-6 functions to inhibit sensory processing.

Several mutants show food preference stronger than the wild type. *egl-4* and *osm-9* phenotypes have been reproduced with both food combinations (Fig 19B).

In chapter 3.4 on leaving behavior I noted that sensory adaptation in *C.elegans* is somewhat similar to leaving behavior on poor food, since in both cases the animal's attractive response changes to avoidance. Interestingly, *osm-9* and *egl-4* are defective in olfactory adaptation to chemicals sensed by the AWC neurons, while *tax-6*, on the contrary, adapts at an increased rate to AWC-sensed odorants. These phenotypes are inverse to the observed food preference defects: *egl-4* and *osm-9* show preference faster than the wild type, while *tax-6* is weaker. This is counterintuitive. We would expect animals that adapt poorly to

stay longer in bad bacteria, while hyper-adapting ones would leave the poor food more rapidly and find the good food in the center. However, it is not clear whether AWC itself is needed for food preference, since *odr-2* and *odr-3* mutants, defective in AWC function, only show a food choice defect on the more sensitive DA837 circle/*Comamonas* center pair (Fig.19B); on the *B.megaterium* circle/HB101 center pair (Fig. 19A) their behavior is wild type. It is possible that *osm-9*, *tax-6*, and *egl-4* affect this behavior in other neurons, where their mode of action is different from the one in AWC. Interestingly, the AWCs have been implicated in olfactory avoidance learning in response to pathogenic bacteria (Zhang et al., 2004).

My preliminary data suggest that *tax-6* shows a defect in the food-dependent regulation of locomotion (Fig. 27, see text below).

It is surprising that strong *unc* mutants, such as *unc-29*, which lack a body wall acetylcholine receptor), *unc-2* (the N-type Ca channel α–subunit) and *unc-36* (the N-type Ca channel β–subunit) have defects weaker than expected. Only *unc-29,* a very slow moving *unc*, shows a defect that is rather strong, although still weaker than that of *ttx-3*. That suggests that locomotion defects do not necessarily cause failure to locate the good food in this assay, probably because the distance between the inner border of the circle and the outer border of the central colony is quite small, about 1.5 mm (6 lengths of an L1), while the time of the assay is very long, 7 and 21 hours.

Mutants in serotonin and/or dopamine synthesis (*bas-1*, *cat-4*, *cat-2*, *tph-1* and some double combinations) show mild to moderate food preference defects. The data on involvement of dopamine and serotonin in *C.elegans* behavior, particularly in response to

food, is so vast, that these results are hardly surprising. In this assay, mutants defective in serotonin, *bas-1* and *tph-1*, do not show large food preference defects. *cat-4*, on the other hand, is defective in both serotonin and dopamine; the levels of both of these neurotransmitters are greatly reduced (Loer and Kenyon, 1993; Ranganathan et al., 2001; Sulston et al., 1975) . *cat-2* is specifically defective in dopamine (Loer and Kenyon, 1993; Sulston et al., 1975). That *cat-2* and *cat-4* are deficient in food preference while the serotonin-null *tph-1* is almost wild type suggests that dopamine is more important in the food preference behavior.

When worms enter a bacterial lawn, they dramatically slow down locomotion (basic slowing response) (Sawin et al., 2000). In fact, they also slow down locomotion upon entering an inedible substrate. This slowing response is dependent on dopaminergic neurons and is rescued by exogenous dopamine. Dopamine has also been implicated in area-restricted search behavior (Hills et al., 2004). When a worm is taken off food and transferred onto an empty plate, the frequency of reversals is transiently increased, presumably because an animal searches for food in the immediate vicinity. This behavior also requires dopaminergic neurons.

One would think that *cat-2*, *cat-4*, or *tph-1;bas-1* mutants, which do not slow down upon entering food as much as the wild type, run through either good or bad bacteria, which results in the food preference defect. I did not investigate this possibility, but it seems that *tph-1;bas-1* animals show a locomotion defect, tending to move in circles (Fig. 27, see below).

In subsequent work, I focused on *ttx-3* and *osm-6* mutants. I hypothesized that the *osm-6* and *ttx-3* defects in the regulation of locomotion in response to chemical cues and food (Fujiwara et al., 2002; Tsalik and Hobert, 2003) underlie the food preference defects of both of these mutants. *ttx-3* was interesting for several reasons. First, it produces the strongest food choice deficiency among mutants tested. Although *ttx-3* has not been described as an *unc*, its food preference defect is even worse that that of *unc-29*. Second, a trivial explanation for the *ttx-3* defect cannot be found. For example, it is clear and uninteresting why *unc-29* is defective; defects of sensory mutations such as *osm-6*, *osm-1* and *tax-6* can also be explained because chemo- and odorsensation is likely to be important for food seeking. *ttx-3*, on the other hand, is defective in thermotaxis (Mori and Ohshima, 1995), and it is not clear why this would cause such a strong food choice deficiency. Finally, the function of *ttx-3* in thermotaxis has been mapped to a single pair of interneurons, the AIYs (Altun-Gultekin et al., 2001; Hobert et al., 1997). The hypothesis that AIY is important is supported by the food choice defect of *ceh-10*, another gene involved in AIY differentiation. Because *C.elegans* thermotaxis is a learned temperature-food association, the possibility that AIY is also important for food choice behavior seemed intriguing.

The defect of *osm-6* is weaker than that of *ttx-3* on 2 out of 3 food combinations. This gene is expressed in many neurons, so it possibly affects many processes. It was identified by a failure to avoid high osmolarity; and more alleles were identified in screens for the failure of amphid sensory neurons to take up fluorescent dye, indicating a defect in sensory cilia development. In o*sm-6* mutants, the ultrastructure of the sensory cilia of amphid sensory neurons is abnormal, resulting in defects in mechano-, osmo- and chemosensation (Culotti

and Russell, 1978; Starich et al., 1995). A GFP protein fusion is expressed in 56 neurons, including 24 amphid neurons. (Collet et al., 1998). That *osm-6* is chemotaxis-deficient may be a trivial explanation for its food choice defect. This idea is undermined, however, by the observation that other chemotaxis-deficient mutants are normal in food choice.

On looking closer, I found that there is a common phenotype in *ttx-3* and *osm-6,* which may explain the food preference defects of both: a perturbed equilibrium between the roaming and dwelling modes of locomotion.

3.7. Food quality regulates the balance between two modes of *C.elegans* locomotion, dwelling and roaming.

On a standard food, the *E.coli* strain OP50, *C.elegans* exhibits two modes of locomotion, called roaming and dwelling (Fujiwara et al., 2002). Roaming or running is a rapid straight movement; dwelling consists of short movements with frequent reversals and turns. On food, wild type adult worms spend about 75% of the time in the dwelling mode and 25% in the roaming mode. Although *osm-6* and other dye filling mutants were not originally described as locomotion-deficient, it was later shown that they are defective in roaming, and spend more than 90% of the time in the dwelling mode (Fujiwara et al., 2002). This defect is rescued by the e*gl-4* mutation, which is a cGMP-dependent protein kinase; the *egl-4* mutant is shifted toward roaming. On the other hand, eat-7, which turned out to the gain-of-function allele of *egl-4*, may cause an increase in "developmental quiescence" (Raizen, 2004).

When worms exit a colony of poor food, they move in a straight trajectory for some time, then stop or reverse (Fig.16). This led me to hypothesize that the role of roaming is exploration of the environment in search of high quality food. To test this, I video recorded locomotion of wild type naïve L1s on different foods (Fig. 20). (The lawn of bacterial food fits into the 10.3 mm wide video field). Indeed, the locomotion of worms on food of different quality is strikingly different. On good food, such as *E.coli* HB101 (Fig. 20A and B) or *Comamonas* (C and D), the worm trajectory is very compact; there are very few periods of straight movement. In contrast, on mediocre food, *E.coli* DA837 (E and F) and *B.megaterium*

(G and H), the animals' trajectory is spread over the whole field of view, and worms traverse the bacterial lawn many times during the 10-hour experiment. Some periods of movement culminate in leaving the bacterial lawn.

Here, the difference between DA837 and HB101 is somewhat higher than expected. In unbiased choice assay (Fig. 15), the wild type only shows a weak preference toward HB101. In the leaving assay (Fig. 16), P(leaving) of the wild type on DA837 is very low. But in that experiment it was only measured within a 1 to 2 hour test interval. I observed that P(leaving) of the wild type on DA837 increases after 4-6 hours. It just seems to take longer for the wild type to start leaving DA837 (data not shown). Leaving or food choice is an "all-or-none", discrete behavior; that is, an animal has to leave the food and/or switch from one food to another; so in these assays, we cannot see the intermediate state. Locomotion, on the other hand, is not discrete, so even small variations show up.

The way food quality affects locomotion is also apparent when the speed of movement and the turning angle (change of direction) are plotted against time (Fig. 21). On the good food HB101, the speed stays low and the turning angle is high, indicating frequent direction change or no net movement. On mediocre food, DA837, periods of rapid movement are common, in which the speed reaches 80 μm/sec. During these periods, the turning angle stays low, indicating that movement is straight. The distribution of movement speed is shown in a histogram in Fig. 22A. On mediocre food, worms spend a large part of their time moving rapidly.

To quantify these affects, I have used the locomotion analysis procedure developed by (Pierce-Shimomura, 1999). First, the trajectory is split into movement segments, each new

segment starting when the direction change exceeds 50^{o}. These segments are then arranged into a histogram by their duration (Fig. 22B). On mediocre food, the population of longer straight movements is significant, while it is much smaller on good food (Fig. 22B, right panel). The duration histogram of wild type movement on DA837, where both short and long movements are represented, is well fit with the sum of two exponentials. Their intersection is a threshold duration, T(critical), and is used to extract long movements, which are thought to represent the roaming mode of locomotion (Fujiwara et al., 2002). This principle is shown in Fig. 22G, and arrows in Fig 22B show the T(critical) for the wild type on DA837. The same T(critical) was used as a threshold for the duration histogram data on other food sources. The effect of food quality is most prominent has its most prominent effect on the population of long movements.

First, the total time spent in long events, relative to the total time of an analyzed recording, is about 30% on poor food, while it is 5% or less on good food (Fig. 22C). The frequency of long events relative to the total time of recording analyzed is also 3 to 6 fold higher on poor food than on good food (Fig. 22D). The mean duration of long event is increased two fold on poor food (Fig. 22E); and the speed of locomotion during long movements is increased about 2.5 fold (Fig. 22F)*.

The fact that high quality food causes a decrease in the total time spent roaming results from a combined effect on the frequency of long movements and on their duration. Of these two effects, the effect on the frequency is larger (compare Fig. 22D and E). The frequency of long events is proportional to the ability to initiate roaming, to switch from dwelling mode into roaming mode. The duration of roaming events is proportional to the

*Note that the trajectory on *B.megaterium* is fragmented due to poor contrast, so the population of long events is artificially decreased because many are interrupted by the inability to record the worm trajectory. The increased roaming on *B.megaterium* is still obvious, but this effect should have been even bigger; see, for example the speed histogram in 22A.

inverse of the ability to switch from roaming mode back to dwelling*. As Fig. 22 shows, both processes are affected, but the effect on the dwelling-to-roaming transition (frequency) is larger. Therefore, the dwelling-to-roaming transition is likely to be more important for the animals' ability to find the high quality food in the environment where foods of different kinds are present. The roaming-to-dwelling transition is also modulated, but the effect is not as big.

The long event duration, which reflects the roaming-to-dwelling transition, is highly variable. The error bars seem small in Fig. 22E, but these data are the average of mean movement durations of single worms. As seen on the Fig. 22B, the spread of durations is very large; although mean is about 55 sec, some movements are 100 to 120 seconds. This upper limit is likely not a true value, because the bacterial lawn is limited and the worm usually stops when it reaches the border.

Looking at the trajectory plots in Fig. 20, one would say that the effect on movement duration is very large: there seem to be very few long segments on HB101 but a lot on DA837. The length of these segments, however, is also dependent on the speed, which is decreased about 3-fold on good food (Fig. 22F), so an average 6-fold decrease in the length of movement segments is expected. This also seems too small an effect to account for the difference between trajectories on good and bad food. What happens here is that it is the longest movements that mainly account for the difference, they are the ones that make the trajectory take the whole field of view. The T(critical) obtained in the analysis procedure is only 16.2 seconds, so many short segments are included in both the HB101 and DA837 data, and their number is much larger than the number of long segments. In analysis, they mask the

*The frequency of long events is analogous to the channel opening probability in the single ion channel analysis. The long event duration is analogous to the mean open time.

difference in the number of very long movements, which mostly accounts for the difference in trajectories. As a result, the effect of the food quality change on the mean movement duration in the bar graph (Fig. 22E) is not as big as one would expect from the difference in trajectory plots (Fig. 20). That the population of long runs is dramatically increased on poor food is best seen on the movement duration histogram (Fig. 22B). It is because of these very long runs the trajectories on good and bad food look so different.

3.8. *osm-6* and *ttx-3* mutants are defective in roaming.

osm-6 and *ttx-3* mutants are defective in food choice behavior (Fig 19). Using the locomotion assay, I found that both of these mutants show abnormal equilibrium of the two locomotion states: the frequency, the duration, and the speed of long movements, representing roaming, is decreased. The trajectories of these mutants as well as the *osm-6; ttx-3* double mutant are shown in Fig. 23. It is obvious that on DA837, *osm-6* (Fig. 23G) and *ttx-3* (Fig. 23C), show far fewer long movements than the wild type, and these defects add up in the double mutant (Fig. 23E). The movement speed of *osm-6* and *ttx-3* is also decreased, as shown on speed histograms (Fig. 24A).

The population of long movements in *ttx-3*, *osm-6* and the double mutant is much smaller than in the wild type (Fig 24B). The fraction of time spent in long movements is also decreased, and in *osm-6* and the *osm-6; ttx-3* double is close to the fraction of time spent in long events for the wild type on good food, *E.coli* HB101 (Fig. 24C).

In *ttx-3* the mutant, both the frequency (Fig. 24D) and the duration of long movements (Fig. 24E) are decreased. In the wild type, good food causes a much larger decrease in frequency than in duration (Fig. 22D vs. 22E). But in *ttx-3*, the effect on the frequency is rather modest, about 30%. Thus the effect of the *ttx-3* mutation on wild-type is far less than the effect of good food on wild-type (Fig. 24D, compare with the wild type on HB101). The effect of *ttx-3* on the long movement duration, however, is two-fold (Fig. 24E), which completely phenocopies the effect of good food on the wild type. This suggests that

the TTX-3 functions to suppress the roaming-to-dwelling transition on bad food; when it is knocked out, the roaming-to-dwelling transition is as likely as it is on good food. The *ttx-3* mutation also causes a two-fold decrease in roaming speed, which is comparable to the 3-fold effect of HB101 on the wild type (Fig. 24F).

The food-dependent regulation of locomotion is preserved in the *ttx-3* mutant: on the good food HB101, its trajectory is even more compact and roaming is further decreased (Fig. 23D). What is interesting, however, is that the frequency of long events in *ttx-3* on HB101 is 2.5-fold higher that in the wild type (Fig 24D). It almost looks as if in the *ttx-3* mutant, there is a population of short but frequent movements on any food, which masks the food-dependent regulation of locomotion and causes the food preference deficiency. The food-dependent regulation of locomotion can be presented as a ratio of locomotion parameters on two different foods (Fig. 24G).

3.9. *ttx-3* mutant phenotype is partially reproduced by laser ablation of AIY interneurons.

The gene *ttx-3* encodes a LIM homeodomain transcription factor required for the differentiation of AIY thermosensory interneurons (Altun-Gultekin et al., 2001; Hobert et al., 1997). It is also expressed in 3 other neuronal types: AIA, ADL and ASI, where its role is unknown*. AIY is required for *C.elegans* thermotaxis, a learned association of temperature with food. Wild type worms, after having been conditioned with food and transferred to an empty plate, migrate to the cultivation temperature and move in straight trajectories while remaining at the same temperature (isothermal tracking) (Hedgecock and Russell, 1975). *ttx-3* mutants or worms in which AIY is ablated with the laser are incapable of isothermal tracking and migrate to cooler temperatures (cryophilic phenotype) (Mori and Ohshima, 1995).

Since the role of *ttx-3* in AIY development was already known, I tested whether *ttx-3* also works in AIY to regulate food seeking behavior. Using a strain expressing GFP in AIY, I ablated both AIY neurons with the laser and tested these animals in food choice and locomotion assays.

On visual inspection, the locomotion of the AIY ablated worms is phenotypically between the wild type and *ttx-3* (Fig. 25). There are fewer long straight periods of movement than in the wild type. In the histogram of movement durations, the population of long movements is decreased compared to the control group (Fig.26A). The total fraction of time spent in long movements is decreased by about 40% (Fig. 26C, compare with 2.5 fold

*In another paper (Tsalik and Hobert, 2003) say that *ttx-3* is expressed in ADF, not in ADL

decrease in *ttx-3*, Fig. 24), the frequency of long events is unchanged (Fig. 26D, 30% decrease in *ttx-3*), the mean duration of long events is decreased by about 2 fold (Fig. 26E, same as in *ttx-3*), and speed is only slightly decreased (Fig. 26F, two fold decrease in *ttx-3*). Therefore, AIY ablation does not affect the frequency and only weakly affects the speed, but the effect on roaming event duration is about the same as the effect of the *ttx-3* mutation. The decrease in roaming event duration caused by AIY ablation is also about the same as the one caused by the substitution of mediocre food, *E.coli* DA837, with good food, *E.coli* HB101 (Fig. 24E). The long event duration measures the inverse of the roaming-to-dwelling switch rate: the lower the probability of transition from roaming to dwelling, the longer roaming events are on average. That laser ablation of AIY causes about the same decrease in roaming event duration as the substitution of mediocre food with a good one, suggests as the simplest hypothesis that AIY normally inhibits the transition from roaming to dwelling, which results in the increase in population of longer "runs" (Fig. 26G).

The observed effect of AIY ablation is consistent with other studies, which suggest that AIY suppresses reversals (Gray et al., 2004a; Tsalik and Hobert, 2003). (Tsalik and Hobert, 2003) have shown that in *ttx-3* mutant the reversal frequency is increased at higher temperatures (20 and 25^{o}C), but not at 15 ^{o}C. My experiments were done at 18 ^{o}C. Interestingly, worms downregulate the frequency of reversals in response to stimuli sensed by AWA and ASE neurons, which directly synapse onto the AIYs. *ttx-3* is required for this regulation at all temperatures (Tsalik and Hobert, 2003). This may represent a "novelty response" in worms: a food-deprived animal is attempting to follow an unknown cue in

search for food. This *ttx-3* defect is consistent with an inability to suppress reversals and increase roaming in response to poor food.

Next, I tested AIY ablated animals in the biased food choice assay. After ablation, worms were put on plates with a circle of *B.megaterium* surrounding a central colony of HB101. While about 90% of the wild type concentrate in the center after 20 hours, only 40% of AIY- worms do (Fig. 26B). Ablation of the ASI neuron, which is a chemosensory neuron in which *ttx-3* is expressed, also results in a food choice defect, which is milder than the effect of AIY ablation. ASI and AIY ablations do not interact: ASI, AIY double ablation has the same effect as AIY.

These results suggest that TTX-3 works in AIY to regulate locomotion in response to the food quality. However, the phenotype of AIY-ablated animals is not as severe as that of the *ttx-3* mutant, suggesting that other neurons are also involved in this regulation.

3.10. *tax-6* shows increased roaming on high quality food.

As seen in fig. 19, *tax-6* mutants show a food choice defect on both combinations of bacteria. *tax-6* encodes *C.elegans* calcineurin ortholog (Kuhara et al., 2002). This gene is expressed in a number of sensory neurons, including thermosensory AFD neurons, chemosensory ASE, AWA, ASH, ASI, ADF, ADL neurons, odorsensory AWC neurons, and interneurons such as AIY and AIZ. Some phenotypes of the *tax-6* loss-of-function mutant can be explained by the hyperactivation of neurons where it is expressed. These mutants are hypersensitive to osmotic stimuli, they adapt to the AWC-sensed odorants faster than the wild type and they are thermophilic, that is, they migrate to the warm temperature in the thermotaxis assay. It has been shown that the thermophilic phenotype may result from the hypeactivation of the AFD neurons that sense the warm temperature. AFD synapses onto the AIY interneurons. The possibility that AIY is activated in *tax-6* has not been excluded, however.

Interestingly, I found that *tax-6* mutants show increased roaming behavior on the high quality food (Fig. 27, C and D), which may explain their food choice defect. This phenotype is opposite to the AIY null *ttx-3*, and is consistent with the AIY being hyperactive in *tax-6*. AIY may be activated directly or via synaptic inputs from other neurons such as AFD. On the other hand, AFD is probably not essential for the AIY influence on locomotion, because *ttx-1* mutant, an AFD null, does not exhibit any food choice defect (Fig. 19). To test if AFD is required for the *tax-6* increased roaming phenotype, *ttx-1;tax-6* double mutant is needed

In addition, some mutants defective in the biogenic amine metabolism (*cat-2*, *cat-4*, *tph-1;bas-1*) show food preference defects (Fig. 19, see discussion above). Preliminary studies of two of these mutants, *cat-2* and *tph-1;bas-1* double revealed locomotion defects in *tph-1;bas-1*: these animals tend to move in circles (Fig 27, E). The roaming activity might also be decreased, but this is hard to interpret because of the clear locomotion defect. Another mutant with a rather mild food choice defect, *cat-2*, did not show dramatic abnormalities in the roaming-dwelling equilibrium (Fig. 27, G and H). Its roaming activity on DA837 may be decreased compared to the wild type, but I have not done enough worms to quantify this.

3.11. A screen for the mutants defective in the food choice behavior

I attempted to screen for mutants in the food choice behavior. Starved synchronized F2s were conditioned for 7 hours on a high quality food, and then subject to a selection on a food choice plate, as shown in Fig. 28A and described in the legend to this figure. Animals that failed to select the good food were picked and retested. A number of putative mutants were isolated, but most of them turned out to have defects in the sensory neuron anatomy, as determined by the fluorescent dye staining (Fig. 28, B and C). These mutants are therefore similar to *osm-6*. A few mutants seemed to stain with the dye, although it is still possible that they have more subtle defects in the sensory neuron anatomy or development.

One thing to mention is that mutants that fail to stain differ widely in the severity of their food choice defect. This may indicate that it is not the ability to sense external stimuli that is important for the food quality detection. Some other property of sensory neurons is essential, which does not require the contact of the sensory cilia with the external world. Alternatively, it is not even sensory amphid neurons that are essential; it is some other neurons that require the same genes for normal development or function. Laser ablation studies are needed to elucidate what those are.

This screen is only preliminary. If I were to re-do it, I would do a dye staining selection of the candidates before retesting them in the food choice assay, since the former is much easier to do.

3.12. Conclusions

In the project described in Chapter 3, I have described novel behavioral paradigms in *C.elegans*, food seeking and food preference, and my initial attempts to study mechanisms of these behaviors.

Mammalian food seeking is a subclass of motivated behaviors (Skinner, 1938; Stellar and Stellar, 1985), with food being the reward. Mammalian food preferences are determined both by the nutritional content of food and by the sensory stimulation it delivers (Capaldi, 1996; Sclafani, 2001). There are inborn preferences, such as that for sweet taste, but many food choices are learned during life and reinforced via the feedback the food provides when nutrients are absorbed and animal's energy stores are replenished.

In *Drosophila* or *C.elegans*, food seeking behavior has not been studied, so there is no genetic system available. In this work I attempt to establish the *C.elegans* system. *C.elegans*'s food is soil bacteria. In a simplified laboratory environment, the roundworm *Caenorhabditis elegans* is routinely fed the intestinal symbiotic bacteria *Escherichia coli*. In the wild, worms are likely exposed to a variety of bacterial food. How they deal with this choice is unknown. Do worms eat the first type of bacteria they encounter or try to search for food of higher quality?

First, I have identified non-*E.coli* worm foods to establish the range of food quality as measured by the food's ability to support growth. Interestingly, the food quality correlates

inversely with the size of bacteria: big bacteria tend to be poor food and small bacteria tend to be good food.

Next, I found that *C.elegans* exhibits food choice behavior: it prefers the high quality food, the one that better supports growth. This choice develops with time, suggesting that animals need to try the food to make a decision. Using *eat* mutants, I show that this choice requires food assessment via feeding. This is similar to mammals that are also capable of selecting the more nutritive food that better supports growth and also try both foods before making a choice (Osborne and Mendel, 1918; Young, 1941).

In previous studies, the effect of food on *C.elegans* behavior was measured by its presence versus absence (Hobert, 2003). The food was thought of mainly as a sensory stimulus acting via worm's odor and taste perception. The fact that food is a reinforcement that provides feedback after it is eaten has not been directly addressed, although this is the key biological significance of food. I show, for example, that after worms find the food, there is a chance that they leave, and this probability is higher if the food is bad. My data suggest that leaving food is an exploratory food seeking behavior.

Interestingly, this behavior is modified by experience: worms that have experienced high quality food show higher exploratory drive after switching to poor food, compared to the ones that have only experienced poor or no food. This phenomenon is similar to the human "food craving" and "carbohydrate craving"; mammals also form strong feeding habits (Capaldi, 1996).

Finally, I show that *C.elegans* locomotion, in particular the equilibrium between roaming, rapid straight movement, and dwelling, slow movement with frequent reversals and

stops, is affected by the food source. On poor food, roaming is drastically increased, while dwelling is predominant on high quality food. These results suggest that at least one biological role of roaming is exploration of the environment in search for the good food.

I identified mutants defective in food preference behavior; and two of them, *osm-6* and *ttx-3* are also defective in roaming. TTX-3 is a transcription factor required for the differentiation of the AIY thermosensory interneuron. The defects of the *ttx-3* mutant are partially reproduced by AIY laser ablation. The biggest effect of AIY laser ablation is on the mean duration of longer movement periods, suggesting that AIY functions to suppress the roaming-to-dwelling transition and to extend the food-seeking periods.

On the other hand, *tax-6* mutants show increased roaming periods on the good food, *E.coli* HB101. This is consistent with the hypothesis that in *tax-6*, AIY is hyperactive. This hypothesis is supported by the observation that the phenotype of *tax-6* in relation to the temperature (thermophilic) is opposite to that of *ttx-3* (cryophilic).

This study is in no way complete and is only a start. My preliminary results, not reported here, suggest that it is possible to design screens to search for mutants defective in food preference. If this works, the molecular mechanism of this behavior can be uncovered which can add a lot to our knowledge of food seeking behavior in animals.

3.13. Methods

Worm culture and strains: For routine purposes, worms were grown on NGMSR (Davis et al., 1995) plates seeded with *E.coli* strain HB101 at 18 ^{o}C. The strains used were: wild type Bristol strain N2, wild type Hawaiian strain CB4856, DA465 *eat-2(ad465) II* (McKay et al., 2004; Raizen et al., 1995), MT6308 *eat-4(ky5) III* (Lee et al., 1999b) and DA1402 *eat-5(ad1402) I* (Starich et al., 1996). For AIY laser ablations, an *mgIs18[ttx-3p::GFP]* integrated line was used (a gift from Dr. Oliver Hobert). Detailed descriptions of mutants tested in Fig.19 are given in Table 1 of the Appendix.

For behavioral assays, two *E.coli* strains were used: HB101 (Boyer and Roulland-Dussoix, 1969) and DA837. DA837 was derived from OP50 (Brenner, 1974) strain by selection for resistance to streptomycin (Davis et al., 1995).

Isolation and identification of soil bacteria was as described in (Avery and Shtonda, 2003). Briefly, soil samples collected at five Dallas locations were suspended in water and plated on LB plates to isolate single colonies. Identification of bacteria was done via 16S rDNA sequencing by Midilabs, DE.

Growth rate measurements: Experiment in Fig. 13 was done as described by (Avery and Shtonda, 2003). Experiment in Fig. 14 was done in a similar way, except all bacteria were grown on standard NGM (Sulston and Hodgkin, 1988) plates. 2-5 day old

bacterial plates were used for these and all other experiments. Hermaphrodites were lysed in 40% bleach (Chlorox), 0.5 M NaOH until fragmented, and eggs were incubated overnight (14-18 hours) at 18^{o}C to allow L1 larvae to hatch. Larvae were washed once in M9 buffer (Lewis and Fleming, 1995); and 50-100 L1s were plated on each plate, kept at 18 ^{o}C and observed repeatedly every 2-6 hours. The growth rate was calculated as the inverse of number of days it took for animals to reach adulthood, as recognized by the shape of the vulva and by the presence of eggs. The experiment shown in Fig. 13 was a single series done the same day. The experiment in Fig. 14 was done over many days, each data point representing one series, and the results were averaged. As mentioned in the legend to Fig.14, in three cases (*eat-5* on DA837, *eat-2* on *Bacillus megaterium*, and *eat-5* on *Bacillus megaterium*) the growth rate variability between animals was too high to determine the growth rate by looking at the population of worms. In these cases, the same assay was done with one larva on each plate, and the results were averaged.

Food choice assays: For the experiments in Fig. 15 (unbiased food preference assays), bacteria were grown overnight at 37 ^{o}C and then used within 5 days. Assays were done on standard 50 mm polystyrene plates filled with NGM medium from which the bactopeptone was omitted to slow bacterial growth during the experiment. Bacterial food was placed on assay plates in three different arrangements with a worm pick, as shown on Fig. 15D. Distances were controlled with an ocular micrometer. Experiments were done the next day. Egg-synchronized L1s, prepared as for growth measurements, were washed once in M9 and placed in the center of the assay plate in a 1-1.5 μl drop of M9 buffer, 70 to 150 worms

per plate. (The number of worms could not be strictly controlled. I found, however, that within this range the exact number of worms used did not affect food choice.) Assays were done at 18^{o}C in a temperature-controlled room. At the time points shown in Fig. 15D, worms were killed by inverting the plates over chloroform, then plates were kept at 4 ^{o}C and the number of worms in each bacterial food and outside of the bacteria was counted. Data for all colonies of the same type on a single plate were pooled together; thus each data point represents one plate. In Fig. 15, the fractions of worms in each type of food correspond to the plot areas as explained in the legend.

For the experiments shown in Fig. 18 and 19 (circle, or biased food choice assay), the bacterial source plates were the same as described above, but the assay plates were normal NGM plates (with bactopeptone). The outer circle of bacterial food was made by putting the back end of the Pasteur pipette in the corresponding bacterial source plate and touching the assay plate. These circles ware grown overnight at 37 ^{o}C. Next day, chunks of another bacterial food were placed in the center of the circle with worm pick to obtain the arrangement shown in Fig. 18. On each plate, two such circles were made on two sides of the plate. The assay plates were stored overnight at room temperature to be used the next day. Egg synchronized L1 larvae were plated outside of the circle as shown in Fig. 18, followed by incubation at 18 ^{o}C. At the given time points, described in the legends for Fig. 18 and 19, worms were killed by chloroform vapors, stored at 4 ^{o}C and counted. Each data point represents one circle, thus each assay plate yielded 2 data points. For Fig. 19, experiments done over many days were averaged. For Fig. 18 an assay was done with 10 plates (20

circles) on a single day, resulting in much less variability. Similar results were obtained on a different day (data not shown).

Leaving assay: For a population leaving assay (Fig. 16A, Fig. 17), assay plates were standard NGM plates. Chunks of bacteria were transferred from bacterial food plates (prepared as described above) onto assay plates with a worm pick and shaped into a small, roughly ellipsoid colony with the smaller dimension >0.5 mm and the bigger dimension <1 mm, as measured with an ocular micrometer. One colony was made on each plate; plates were immediately used in the assay. L1 larvae were prepared by egg synchronization and allowed 15-18 hours to hatch. 40-60 larvae were placed in a 1-1.5µl drop of M9 close to the food colony. Plates were placed on a video recording apparatus (see below) for recording. Video recordings were analyzed using Adobe Premiere 6.5 software. The moment at which the first worm entered the colony was time point 0. Then, the number of worms entering and leaving the colony each minute was counted. The leaving probability, P(leaving) in each minute of the recording was determined as the ratio of the number of worms that left the colony during this minute to the total number of worms in the colony at the start of that minute. For Fig. 16A, the per-minute probability was averaged between 1 and 2 hours of the recording (i.e., for minutes 61 - 120); for Fig. 17 P(leaving) was averaged in several intervals as described in the legend. Leaving assays on single worms over long times (Fig 16B, C and D) were done on NGM plates from which the bactopeptone was omitted and (for C and D only) agar replaced with agarose to limit the growth of the colony during the experiment. In single worm assays, a late stage (pretzel) embryo was placed close to the colony. The larva

usually hatched within the next 3 hours, and time point 0 was the time at which it first entered the colony. The experiment in Fig. 16A was done over many days, and results were averaged.

For the experiments in Fig. 17 larvae were prepared in the same way, but incubated strictly for 15 hours. This experiment was done on 5 consecutive days, and each time all five conditions were run in parallel. Naïve synchronized L1s were placed on different conditioning plates, seeded with bacterial food or unseeded (empty) as described in the legend. After 3 hours, worms were washed off with 1 mL of M9 and washed three times with 1 mL of M9, with each wash followed by a 1 min spin at 1000rpm in a swinging-bucket rotor in a microcentrifuge. After the final spin, larvae were transferred onto assay plates in a small drop of M9 for the leaving assay as described above. All incubations and video recordings were done at 18 ^{o}C.

Laser ablations: Laser ablations were performed as described in (Bargmann and Avery, 1995). AIY neurons were identified by GFP epifluorescence in the *mgIs18[ttx-3p::GFP]* strain. ADL, ASI, ASK and ASH were identified by staining with the fluorescent dye DiO. For the food preference assay (Fig. 26B), eggs obtained by bleaching adults were incubated for 14-15 hours to get synchronized L1 larvae. After one M9 wash, worms were incubated in 0.01 mg/mL DiO in M9 for 2 hours. Then, animals were destained for 1 hour on an unseeded NGM plate and transferred from this plate onto 3% agarose pads containing 3mM NaN_3 for the laser ablation. Ablations were monitored by GFP or DiO bleaching by the laser beam. All groups shown in Fig. 26B were treated the same, except that

in the control group lasering was omitted. After ablation, worms were transferred in M9 onto an empty NGM plates for a 2 hour recovery and then plated on food preference assay plates, with one circle assay per plate. On each plate, 2 to 4 worms were assayed (usually from one ablated batch). After 20 hours, plates were scored.

For the trajectory analysis on AIY-ablated animals (Fig 25), eggs were obtained by bleaching and plated on the NGM plate. After 1 hour, larvae were picked for ablations. Ablations were performed as described above, except DiO staining was omitted (AIY neurons were identified by GFP in the *ttx3::GFP* strain). Controls were treated the same, except that neurons were not ablated. After a 2 hour recovery, single worms were transferred onto assay plates for trajectory recordings (see below).

Video recordings: For the leaving assay and trajectory recordings, a 9 worm recording station was built. Nine PC23C (Supercircuits, TX) monochrome cameras (640x480 resolution) were mounted on a custom-made rack and connected to the 16 port GV-600 recording board (Geovision, Taiwan), which was installed in the Pentium 4 Windows 2000 computer (Appendix, Fig. 4). The light sources were also custom built (Appendix, Fig. 5). Recordings were done using the Geovision software at a rate of approximately 1 frame per second; video files were automatically saved every 5 min. These files were then compiled into one large continuous file using Adobe Premiere 6.5 and analyzed as described below. All recording experiments were done in a temperature-controlled 18^{o}C room.

Trajectory recordings and analysis:

For the trajectory assay (Fig. 20, 23, 25), thin, roughly rectangular lawns of bacteria were streaked with the small (about 4 mm long) streaker made of a Pasteur pipette, and then grown on standard NGM plates for 3.5-5 hours at 37^{o}C to produce a thin smooth lawn of about 9x4 mm in size. Different bacteria were found to grow at different rates: *B.megaterium* is the fastest; *E.coli* DA837 is intermediate*, and* Comamonas and *E.coli* HB101 are the slowest. The incubation times were adjusted correspondingly to produce lawns of about equal thickness. Eggs were obtained by bleaching, and L1 larvae hatched within an hour were transferred in a small (1-1.5 μL) drop of M9 onto the trajectory assay plates. The video field for the trajectory recording was 10.3 mm wide, which was found to be the maximal size to allow an automated tracking of an L1 larva. For experiment in Fig.25, laser ablations were performed as described above. Video recordings were done using an apparatus described above.

Video files were analyzed using the custom worm tracking software written with Microsoft Visual C++ 6 (Appendix, Fig. 7). Every frame, worm coordinates were recorded. For the locomotion analysis, the trajectory of the worm from 2 to 10 hours from the start of the recording was used. These regions were run through the custom-written Labview 6 (National Instruments) (Appendix, Fig. 6) software to extract movement segments using the segmentation procedure described in (Pierce-Shimomura et al., 1999). Coordinates of every fifth frame (on average, every 5.37 seconds) were used to calculate the movement speed and turning angles. Every turn of more than 50^{o} was considered direction change and a start of the new movement segment. Unlike previous reports (Fujiwara et al., 2002; Pierce-Shimomura et al., 1999), I found that on good food, wild type larvae exhibit extended periods of no

movement. This cannot be due to sickness, since it was found in almost all experiments and, most importantly, the behavior was very different on mediocre food (Fig 20). During periods of no movement, direction change (turning angle) is undefined. We assigned 180^{o} to the value of turning angle during these periods, because no movement is a behavior totally opposite to the rapid straight locomotion, when the turning angle stays low, close to 0. Moreover, periods of no movement are indistinguishable from very small movements at our video and time resolution and from noise resulting from brightness and contrast variations. Therefore, the dwelling mode of locomotion (Fujiwara et al., 2002) in our analysis includes both periods of small movement and frequent direction change, as well as periods of no movement. Only running periods, when direction change stays $<50^{o}$, were extracted.

Using the two exponential fitting and thresholding procedure (Pierce-Shimomura et al., 1999), a population of long locomotion events (representing roaming, or running mode of locomotion) was isolated. Using Labview software (Appendix, Fig. 6), various parameters of these "runs" were determined, such as their frequency, the fraction of the total time spent running, mean duration and mean running speed (Fig. 22,24,26).

Unfortunately, on *B.megaterium* lawn the contrast was so poor that the L1 cannot be seen for a large fraction of the time, so the trajectory is fragmented. This creates a bias in favor for the short movements, because the long ones are often interrupted (interrupted segments were always discarded). Trajectories on *B.megaterium* are poorly suited for analysis, and this data should be treated with caution. Most mutant and laser ablation analyzes were done on HB101 and DA837 strains of *E.coli*.

Data presentation and statistics: Data are presented as mean ± standard deviation (SD) or standard error of the mean (SEM), as stated in figure legends. Comparisons are made by the Student's T-test or the chi-squared test of independence.

APPENDIX

Table 1. **Mutants tested in the circle (biased) food preference assay (Fig 19).** Many text descriptions are adapted from WormBase (www.wormbase.org).

gene	strain (allele)	Protein/function	phenotype	expression
ttx-3	OH161 (ot22) X FK134 (ks5)	LIM homeodomain protein. Required for the differentiation of the AIY thermosensory interneuron (Altun-Gultekin et al., 2001; Hobert et al., 1997).	Cryophilic, almost completely defective in isothermal tracking. (Mori and Ohshima, 1995). Increased frequency of turns and reversals during locomotion (Tsalik and Hobert, 2003).	Consistent expression in the AIY interneuron; slightly weaker but still very consistent expression is also observed in the AIA interneuron and less consistent and weaker expression can be observed in the ADL and ASI sensory classes as well as two pharyngeal neurons. (Altun-Gultekin et al., 2001)
osm-6	PR811 (p811) V	Putative N-acetyllactoseamine synthase. Functions in the outgrowth of axonemes of the ciliated censory neurons (Collet et al., 1998)	Fails to avoid 4M fructose or 4M NaCl; poor chemotaxis to NaCl; normal thermotaxis; fails to take up FITC; dauer defective; severely shortened axonemes, ectopic assembly of ciliary structures and microtubules in many sensory neurons (Collet et al., 1998; Starich et al., 1995)	56 cells in the hermaphrodite: the 24 amphid neurons, twelve inner labial neurons, six outer labial neurons, four CEPs, two ADEs, four phasmid cells in all stages from late embryo through adult; AQR and PQR at L1 through adult PDE cells at L2 through adult. Additional expression in male-specific cells: CEM cells and male tail sensory cells (Collet et al., 1998)
egl-4	MT1073 (n1073) IV	PKG, cGMP-dependent protein kinase. May act through the TGF-beta signalling pathway relay sensory cues that modulate chemosensory behavior, dauer formation, foraging and egg-laying. (Fujiwara et al., 2002; Hirose et al., 2003; L'Etoile et al., 2002)	Increased body size (due to increase cell size), delayed egg-laying, increased life span, increased roaming on food, defects in chemosensation by the AWA and AWC, defects in olfactory adaptation, hypersensitive to dauer pheromone. (Fujiwara et al., 2002; Hirose et al., 2003; L'Etoile et al., 2002)	Predominantly expressed in head neurons, a few cells in the tail and hypodermis except for seam cells. Stronger or more consistent expression was observed in RMDV, RMD, SMDV, RIB, ASK and probably RMDD and SMDD neurons. Expression in AWC, ASE, AVJ and ASH was sometimes seen. In the tail, DVB and DVC neurons were probably expressing. GFP was also expressed in ventral cord neurons and intestine, typically near the tail. (Hirose et al., 2003)

osm-1	PR808 (p808) X	Putative leucine zipper transcription factor of unknown function.	Phenotypes same as in *osm-6* (Culotti and Russell, 1978; Starich et al., 1996).	N/d
che-2	CB1033 (e1033) X	A protein containing G-protein beta-like WD-40 repeats (Fujiwara et al., 1999).	Non-chemotactic to Na^+; slightly small; defective osmotic and copper avoidance; defective dauer formation; males impotent; no FITC uptake; ciliated neurons have abnormal stunted ultrastructure. (Fujiwara et al., 1999; Starich et al., 1995).	Sensory cilia of most ciliated sensory neurons. All amphid sensory neurons except AFD, phasmid neurons PHA and PHB, all the inner and outer labial neurons (IL1, IL2, OLQ and OLL), CEP, PDE, FLP, PQR, and three unidentified neurons (perhaps AQR and ADEL/R). GFP expression in N2 male tails, where there are many male-specific sensory neurons required for mating behavior. (Fujiwara et al., 1999)
osm-2 (che-3)	PR802 (p802) I	The dynein heavy chain (DHC) 1b isoform. Required for the structural integrity of sensory cilia, presumably functions in the intraflagellar transport. (Wicks et al., 2000).	Fails to take up FITC, defective chemotaxis, defective copper avoidance. Progressive developmental defects of the chemosensory cilia. (Culotti and Russell, 1978; Wicks et al., 2000).	Temporally and spatially restricted expression in ciliated sensory neurons, including: ADL, ASH, ASI, ASJ, PHA, PHB, AQR, PQR, ASE, ASG, ADF, AFD, FLP, ADE.(Wicks et al., 2000)
osm-3	PR802 (p802) IV	Heteromeric anterograde motor kinesin heavy chain subunit; required for formation of the distal segment of amphid channel cilia. May form a structural complex with KLP-11 and KAP-1 (Khan et al., 2000).	Fails to avoid 4M fructose or 4M NaCl; non-chemotactic; defective dauer formation; normal thermotaxis; fails to take up FITC (except ADF); eliminates distal segment of amphid channel; cilia in other ciliated neurons normal; accumulation of dense matrix material in the amphid sheath cytoplasm and a shortened distal segment of the amphid channel cilium octopamine-deficient. (Culotti and Russell, 1978; Shakir et al., 1993; Starich et al., 1995; Tabish et al., 1995).	26 chemosensory neurons whose dendritic endings are exposed to the external environment, including six IL2 neurons of the inner labial sensilla, eight pairs of amphid neurons (ADE ADL, ASE, ASG, ASH, ASI, ASJ, ASK) in the head, and two pairs of phasmid neurons (PHA and PHB) in the tail (Tabish et al., 1995).
ttx-1	PR767 (p767) V	OTD/OTX family homeodomain transcription factor. (Satterlee et al., 2001).	Strongly cryophilic; hypersensitive to dauer pheromone; neuron AFD lacks "fingers" (microvilli). (Mori and Ohshima, 1995; Satterlee et al., 2001).	AFD neurons, nine pharyngeal marginal cells (Satterlee et al., 2001).

odr-2	CX2304 (n2145) V	Encodes three isoforms of a predicted membrane-associated protein related to the Ly-6 (leukocyte antigen-6) family of GPI-linked signaling proteins (Chou et al., 2001).	Defective odortaxis to AWC-sensed odorants (e.g, 2,3-pentanedione) (Chou et al., 2001).	Expression driven by the 2kb upstream region was observed in AIZ, AIB, AVG, RIF, PVP, and RIV interneurons, SIAV motor neurons, and IL2 and ASG sensory neurons. Faint expression driven by the 16 kb upstream region was observed in SMD and RME motor neurons, as well as in several other neurons in a variable pattern. Expression driven by the 18 kb upstream region was observed in SMB and RME motor neurons, in ALN and PLN sensory neurons, and in RIG interneurons. Protein localizes to axons. (Chou et al., 2001).
odr-3	CX2205 (n2150) V	G protein alpha subunit (Roayaie et al., 1998).	Reduced response to all volatile odorants; defective osmotic avoidance; some chemotactic defects. Cilia of sensory neuron AWC stunted (Roayaie et al., 1998).	Expression of the GFP reporter was observed in AWA, AWB, AWC, ASH, and ADF neurons. The AWC neurons consistently expressed GFP most brightly, the AWB neurons less well, and the AWA, ASH, and ADF neurons only weakly (Roayaie et al., 1998).
odr-7	CX4 (ky4) X	A nuclear hormone receptor. Specifies AWA sensory identity by promoting the expression of AWA-specific signaling genes. (Colosimo et al., 2003; Sengupta et al., 1994)	Defective in response to diacetyl, pyrazine, some other attractants, normal response to benzaldehyde, butanone, isoamyl alcohol -- phenotype similar to AWA kill (Sengupta et al., 1994).	Only in AWA neurons (Sengupta et al., 1994).
tax-1 (che-1)	PR679 (p679) I	Zinc-finger protein. Similar to the GLASS transcription factor required for photoreceptor cell differentiation in Drosophila. Essential for specification and function of ASE neurons (Uchida et al., 2003).	Defective chemotaxis to ASE-sensed Na^+ and Cl^-. Abnormal sensory neuroanatomy especially of AFD, IL2 cells (Dusenbery et al., 1975; Uchida et al., 2003).	Only in ASE neurons (Uchida et al., 2003)

tax-6	PR675 (p675) IV	Serine/threonine protein phosphatase calcineurin A ortholog (Kuhara et al., 2002).	Small body size. Thermophylic (migrates to the temperature higher than the cultivation temperature). Hypersensitive to the osmotic stimuli sensed by the ASH neurons. Defective in odortaxis to AWA and AWC-sensed odorants. Enhanced olfactory adaptation. (Kuhara et al., 2002)	A variety of neurons, including thermosensory AFD neurons, the chemosensory ASE, AWA, and AWC neurons, osmosensory ASH neurons, ASI, ADF, ASK, ADL, AUA, PHA, PHB, AVE, AIB, AIY, AIZ, RIA, RIB, RIS, RIM, AVK, AIM, RMDV, AVA and muscle cells. (Kuhara et al., 2002)
tax-2	PR671 (p671) II	Ortholog of the human rod photoreceptor cGMP-gated channel beta subunit (Coburn et al., 1998).	Defects in thermo-, odor-, and chemotaxis. Some sensory neurons display axon outgrowth defects. (Coburn and Bargmann, 1996; Dusenbery et al., 1975).	AWC, AFD, ASE, ASG, ASJ, AQR, PQR, BAG, ASK, ASI, and AWB neurons. Tax-2::GFP fusion protein is present both in sensory cilia and in sensory axons. (Coburn and Bargmann, 1996)
osm-7	MT3564 (n1515) III	unknown	Defective osmotic avoidance; defective chemotaxis; slow pharyngeal pumping; FITC uptake normal (Thomas JH and HR, 1988).	N/d
osm-9	CX10 (ky10) IV	TRP channel, similar to the mammalian capsaicin receptor VR1 (Colbert et al., 1997).	Defective in osmotic and nose touch avoidance; partly defective adaptation to isoamyl alcohol and butanone; normal chemotaxis. (Colbert et al., 1997)	Neurons: OLQ and IL2 neurons in the anterior ganglion, the AWA, AWC, ASE, ADF, ASG, ASH, ASI, ASJ, ASK, and ADL neurons in the amphid sensory structure, the FLP and PVD neurons in the body, the PHA and PHB neurons in the phasmid sensory structure. Rectal gland cells and few cells in the ventral uterine region (Colbert et al., 1997).
ncs-1	XA406 (qa406) X	Neuronal calcium sensor. Regulates thermotactic behavior. NCS-1 is necessary in the AIY interneuron, but not in the AFD sensory neuron (Gomez et al., 2001).	Defective isothermal tracking behavior. Chemotactis, locomototion, and thermal avoidance are normal. (Gomez et al., 2001)	Sensory neurons (10 pairs: AWC, ASE, AWB, BAG, PHB, AWA, AFD, ADF, ASG, PHA), two pairs of interneurons (AVK, AIY), one motor neuron (RMG), and one pharyngeal muscle cell pm1 (Gomez et al., 2001).
mec-3	CB1338 (e1338) IV	LIM homeodomain transcription factor essential for proper differentiation of the set of six touch receptor neurons in C. elegans (Way and Chalfie, 1988).	Touch insensitive, lethargic. Abnormal processes of mechanosensory neurons. (Chalfie and Sulston, 1981; Way and Chalfie, 1988).	Touch receptor neurons: ALML/R, AVM, PVM and PLML/R, FLPL/R and PVDL/R (Way and Chalfie, 1988).

unc-86	CB1416 (e1416) III	POU-type homeodomain transcription factor; human BRN-3 ortholog. Required for the fate determination in diverse neuronal lineages, including egg-laying, mechanosensory, and chemosensory neurons. Positively regulates MEC-3. (Finney and Ruvkun, 1990; Xue et al., 1992).	Touch insensitive (touch cells absent); lethargic, egg-laying-defective (HSN cells fail to differentiate); non-chemotactic to NaCl; multiple neuronal lineage abnormalities. AIZ interneurons fail to develop (Finney and Ruvkun, 1990).	Neurons, including RIH, RIR, PVR, IL2L/R, URYVL/R, RIPL/R, AIZL/R, FLPL/R, ADAL/R, RMGL/R, BPUL/R, PLML/R, ALML/R, ALNL/R, HSNL/R, URBL/R, NSML/R, URADL/R, URADL/R, IL2DL/R, I2L/R, IL2VL/R, URAVL/R, URXL/R, AIML/R, URYDL/R, PQR, PVM, SDQL/R, PVDL/R, PHCL/R, PLNL/R (Finney and Ruvkun, 1990).
npr-1	DA609 (ad609) X	Neuropeptide Y (NPY) receptor ortholog (de Bono and Bargmann, 1998). Inhibits social feeding. Responsible for the variability in social feeding behavior between different wild *C.elegans* strains.	Social (bordering) behavior: worms clump together on the border of the bacterial lawn (Coates and de Bono, 2002; de Bono and Bargmann, 1998; de Bono et al., 2002).	Neurons: AQR, ASE, ASG, ASH (L4/adult stages only), SDQ, PQR, PHA and PHB. RIV, RIG, URX, IL2L/R and OLQ (with its socket and sheath cells), the interneurons AUA and SAAD, the motor neurons RMG and SMBD, pharyngeal neuron M3. In the ventral nerve cord, in the GABA-containing VD and DD motorneurons. Non-neuronal: terminal bulb of the pharynx, excretory duct cell and excretory canal. (Coates and de Bono, 2002).
hen-1	JC2154 (tm501) X	Secretory protein that contains a low-density lipoprotein receptor class A domain (Ishihara et al., 2002).	Hesitation in crossing an aversive ion. Defective in behavioral plasticity after conditioned with NaCl and starvation or with temperature and starvation (Ishihara et al., 2002).	AIY and ASE neurons; pharyngeal muscles and vulva (Ishihara et al., 2002).
ceh-10	BW506 (ct78) III	Paired-like homeodomain transcription factor. Required for CAN cell fate specification and migration. CEH-10, along with TTX-3 and CEH-23, constitutes a regulatory cascade that controls differentiation of the AIY interneurons. (Altun-Gultekin et al., 2001; Forrester et al., 1998).	Withered tail. Adults shorter than WT. Embryonic cell migrations affected: CAN migration with high penetrance.(Altun-Gultekin et al., 2001; Forrester et al., 1998).	AIYL/R, CEPDL/R, RID, ALA, RMED, AINL/R, AVJL/R and CAN cells (the excretory Canal Associated Neuron) (Svendsen and McGhee, 1995).

bas-1	MT7988 (ad446) III	Serotonin- and dopamine-synthetic aromatic amino acid decarboxylase (AAADC) that is required for the synthesis of serotonin from 5-hydroxytryptophan (Loer and Kenyon, 1993).	Serotonin-deficient (no detectable serotonin immunoreactivity), poor male turning behavior during mating (Loer and Kenyon, 1993).	Serotonergic and dopaminergic neurons, including CEP, ADE, NSM, ADF, HSN, RN, PDE and CP (Hare and Loer, 2004).
cat-4	CB1141 (e1141) V	An ortholog of the human GTP cyclohydrolase I, involved in serotonin and dopamine biosynthesis. Synthesizes the biopterin cofactor required for the TPH-1 activity (Loer and Kenyon, 1993).	Dopamine reduced > 90%, serotonin greatly reduced; poor male turning behavior; enhanced foraging behavior (Loer and Kenyon, 1993; Ranganathan et al., 2001; Sulston et al., 1975).	N/d
cat-2	CB1112 (e1112) II	A putative tyrosine hydroxylase in the dopamine biosynthesis pathway (Lints and Emmons, 1997).	Dopamine reduced > 95%; serotonin normal; no defect in male turning behavior (Loer and Kenyon, 1993; Sulston et al., 1975).	CEP, ADE, and PDE neurons (Suo et al., 2003).
tph-1	GR1321 (mg280) II	Tryptophan hydroxylase involved in serotonin biosynthesis (Sze et al., 2000).	Slow pumping. Egg laying defective. Low frequency of dauer formation. Residual serotonin immunoreactivity, rare and very faint (<1% of NSMs) in most stages, but nearly 100% of CP neurons in adult males show faint to moderate serotonin immunoreactivity (Sze et al., 2000).	Serotonergic neurons: NSM, ADF, hermaphrodite-specific HSN, male-specific CP, and, rarely, AIM and RIH (Sze et al., 2000).
unc-29	CB193 (e193) I	A non-alpha subunit of the nicotinic acetylcholine receptor (nAChR). Neurotransmission to the body wall muscle (Fleming et al., 1997; Richmond and Jorgensen, 1999).	Very sluggish, weak kinker, head region stiff. Moves better in reverse; resistant to 1 mM levamisole; sensitive to hypoosmotic shock (Brenner, 1974).	Body wall muscle (Fleming et al., 1997).

unc-2	CB55 (e55) X	An N-type Ca channel alpha subunit; orthologous to human CACNA1A (Schafer and Kenyon, 1995).	Weak kinker; sluggish; thin; hypersensitive to serotonin, fails to desensitize to dopamine. Defective in MAP kinase activation in odorant-stimulated AWC neurons. (Brenner, 1974; Hirotsu et al., 2000; Schafer and Kenyon, 1995).	Nervous system: most motor neurons in the ventral nerve cord, nerve ring neurons (including AWA), touch cells (including AVM), HSN neurons. A subset of pharyngeal muscle cells. (Mathews et al., 2003).
unc-36	CB251 (e251) III	alpha2/delta subunit of the voltage-dependent Ca^{2+} channel.	Very slow, almost paralysed, thin and slightly small; hypersensitive to serotonin, fails to adapt to dopamine (like *unc-2*); hypersensitive to verapamil. Pharyngeal pumping slow and irregular, slippery corpus and isthmus; increased sensitivity to arecoline. (Avery, 1993a; Brenner, 1974).	N/d

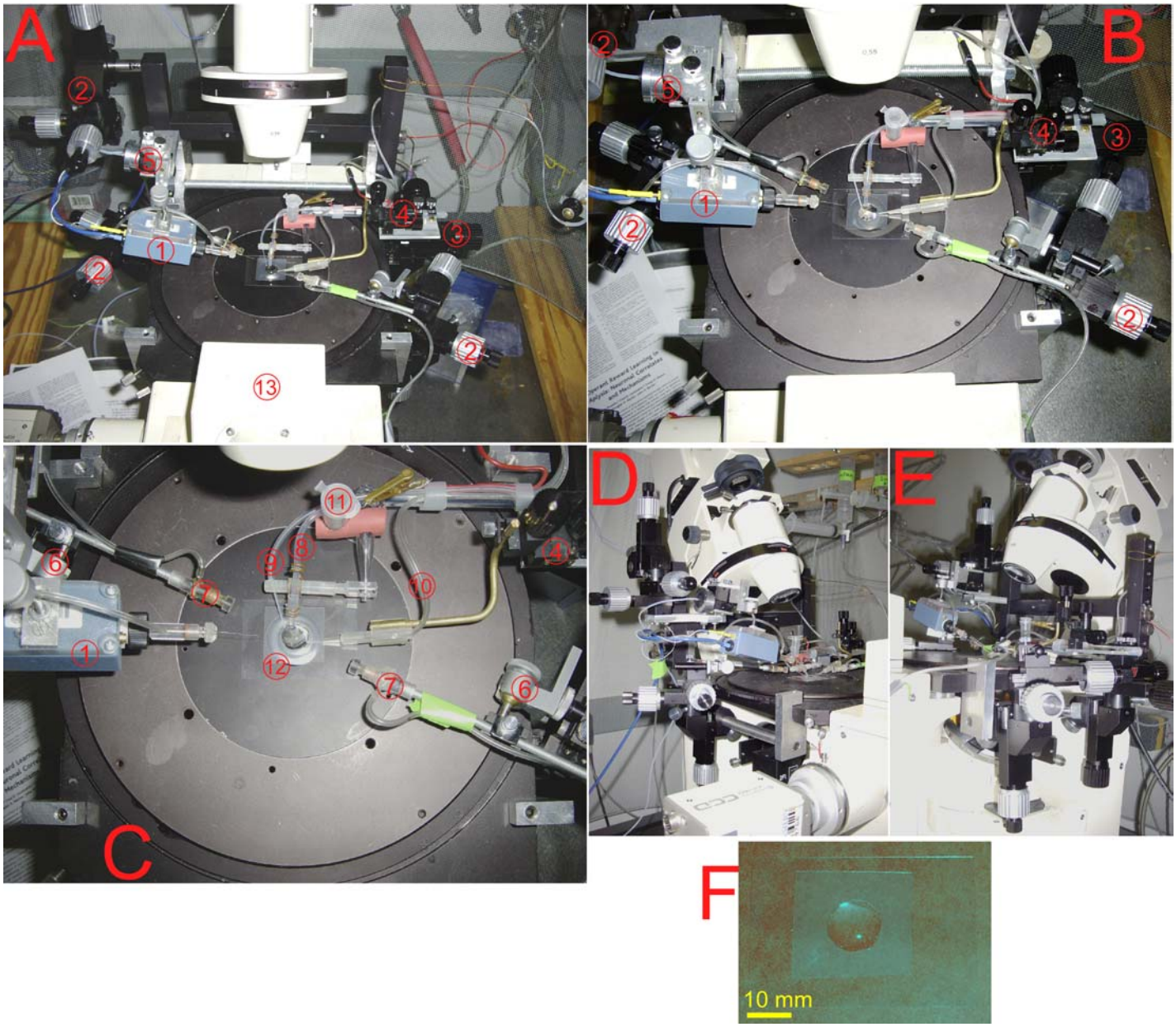

Figure 1. **The voltage clamp setup. (A)** General view. **(B)** Top view. **(C)** Top view, close-up. **(D)** Left view. **(E)** Right view. **(F)** Recording chamber.

Parts: 1) Recording headstage (HS-2A 0.1LU, Axon Instruments, Union City, CA). 2) Manipulator (UMM-3FC, You Ltd, Japan). 3) Manipulator (UMM-3C, You Ltd, Japan). Holds an assembly of items 9 to 11. 4) Manipulator holding the aspiration line (U-3MC, You Ltd, Japan). 5) One-axis water hydraulic manipulator holding the headstage (MHW-4, Narishige, Japan). Attached to the UMM-3FC (2) via the adapter. 6) Ball joint (B-8D, Narishige, Japan). 7) Pipette holder (MPH4, World Precision instruments, Sarasota, FL). Dissection pipettes are fixed in these holders and connected to syringes. 8) 0.5 M NaCl agarose bridge. 9) Perfusion line. 10) Aspiration line. 11) 1.5 mL eppendort tube with 0.5 M NaCl. 12) Recording chamber. 13) Axiovert 35 inverted microscope (Zeiss, Germany).

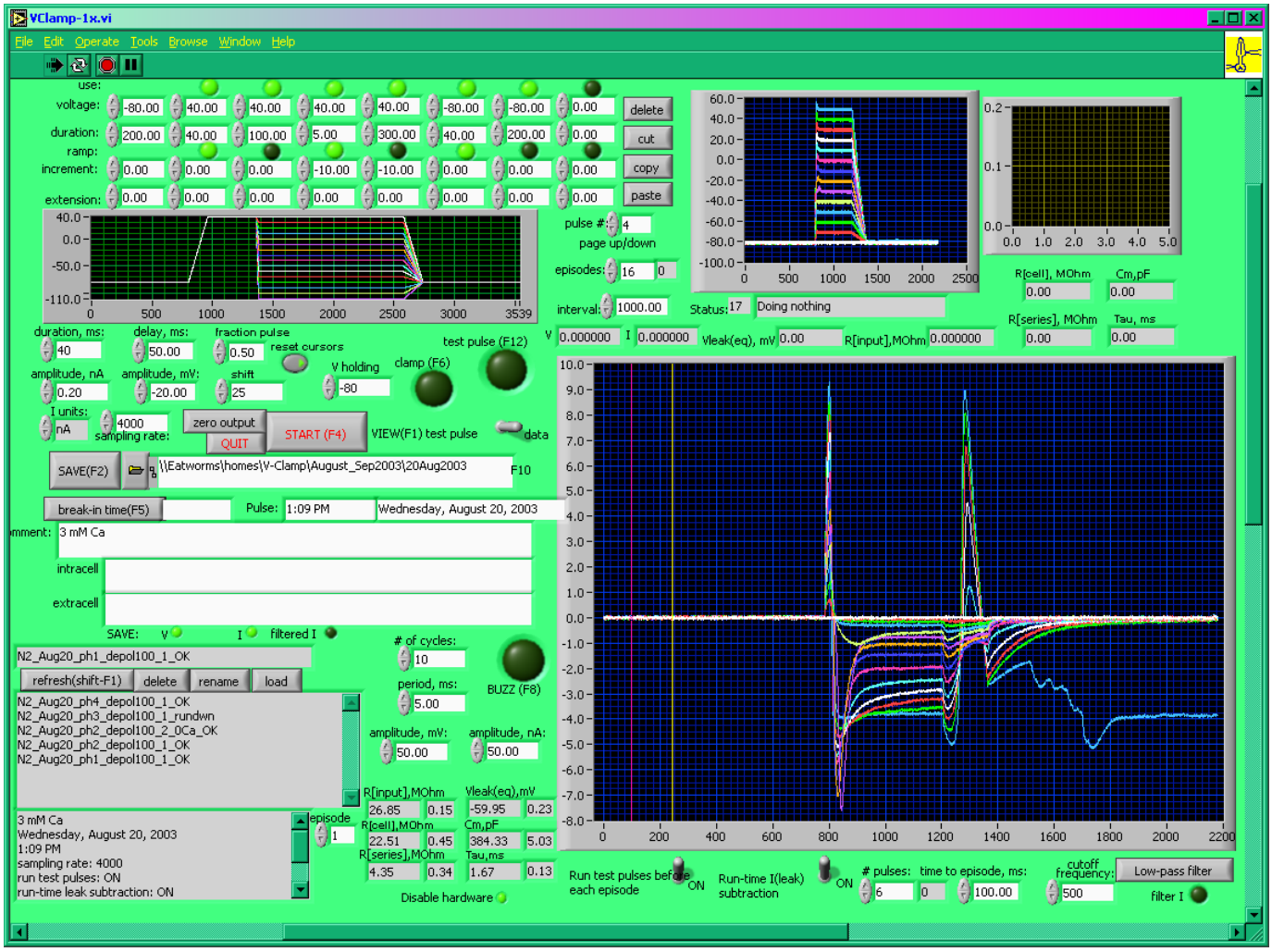

Figure 2. **The Labview program used for voltage clamp experiments.** Allows design of voltage pulses of up to 8 steps. Records both voltage and current, calculates Cm, Rm, Rs, Vleak, can auto-subtract the leak current. Saves data as a text spreadsheet, which can be opened in Microsoft Exel or Microcal Origin. Can also load and view existing data.

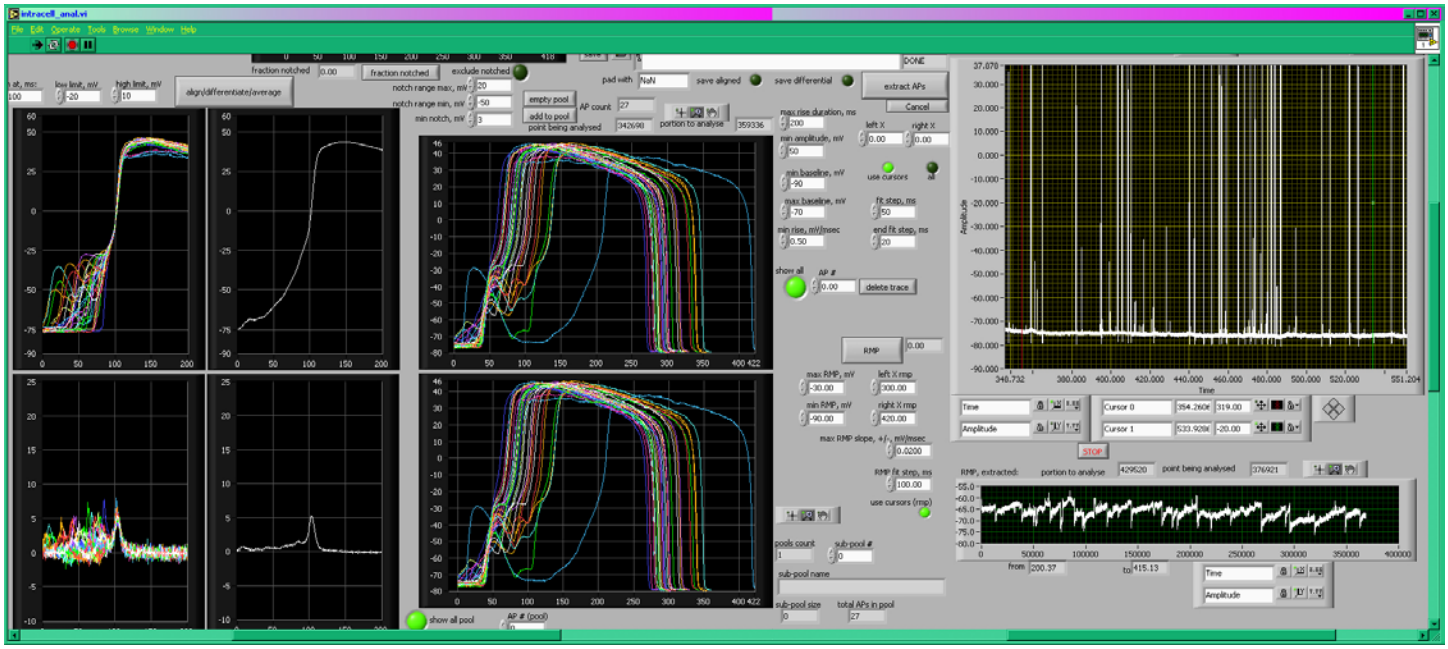

Figure 3. **The Labview program used for analysis of current clamp recordings.** Extracts action potentials from the trace. Calculates RMP. Aligns and differentiates action potentials. Open files saved with Accbin (Raizen and Avery, 1994). Saves data in text format.

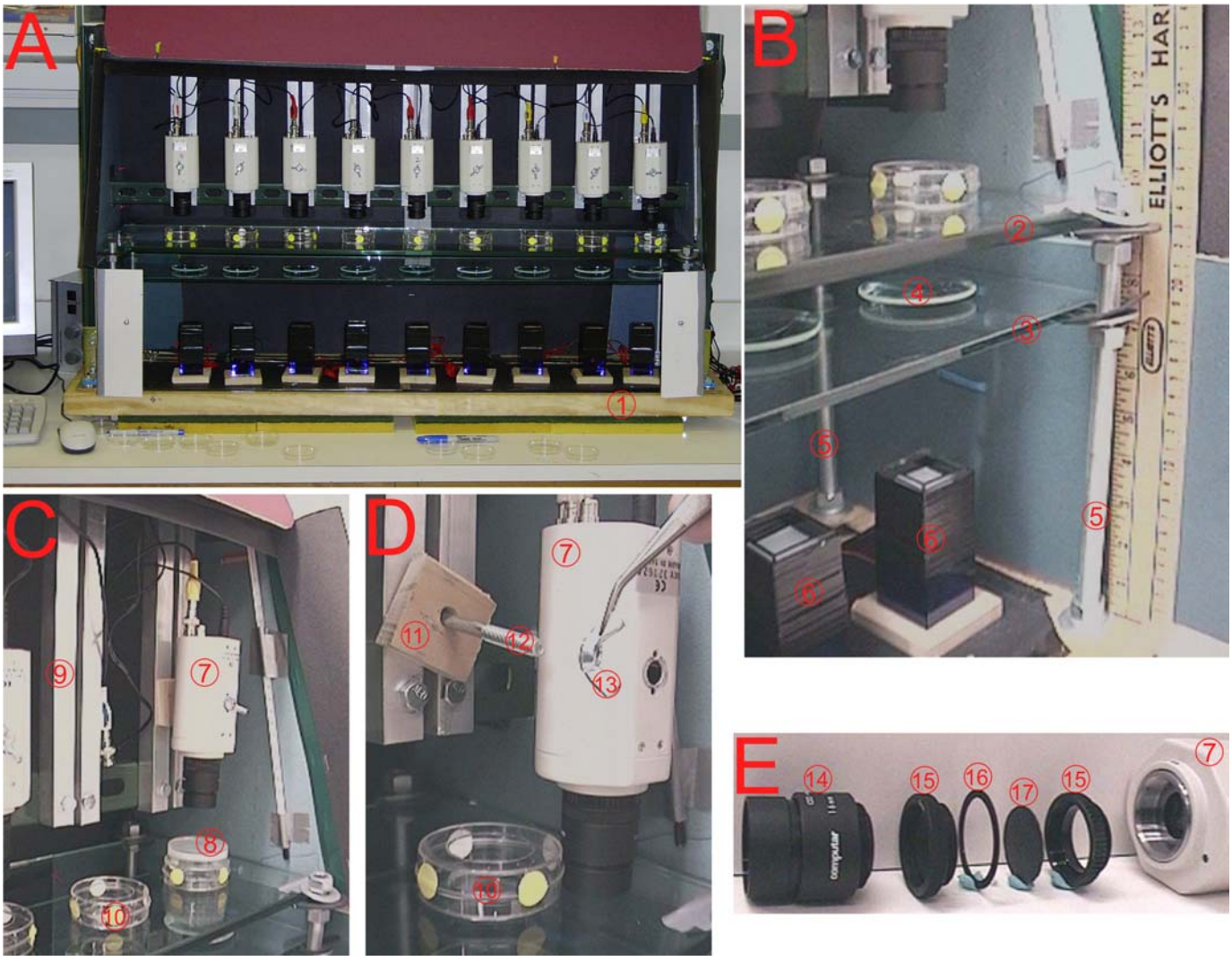

Figure 4. **The video recording apparatus. (A)** General view. The rack was build of steel rails and fixed on the wooden base (1). **(B, (C)** and **(D)** close-ups. Two glass shelves (2,3) were fixed on threaded rods (5) at 19 and 23.5 cm off the base. Condenser lenses (4) were placed on the bottom shelf. Assay plates (8) were placed inverted on the top shelf with the spacer (10) to prevent moisture condensation on the glass shelf. The cameras (7) were fixed on aluminum rails (9) with screws (12) **(E)** Objective assembly. Spacers (15,16) were inserted to increase magnification; a diaphragm (17) was used to kill aberrations.

Parts: 1) Base, a wooden board 114x28cm, 3.5 inch think. 2) Glass shelf, 100.5x21.5 cm, 3/8 inch thick. 3) Glass shelf, 100.5x21.5 cm, 3/16 inch thick. 4) Condenser lens (Magnifier low-grade lens, fd=12.5 cm, Fry's electronics). 5) Steel threaded rods, ½ inch thread, 30 cm long. 6) Light sources (see Appendix Fig. 2). 7) Video camera (PC23C, Supercircuits, Liberty Hill, TX). 8) 50 mm assay plate. 9) Aluminum rails, ¾ inch section, 31 cm long. 10) Spacer, made of two 50 mm plate lids with 30 mm holes drilled in them. 11) Wooden spacer, ½ inch thick. 12) Screw, ¼ inch thread, 3.5 inch long. 13) Nut. 14) Camera lens (M1614, 16mm, monofocal, 2/3" C-Mount, f1.4, Computar, Commack, NY). 15) 5 mm spacer ring (Extension Tube Kit VM100, Computar). 16) 1 mm spacer ring (VM100, Computar). 17) Diaphragm, made of black cardboard; a small hole in the center was burnt with the needle.

Figure 5. **The light source used in video recording apparatus. (A)** Parts. 1) Wooden base (approx. 65 x 65 mm 1/2 inch thick), 2) Condenser lens (a magnifying "bug box", fd = 105mm, lens 30 mm diameter, purchased in Container Store). 3) Light bulb cartridge (Radio Shack). 4) 6V light bulb (Radio Shack). 5) Plastic box (40x40x53 mm, Container Store). 6) A piece of opaque plastic (cut to tightly fit the "bug box", 31x31 mm) **(B)** Top view with lenses removed and the light bulb installed **(C)** Condenser lens assembly. Two magnifying "bug boxes" are taped together with lenses facing each other, so the final focal distance is about 53 mm; the opaque plastic is placed on top. **(D)** The arrangement of parts. **(E)** Final assembly. All parts are fixed together with electric tape.

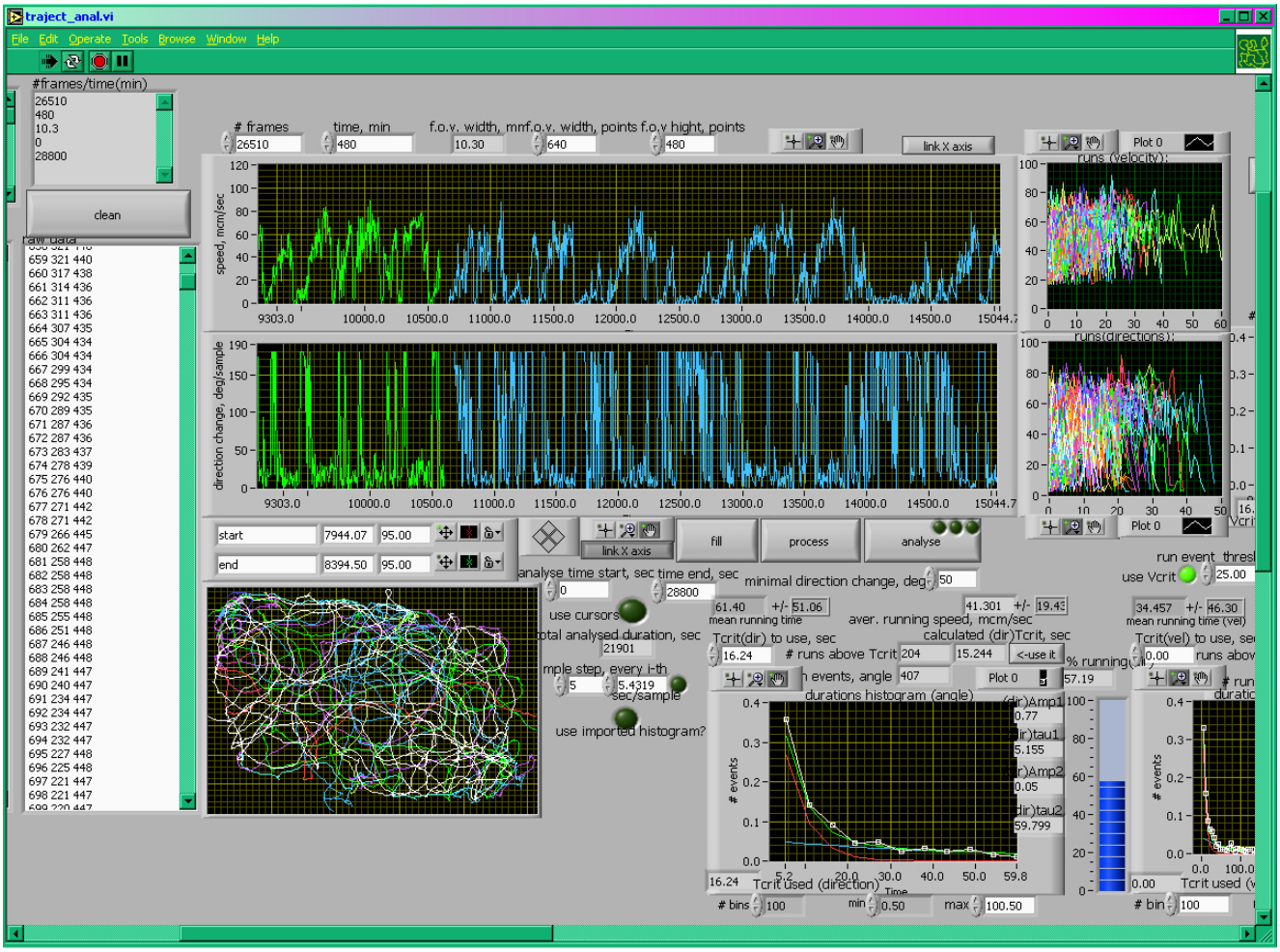

Figure 6. **The Labview program used for the trajectory analysis.** Calculates speed and turning angle from the coordinate data. Extracts long movements using the thresholding procedure (Pierce-Shimomura et al., 1999). Trajectory data can be copied from Exel; histogram data can be copied into the clipboard.

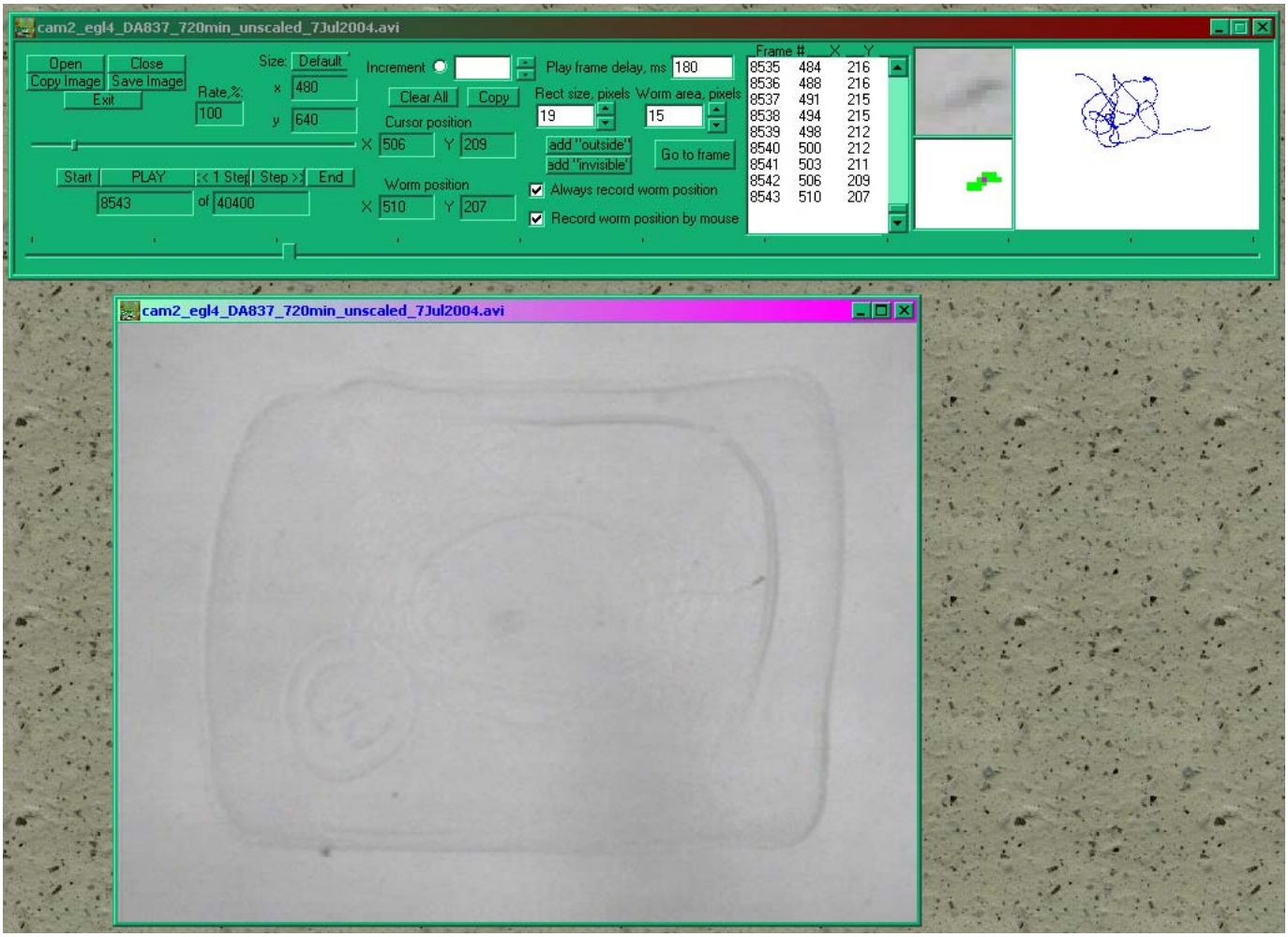

Figure 7. **The program used to trace the worm's trajectory.** Uses Microsoft DirectX 9.0 VMR9 interface (requires the video adapter that supports it). Loads video file of unlimited size. Traces the worm trajectory. Coordinate data can be copied to the clipboard and pasted into Exel.

REFERENCES

Aguinaldo, A.M., Turbeville, J.M., Linford, L.S., Rivera, M.C., Garey, J.R., Raff, R.A. and Lake, J.A. (1997) Evidence for a clade of nematodes, arthropods and other moulting animals. *Nature*, **387**, 489-493.

Albertson, D.G. and Thomson, J.N. (1976) The pharynx of *Caenorhabditis elegans*. *Philos Trans R Soc Lond B Biol Sci.*, **275**, 299-325.

Altun-Gultekin, Z., Andachi, Y., Tsalik, E.L., Pilgrim, D., Kohara, Y. and Hobert, O. (2001) A regulatory cascade of three homeobox genes, ceh-10, ttx-3 and ceh-23, controls cell fate specification of a defined interneuron class in C. elegans. *Development*, **128**, 1951-1969.

Andrew, P.A. and Nicholas, W.L. (1976) Effect of bacteria on dispersal of Caenorhabditis elegans (Rhabditidae). *Nematologica*, **22**, 451-461.

Anokhin, P.K. (1974) *Biology and neurophysiology of the conditioned reflex and its role in adaptive behavior*. Pergamon Press, Oxford, New York,.

Anselmo, S.S. and Avery, L. (2004) eat-17 encodes a putative Rab GTPase activating protein that acts in concert with RAB-6.2 to promote proper grinder formation in C.elegans. *West Coast Worm Meeing Abstracts*, **46**.

Avery, L. (1993a) The genetics of feeding in Caenorhabditis elegans. *Genetics.*, **133**, 897-917.

Avery, L. (1993b) Motor neuron M3 controls pharyngeal muscle relaxation timing in Caenorhabditis elegans. *J Exp Zool.*, **175**, 283-297.

Avery, L. and Horvitz, H.R. (1989) Pharyngeal pumping continues after laser killing of the pharyngeal nervous system of C. elegans. *Neuron.*, **3**, 473-485.

Avery, L. and Horvitz, H.R. (1990) Effects of starvation and neuroactive drugs on feeding in Caenorhabditis elegans. *J Exp Zool.*, **253**, 263-270.

Avery, L. and Shtonda, B.B. (2003) Food transport in the *C elegans* pharynx. *J Exp Biol*, **206**, 2441-2457.

Bargmann, C.I. (1998) Neurobiology of the Caenorhabditis elegans genome. *Science*, **282**, 2028-2033.

Bargmann, C.I. and Avery, L. (1995) Laser killing of cells in Caenorhabditis elegans. *Methods Cell Biol*, **48**, 225-250.

Belluscio, L., Gold, G.H., Nemes, A. and Axel, R. (1998) Mice deficient in G(olf) are anosmic. *Neuron*, **20**, 69-81.

Berridge, K.C. (1996) Food reward: brain substrates of wanting and liking. *Neurosci Biobehav Rev*, **20**, 1-25.

Berridge, K.C. and Robinson, T.E. (2003) Parsing reward. *Trends Neurosci*, **26**, 507-513.

Bessou, C., Giugia, J.B., Franks, C.J., Holden-Dye, L. and Segalat, L. (1998) Mutations in the Caenorhabditis elegans dystrophin-like gene dys-1 lead to hyperactivity and suggest a link with cholinergic transmission. *Neurogenetics*, **2**, 61-72.

Boyer, H.W. and Roulland-Dussoix, D. (1969) A complementation analysis of the restriction and modification of DNA in Escherichia coli. *J Mol Biol*, **41**, 459-472.

Brembs, B., Lorenzetti, F.D., Reyes, F.D., Baxter, D.A. and Byrne, J.H. (2002) Operant reward learning in Aplysia: neuronal correlates and mechanisms. *Science*, **296**, 1706-1709.
Brenner, S. (1974) The genetics of Caenorhabditis elegans. *Genetics*, **77**, 71-94.
Briggs, M.P. (1946) *Culture methods for a free-living soil nematode. M.A. Thesis.* Stanford University, Stanford, CA.
Byerly, L. and Masuda, M.O. (1979) Voltage-clamp analysis of the potassium current that produces a negative-going action potential in Ascaris muscle. *J Physiol*, **288**, 263-284.
Cabanac, M. (1971) Physiological role of pleasure. *Science*, **173**, 1103-1107.
Capaldi, E. (1996) *Why we eat what we eat : the psychology of eating*. American Psychological Association, Washington, DC.
Chalfie M and J, W. (1988) The nervous system. In: The Nematode C. elegans. (Wood W, ed). In, Cold Spring Harbor, New York: Cold Spring Harbor Laboratory, pp. 337-391.
Chalfie, M. and Sulston, J. (1981) Developmental genetics of the mechanosensory neurons of Caenorhabditis elegans. *Dev Biol*, **82**, 358-370.
Chou, J.H., Bargmann, C.I. and Sengupta, P. (2001) The Caenorhabditis elegans odr-2 gene encodes a novel Ly-6-related protein required for olfaction. *Genetics*, **157**, 211-224.
Coates, J.C. and de Bono, M. (2002) Antagonistic pathways in neurons exposed to body fluid regulate social feeding in Caenorhabditis elegans. *Nature*, **419**, 925-929.
Coburn, C.M. and Bargmann, C.I. (1996) A putative cyclic nucleotide-gated channel is required for sensory development and function in C. elegans. *Neuron*, **17**, 695-706.
Coburn, C.M., Mori, I., Ohshima, Y. and Bargmann, C.I. (1998) A cyclic nucleotide-gated channel inhibits sensory axon outgrowth in larval and adult Caenorhabditis elegans: a distinct pathway for maintenance of sensory axon structure. *Development*, **125**, 249-258.
Colbert, H.A. and Bargmann, C.I. (1995) Odorant-specific adaptation pathways generate olfactory plasticity in C. elegans. *Neuron*, **14**, 803-812.
Colbert, H.A. and Bargmann, C.I. (1997) Environmental signals modulate olfactory acuity, discrimination, and memory in Caenorhabditis elegans. *Learn Mem*, **4**, 179-191.
Colbert, H.A., Smith, T.L. and Bargmann, C.I. (1997) OSM-9, a novel protein with structural similarity to channels, is required for olfaction, mechanosensation, and olfactory adaptation in Caenorhabditis elegans. *J Neurosci*, **17**, 8259-8269.
Collet, J., Spike, C.A., Lundquist, E.A., Shaw, J.E. and Herman, R.K. (1998) Analysis of osm-6, a gene that affects sensory cilium structure and sensory neuron function in Caenorhabditis elegans. *Genetics*, **148**, 187-200.
Colosimo, M.E., Tran, S. and Sengupta, P. (2003) The divergent orphan nuclear receptor ODR-7 regulates olfactory neuron gene expression via multiple mechanisms in Caenorhabditis elegans. *Genetics*, **165**, 1779-1791.
Croll, N.A. (1975) Components and patterns in the behavior of the nematode Caenorhabditis elegans. *J. Zool. (Lond.)*, **176**, 159-176.
Culotti, J.G. and Russell, R.L. (1978) Osmotic avoidance defective mutants of the nematode Caenorhabditis elegans. *Genetics*, **90**, 243-256.

Curtis, H.J. and Cole, K.S. (1938) Transverse electric impedance of the squid giant axon. *J. Gen. Physiol.*, **21**, 757-765.
Davis, M.W. (1995) Intracellular recording from pharyngeal muscles. *Worm Breeder's Gazette*, **13**, 34.
Davis, M.W. (1999) *Regulation of the relaxation phase of the C. elegans pharyngeal muscle action potential. In: PhD dissertation The University of Texas Southwestern Medical Center at Dallas.*
Davis, M.W., Fleischhauer, R., Dent, J.A., Joho, R.H. and Avery, L. (1999) A mutation in the C. elegans EXP-2 potassium channel that alters feeding behavior. *Science.*, **286**, 2501-2504.
Davis, M.W., Somerville, D., Lee, R.Y., Lockery, S., Avery, L. and Fambrough, D.M. (1995) Mutations in the Caenorhabditis elegans Na,K-ATPase alpha-subunit gene, eat-6, disrupt excitable cell function. *J Neurosci*, **15**, 8408-8418.
de Bono, M. and Bargmann, C.I. (1998) Natural variation in a neuropeptide Y receptor homolog modifies social behavior and food response in C. elegans. *Cell*, **94**, 679-689.
de Bono, M., Tobin, D.M., Davis, M.W., Avery, L. and Bargmann, C.I. (2002) Social feeding in Caenorhabditis elegans is induced by neurons that detect aversive stimuli. *Nature*, **419**, 899-903.
Dent, J.A. and Avery, L. (1993) A defined medium for the pharynx. *Worm Breeder's Gazette*, **13**, 44.
Dent, J.A., Davis, M.W. and Avery, L. (1997) avr-15 encodes a chloride channel subunit that mediates inhibitory glutamatergic neurotransmission and ivermectin sensitivity in Caenorhabditis elegans. *EMBO J.*, **16**, 5867-5879.
DiFrancesco, D. (1993) Pacemaker mechanisms in cardiac tissue. *Annu Rev Physiol*, **55**, 455-472.
DiLeone, R.J., Georgescu, D. and Nestler, E.J. (2003) Lateral hypothalamic neuropeptides in reward and drug addiction. *Life Sci*, **73**, 759-768.
Doncaster, C.C. (1962) Nematode feeding mechanisms. I. Observations on *Rhabditis* and *Pelodera*. *Nematologica.*, **8**, 313-320.
Dusenbery, D.B., Sheridan, R.E. and Russell, R.L. (1975) Chemotaxis-defective mutants of the nematode Caenorhabditis elegans. *Genetics*, **80**, 297-309.
Elizalde, G. and Sclafani, A. (1990) Flavor preferences conditioned by intragastric polycose infusions: a detailed analysis using an electronic esophagus preparation. *Physiol Behav*, **47**, 63-77.
Finney, M. and Ruvkun, G. (1990) The unc-86 gene product couples cell lineage and cell identity in C. elegans. *Cell*, **63**, 895-905.
Fleischhauer, R., Davis, M.W., Dzhura, I., Neely, A., Avery, L. and Joho, R.H. (2000) Ultrafast inactivation causes inward rectification in a voltage-gated K(+) channel from Caenorhabditis elegans. *J Neurosci*, **20**, 511-520.
Fleming, J.T., Squire, M.D., Barnes, T.M., Tornoe, C., Matsuda, K., Ahnn, J., Fire, A., Sulston, J.E., Barnard, E.A., Sattelle, D.B. and Lewis, J.A. (1997) Caenorhabditis elegans levamisole resistance genes lev-1, unc-29, and unc-38 encode functional nicotinic acetylcholine receptor subunits. *J Neurosci*, **17**, 5843-5857.

Forrester, W.C., Perens, E., Zallen, J.A. and Garriga, G. (1998) Identification of Caenorhabditis elegans genes required for neuronal differentiation and migration. *Genetics*, **148**, 151-165.

Francis, M.M., Mellem, J.E. and Maricq, A.V. (2003) Bridging the gap between genes and behavior: recent advances in the electrophysiological analysis of neural function in Caenorhabditis elegans. *Trends Neurosci*, **26**, 90-99.

Franks, C.J., Pemberton, D., Vinogradova, I., Cook, A., Walker, R.J. and Holden-Dye, L. (2002) Ionic basis of the resting membrane potential and action potential in the pharyngeal muscle of Caenorhabditis elegans. *J Neurophysiol*, **87**, 954-961.

Fujiwara, M., Ishihara, T. and Katsura, I. (1999) A novel WD40 protein, CHE-2, acts cell-autonomously in the formation of C. elegans sensory cilia. *Development*, **126**, 4839-4848.

Fujiwara, M., Sengupta, P. and McIntire, S.L. (2002) Regulation of body size and behavioral state of C. elegans by sensory perception and the EGL-4 cGMP-dependent protein kinase. *Neuron*, **36**, 1091-1102.

Galef, B.G., Jr., Kenneth, D.J. and Wigmore, S.W. (1984) Transfer of information concerning distant food in rats: A robust phenomenon. *Animal Learning and Behavior*, **12**, 292-296.

Garcia, J., Kimeldorf, D.J. and Koelling, R.A. (1955) Conditioned aversion to saccharin resulting from exposure to gamma radiation. *Science*, **122**, 157-158.

Garcia, J., McGowan, B.K., Ervin, F.R. and Koelling, R.A. (1968) Cues: their relative effectiveness as a function of the reinforcer. *Science*, **160**, 794-795.

Garsin, D.A., Sifri, C.D., Mylonakis, E., Qin, X., Singh, K.V., Murray, B.E., Calderwood, S.B. and Ausubel, F.M. (2001) A simple model host for identifying Gram-positive virulence factors. *Proc Natl Acad Sci U S A*, **98**, 10892-10897.

Gentet, L.J., Stuart, G.J. and Clements, J.D. (2000) Direct measurement of specific membrane capacitance in neurons. *Biophys J*, **79**, 314-320.

Ghosh, R., Lipton, J.O. and Emmons, S.W. (2003) Molecular genetics of male leaving, a sexually dimorphic behavior in C.elegans. *International Worm Meeting Abstracts*, 427.

Gillessen, T. and Alzheimer, C. (1997) Amplification of EPSPs by low Ni(2+)- and amiloride-sensitive Ca2+ channels in apical dendrites of rat CA1 pyramidal neurons. *J Neurophysiol*, **77**, 1639-1643.

Gomez, M., De Castro, E., Guarin, E., Sasakura, H., Kuhara, A., Mori, I., Bartfai, T., Bargmann, C.I. and Nef, P. (2001) Ca2+ signaling via the neuronal calcium sensor-1 regulates associative learning and memory in C. elegans. *Neuron*, **30**, 241-248.

Goodman, M.B., Hall, D.H., Avery, L. and Lockery, S.R. (1998) Active currents regulate sensitivity and dynamic range in C. elegans neurons. *Neuron*, **20**, 763-772.

Gray, J.M., Hill, J.J. and Bargmann, C.I. (2004a) Mapping a navigational circuit in C.elegans. *West Coast Worm Meeing Abstracts*, **36**.

Gray, J.M., Karow, D.S., Lu, H., Chang, A.J., Chang, J.S., Ellis, R.E., Marletta, M.A. and Bargmann, C.I. (2004b) Oxygen sensation and social feeding mediated by a C. elegans guanylate cyclase homologue. *Nature*, **430**, 317-322.

Grewal, P.S. and Wright, D.J. (1992) Migration of *Caenorhabditis elegans* (Nematoda : Rhabditidae) larvae towards bacteria and the nature of the bacterial stimulus. *Fundam. appl. Nematol.*, **15**, 159-166.

Grill, H.J. and Norgren, R. (1978a) The taste reactivity test. I. Mimetic responses to gustatory stimuli in neurologically normal rats. *Brain Res*, **143**, 263-279.

Grill, H.J. and Norgren, R. (1978b) The taste reactivity test. II. Mimetic responses to gustatory stimuli in chronic thalamic and chronic decerebrate rats. *Brain Res*, **143**, 281-297.

Hagiwara, N., Irisawa, H. and Kameyama, M. (1988) Contribution of two types of calcium currents to the pacemaker potentials of rabbit sino-atrial node cells. *J Physiol (Lond).* **395**, 233-253.

Hare, E.E. and Loer, C.M. (2004) Function and evolution of the serotonin-synthetic bas-1 gene and other aromatic amino acid decarboxylase genes in Caenorhabditis. *BMC Evol Biol*, **4**, 24.

Harris, L.J., Clay, J., Hargreaves, F.J. and Ward, A. (1933) Appetite and choice of diet; the ability of the vitamin B deficient rat to discriminate between diets containing and lacking the vitamin. *Proc. Royal Soc.*, **113**, 161-190.

Hedgecock, E.M. and Russell, R.L. (1975) Normal and mutant thermotaxis in the nematode Caenorhabditis elegans. *Proc Natl Acad Sci U S A*, **72**, 4061-4065.

Hille, B. (2001) *Ion channels of excitable membranes*. Sinauer, Sunderland, Mass.

Hills, T., Brockie, P.J. and Maricq, A.V. (2004) Dopamine and glutamate control area-restricted search behavior in Caenorhabditis elegans. *J Neurosci*, **24**, 1217-1225.

Hirose, T., Nakano, Y., Nagamatsu, Y., Misumi, T., Ohta, H. and Ohshima, Y. (2003) Cyclic GMP-dependent protein kinase EGL-4 controls body size and lifespan in C elegans. *Development*, **130**, 1089-1099.

Hirotsu, T., Saeki, S., Yamamoto, M. and Iino, Y. (2000) The Ras-MAPK pathway is important for olfaction in Caenorhabditis elegans. *Nature*, **404**, 289-293.

Hobert, O. (2003) Behavioral plasticity in C. elegans: paradigms, circuits, genes. *J Neurobiol*, **54**, 203-223.

Hobert, O., Mori, I., Yamashita, Y., Honda, H., Ohshima, Y., Liu, Y. and Ruvkun, G. (1997) Regulation of interneuron function in the C. elegans thermoregulatory pathway by the ttx-3 LIM homeobox gene. *Neuron*, **19**, 345-357.

Hullar, I., Fekete, S., Andrasofszky, E., Szocs, Z. and Berkenyi, T. (2001) Factors influencing the food preference of cats. *J Anim Physiol Anim Nutr (Berl)*, **85**, 205-211.

Ishihara, T., Iino, Y., Mohri, A., Mori, I., Gengyo-Ando, K., Mitani, S. and Katsura, I. (2002) HEN-1, a secretory protein with an LDL receptor motif, regulates sensory integration and learning in Caenorhabditis elegans. *Cell*, **109**, 639-649.

Jaffe, J.H., Cascella, N.G., Kumor, K.M. and Sherer, M.A. (1989) Cocaine-induced cocaine craving. *Psychopharmacology (Berl)*, **97**, 59-64.

Jansson, H.-B. (1994) Adhesion of conidia of Drechmeria coniospora to Caenorhabditis elegans wild type and mutants. *Journal of Nematology*, **26**, 430-435.

Jospin, M., Jacquemond, V., Mariol, M.C., Segalat, L. and Allard, B. (2002a) The L-type voltage-dependent Ca2+ channel EGL-19 controls body wall muscle function in Caenorhabditis elegans. *J Cell Biol*, **159**, 337-348.

Jospin, M., Mariol, M.C., Segalat, L. and Allard, B. (2002b) Characterization of K(+) currents using an in situ patch clamp technique in body wall muscle cells from Caenorhabditis elegans. *J Physiol*, **544**, 373-384.

Keane, J. and Avery, L. (2003) Mechanosensory inputs influence Caenorhabditis elegans pharyngeal activity via ivermectin sensitivity genes. *Genetics*, **164**, 153-162.

Khan, M.L., Ali, M.Y., Siddiqui, Z.K., Shakir, M.A., Ohnishi, H., Nishikawa, K. and Siddiqui, S.S. (2000) C. elegans KLP-11/OSM-3/KAP-1: orthologs of the sea urchin kinesin-II, and mouse KIF3A/KIFB/KAP3 kinesin complexes. *DNA Res*, **7**, 121-125.

Kuhara, A., Inada, H., Katsura, I. and Mori, I. (2002) Negative regulation and gain control of sensory neurons by the C. elegans calcineurin TAX-6. *Neuron*, **33**, 751-763.

Lee, J.H., Gomora, J.C., Cribbs, L.L. and Perez-Reyes, E. (1999a) Nickel block of three cloned T-type calcium channels: low concentrations selectively block alpha1H. *Biophys J*, **77**, 3034-3042.

Lee, R.Y., Lobel, L., Hengartner, M., Horvitz, H.R. and Avery, L. (1997) Mutations in the alpha1 subunit of an L-type voltage-activated Ca2+ channel cause myotonia in Caenorhabditis elegans. *EMBO J.*, **16**, 6066-6076.

Lee, R.Y., Sawin, E.R., Chalfie, M., Horvitz, H.R. and Avery, L. (1999b) EAT-4, a homolog of a mammalian sodium-dependent inorganic phosphate cotransporter, is necessary for glutamatergic neurotransmission in caenorhabditis elegans. *J Neurosci*, **19**, 159-167.

L'Etoile, N.D., Coburn, C.M., Eastham, J., Kistler, A., Gallegos, G. and Bargmann, C.I. (2002) The cyclic GMP-dependent protein kinase EGL-4 regulates olfactory adaptation in C. elegans. *Neuron*, **36**, 1079-1089.

Lewis, J.A. and Fleming, J.T. (1995) Basic Culture Methods. *Methods Cell Biol*, **48**, 3-29.

Lien, C.W., Hisatsune, T. and Kaminogawa, S. (1999) Role of olfaction in food preference as evaluated in an animal model. *Biosci Biotechnol Biochem*, **63**, 1553-1556.

Lints, R. and Emmons, S.W. (1997) Genetic analysis of dopaminergic neuron specification in the male tail. *Worm Breeder's Gazette*, **15**, 51.

Lipton, J., Kleemann, G., Ghosh, R., Lints, R. and Emmons, S.W. (2004) Mate searching in Caenorhabditis elegans: a genetic model for sex drive in a simple invertebrate. *J Neurosci*, **24**, 7427-7434.

Loer, C.M. and Kenyon, C.J. (1993) Serotonin-deficient mutants and male mating behavior in the nematode Caenorhabditis elegans. *J Neurosci*, **13**, 5407-5417.

Lucas, F., Ackroff, K. and Sclafani, A. (1998) High-fat diet preference and overeating mediated by postingestive factors in rats. *Am J Physiol*, **275**, R1511-1522.

Marder, E., Abbott, L.F., Turrigiano, G.G., Liu, Z. and Golowasch, J. (1996) Memory from the dynamics of intrinsic membrane currents. *Proc Natl Acad Sci U S A*, **93**, 13481-13486.

Mathews, E.A., Garcia, E., Santi, C.M., Mullen, G.P., Thacker, C., Moerman, D.G. and Snutch, T.P. (2003) Critical residues of the Caenorhabditis elegans unc-2 voltage-

gated calcium channel that affect behavioral and physiological properties. *J Neurosci*, **23**, 6537-6545.
McKay, J.P., Raizen, D.M., Gottschalk, A., Schafer, W.R. and Avery, L. (2004) eat-2 and eat-18 are required for nicotinic neurotransmission in the Caenorhabditis elegans pharynx. *Genetics*, **166**, 161-169.
McKay, R.M., McKay, J.P., Avery, L. and Graff, J.M. (2003) C elegans: a model for exploring the genetics of fat storage. *Dev Cell*, **4**, 131-142.
Mellem, J.E., Brockie, P.J., Zheng, Y., Madsen, D.M. and Maricq, A.V. (2002) Decoding of polymodal sensory stimuli by postsynaptic glutamate receptors in C. elegans. *Neuron*, **36**, 933-944.
Mori, I. and Ohshima, Y. (1995) Neural regulation of thermotaxis in Caenorhabditis elegans. *Nature*, **376**, 344-348.
Morrison, G.E. and van der Kooy, D. (2001) A mutation in the AMPA-type glutamate receptor, glr-1, blocks olfactory associative and nonassociative learning in Caenorhabditis elegans. *Behav Neurosci*, **115**, 640-649.
Morrison, G.E., Wen, J.Y., Runciman, S. and van der Kooy, D. (1999) Olfactory associative learning in Caenorhabditis elegans is impaired in lrn-1 and lrn-2 mutants. *Behav Neurosci*, **113**, 358-367.
Nicholas, W.L., Dougherty, E.C. and Hansen, E.L. (1959) Axenic cultivation of C. briggsae (Nematoda: Rhabditidae) with chemically undefined supplements; comparative studies with related nematodes. *Ann. N.Y. Acad. Sci.*, **77**, 218-236.
Nicholas, W.L. and M.G., M. (1957) A technique for obtaining axenic cultures of rhabditid nematodes. *J. Helminthology*, **31**, 135-144.
Nuttley, W.M., Atkinson-Leadbeater, K.P. and Van Der Kooy, D. (2002) Serotonin mediates food-odor associative learning in the nematode Caenorhabditiselegans. *Proc Natl Acad Sci U S A*, **99**, 12449-12454.
O'Keefe, J. and Dostrovsky, J. (1971) The hippocampus as a spatial map. Preliminary evidence from unit activity in the freely-moving rat. *Brain Res*, **34**, 171-175.
Osborne, T.B. and Mendel, L.B. (1918) The choice between adequate and inadequate diets, as made by rats. *J. Biol. Chem.*, **35**, 19-27.
Pavlov, I.P. (1927) *Conditioned Reflexes*. Oxford University Press, Oxford.
Perez, C., Fanizza, L.J. and Sclafani, A. (1999) Flavor preferences conditioned by intragastric nutrient infusions in rats fed chow or a cafeteria diet. *Appetite*, **32**, 155-170.
Pierce-Shimomura, J.T., Faumont, S., Gaston, M.R., Pearson, B.J. and Lockery, S.R. (2001) The homeobox gene lim-6 is required for distinct chemosensory representations in C. elegans. *Nature*, **410**, 694-698.
Pierce-Shimomura, J.T. and McIntire, S.L. (2004) Swimming as a distinct form of locomotion in C.elegans: Analysis of the switch between crawling and swimming. *West Coast Worm Meeing Abstracts*, 38.
Pierce-Shimomura, J.T., Morse, T.M. and Lockery, S.R. (1999) The fundamental role of pirouettes in Caenorhabditis elegans chemotaxis. *J Neurosci*, **19**, 9557-9569.
Posadas-Andrews, A. and Roper, T.J. (1983) Social transmission of food preferences in adult rats. *Anim Behav*, **31**, 265-271.

Pujol, N., Link, E.M., Liu, L.X., Kurz, C.L., Alloing, G., Tan, M.W., Ray, K.P., Solari, R., Johnson, C.D. and Ewbank, J.J. (2001) A reverse genetic analysis of components of the Toll signaling pathway in Caenorhabditis elegans. *Curr Biol*, **11**, 809-821.

Raizen, D.M. and Avery, L. (1994) Electrical activity and behavior in the pharynx of Caenorhabditis elegans. *Neuron.*, **12**, 483-495.

Raizen, D.M., Lee, R.Y. and Avery, L. (1995) Interacting genes required for pharyngeal excitation by motor neuron MC in Caenorhabditis elegans. *Genetics.*, **141**, 1365-1382.

Ramirez, I. (1996) Stimulus specificity in flavor acceptance learning. *Physiol Behav*, **60**, 595-610.

Ranganathan, R., Sawin, E.R., Trent, C. and Horvitz, H.R. (2001) Mutations in the Caenorhabditis elegans serotonin reuptake transporter MOD-5 reveal serotonin-dependent and -independent activities of fluoxetine. *J Neurosci*, **21**, 5871-5884.

Richmond, J.E. and Jorgensen, E.M. (1999) One GABA and two acetylcholine receptors function at the C. elegans neuromuscular junction. *Nat Neurosci*, **2**, 791-797.

Richter, C.P. (1936) Increased salt appetite in adrenalectomized rats. *Endocrinology*, **115**, 155-167.

Richter, C.P. and Eckert, J.F. (1937) Increased calcium appetite of parathyroidectomized rats. *Endocrinology*, **21**, 50-54.

Richter, C.P., Holt, L.E. and Barelare, B. (1937) Vitamin B1 craving in rats. *Science*, **86**, 354-355.

Richter, C.P., Holt, L.E. and Barelare, B. (1938) Nutritional requirements for normal growth and reproduction in rats studied by the self-selection method. *Amer. J. Physiol.*, **122**, 734-744.

Roayaie, K., Crump, J.G., Sagasti, A. and Bargmann, C.I. (1998) The G alpha protein ODR-3 mediates olfactory and nociceptive function and controls cilium morphogenesis in C. elegans olfactory neurons. *Neuron*, **20**, 55-67.

Rose, J.K., Kaun, K.R., Chen, S.H. and Rankin, C.H. (2003) GLR-1, a non-NMDA glutamate receptor homolog, is critical for long-term memory in Caenorhabditis elegans. *J Neurosci*, **23**, 9595-9599.

Rose, J.K. and Rankin, C.H. (2001) Analyses of habituation in Caenorhabditis elegans. *Learn Mem*, **8**, 63-69.

Saeki, S., Yamamoto, M. and Iino, Y. (2001) Plasticity of chemotaxis revealed by paired presentation of a chemoattractant and starvation in the nematode Caenorhabditis elegans. *J Exp Biol*, **204**, 1757-1764.

Saper, C.B., Chou, T.C. and Elmquist, J.K. (2002) The need to feed: homeostatic and hedonic control of eating. *Neuron*, **36**, 199-211.

Satterlee, J.S., Sasakura, H., Kuhara, A., Berkeley, M., Mori, I. and Sengupta, P. (2001) Specification of thermosensory neuron fate in C. elegans requires ttx-1, a homolog of otd/Otx. *Neuron*, **31**, 943-956.

Sawin, E.R., Ranganathan, R. and Horvitz, H.R. (2000) C. elegans locomotory rate is modulated by the environment through a dopaminergic pathway and by experience through a serotonergic pathway. *Neuron*, **26**, 619-631.

Schafer, W.R. and Kenyon, C.J. (1995) A calcium-channel homologue required for adaptation to dopamine and serotonin in Caenorhabditis elegans. *Nature*, **375**, 73-78.
Schechter, M.D. and Calcagnetti, D.J. (1993) Trends in place preference conditioning with a cross-indexed bibliography; 1957-1991. *Neurosci Biobehav Rev*, **17**, 21-41.
Schultz, W. (1998) Predictive reward signal of dopamine neurons. *J Neurophysiol*, **80**, 1-27.
Sclafani, A. (1989) Dietary-induced overeating. *Ann N Y Acad Sci*, **575**, 281-289; discussion 290-281.
Sclafani, A. (2001) Psychobiology of food preferences. *Int J Obes Relat Metab Disord*, **25 Suppl 5**, S13-16.
Sclafani, A., Lucas, F. and Ackroff, K. (1996) The importance of taste and palatability in carbohydrate-induced overeating in rats. *Am J Physiol*, **270**, R1197-1202.
Sengupta, P., Colbert, H.A. and Bargmann, C.I. (1994) The C. elegans gene odr-7 encodes an olfactory-specific member of the nuclear receptor superfamily. *Cell*, **79**, 971-980.
Seymour, M.K., Wright, K.A. and Doncaster, C.C. (1983) The action of the anterior feeding apparatus of *Caenorhabditis elegans* (Nematoda: Rhabditida). *J. Zool. (Lond.)*, **201**, 527-539.
Shakir, M.A., Fukushige, T., Yasuda, H., Miwa, J. and Siddiqui, S.S. (1993) C. elegans osm-3 gene mediating osmotic avoidance behaviour encodes a kinesin-like protein. *Neuroreport*, **4**, 891-894.
Sherman-Gold, R. (1993) *The Axon Guide For Electrophysiology & Biophysics Laboratory Techniques*. Axon Instruments, Inc.
Skinner, B.F. (1938) *The behavior of organisms; an experimental analysis*. D. Appleton-Century Company, incorporated, New York, London.
Sokolowski, M.B. (2001) Drosophila: genetics meets behaviour. *Nat Rev Genet*, **2**, 879-890.
Spector, P.S., Curran, M.E., Zou, A., Keating, M.T. and Sanguinetti, M.C. (1996) Fast inactivation causes rectification of the IKr channel. *J Gen Physiol*, **107**, 611-619.
Starich, T.A., Herman, R.K., Kari, C.K., Yeh, W.H., Schackwitz, W.S., Schuyler, M.W., Collet, J., Thomas, J.H. and Riddle, D.L. (1995) Mutations affecting the chemosensory neurons of Caenorhabditis elegans. *Genetics*, **139**, 171-188.
Starich, T.A., Lee, R.Y., Panzarella, C., Avery, L. and Shaw, J.E. (1996) eat-5 and unc-7 represent a multigene family in Caenorhabditis elegans involved in cell-cell coupling. *J Cell Biol.*, **134**, 537-548.
Steger, K.A. (2003) *Cholinergic regulation of feeding in C.elegans: studies of a T-type calcium channel and three muscarinic acetylcholine receptors. In: PhD dissertation The University of Texas Southwestern Medical Center at Dallas.*
Steger, K.A., Shtonda, B.B., Thacker, C., Snutch, T.P. and Avery, L. (2004) The *Caenorhabditis elegans* T-type calcium channel CCA-1 boosts neuromuscular transmission. *submitted*.
Steiner, J.E. (1973) The gustofacial response: observation on normal and anencephalic newborn infants. *Symp Oral Sens Percept*, 254-278.
Steiner, J.E. (1979) Human facial expressions in response to taste and smell stimulation. *Adv Child Dev Behav*, **13**, 257-295.
Stellar, J. and Stellar, E. (1985) *Neurobiology of motivation and reward*. Springer-Verlag, New York.

Sulston, J., Dew, M. and Brenner, S. (1975) Dopaminergic neurons in the nematode Caenorhabditis elegans. *J Comp Neurol*, **163**, 215-226.
Sulston, J. and Hodgkin, J. (1988) Methods. In: The Nematode C. elegans. (Wood W, ed). In, Cold Spring Harbor, New York: Cold Spring Harbor Laboratory, pp. 587-606.
Sulston, J.E. and Horvitz, H.R. (1977) Post-embryonic cell lineages of the nematode, Caenorhabditis elegans. *Dev Biol*, **56**, 110-156.
Suo, S., Sasagawa, N. and Ishiura, S. (2003) Cloning and characterization of a Caenorhabditis elegans D2-like dopamine receptor. *J Neurochem*, **86**, 869-878.
Svendsen, P.C. and McGhee, J.D. (1995) The C. elegans neuronally expressed homeobox gene ceh-10 is closely related to genes expressed in the vertebrate eye. *Development*, **121**, 1253-1262.
Sze, J.Y., Victor, M., Loer, C., Shi, Y. and Ruvkun, G. (2000) Food and metabolic signalling defects in a Caenorhabditis elegans serotonin-synthesis mutant. *Nature*, **403**, 560-564.
Tabish, M., Siddiqui, Z.K., Nishikawa, K. and Siddiqui, S.S. (1995) Exclusive expression of C. elegans osm-3 kinesin gene in chemosensory neurons open to the external environment. *J Mol Biol*, **247**, 377-389.
Thomas JH and HR, H. (1988) Osmotic avoidance mutants with normal sensory endings. *Worm Breeder's Gazette*, **10**, 167.
Thorndike, E. (1965, reprint of 1911 ed.) *Animal intelligence; experimental studies*. Hafner Pub. Co., New York.
Tordoff, M.G. (2002) Obesity by choice: the powerful influence of nutrient availability on nutrient intake. *Am J Physiol Regul Integr Comp Physiol*, **282**, R1536-1539.
Trent, C., Tsuing, N. and Horvitz, H.R. (1983) Egg-laying defective mutants of the nematode Caenorhabditis elegans. *Genetics*, **104**, 619-647.
Tsalik, E.L. and Hobert, O. (2003) Functional mapping of neurons that control locomotory behavior in Caenorhabditis elegans. *J Neurobiol*, **56**, 178-197.
Turrigiano, G., LeMasson, G. and Marder, E. (1995) Selective regulation of current densities underlies spontaneous changes in the activity of cultured neurons. *J Neurosci*, **15**, 3640-3652.
Uchida, O., Nakano, H., Koga, M. and Ohshima, Y. (2003) The C. elegans che-1 gene encodes a zinc finger transcription factor required for specification of the ASE chemosensory neurons. *Development*, **130**, 1215-1224.
Urban, N.N., Henze, D.A. and Barrionuevo, G. (1998) Amplification of perforant-path EPSPs in CA3 pyramidal cells by LVA calcium and sodium channels. *J Neurophysiol*, **80**, 1558-1561.
Way, J.C. and Chalfie, M. (1988) mec-3, a homeobox-containing gene that specifies differentiation of the touch receptor neurons in C. elegans. *Cell*, **54**, 5-16.
White, J., Southgate, E., Thomson, J. and Brenner, S. (1986) The structure of the nervous system of *Caenorhabditis elegans*. *Phil Trans Roy Soc Lond B*, **314**, 1-340.
Wicks, S.R., de Vries, C.J., van Luenen, H.G. and Plasterk, R.H. (2000) CHE-3, a cytosolic dynein heavy chain, is required for sensory cilia structure and function in Caenorhabditis elegans. *Dev Biol*, **221**, 295-307.
Xue, D., Finney, M., Ruvkun, G. and Chalfie, M. (1992) Regulation of the mec-3 gene by the C.elegans homeoproteins UNC-86 and MEC-3. *Embo J*, **11**, 4969-4979.

Yeates, G.W., Bongers, T., DeGoede, R.G.M., Freckman, D.W. and Georgieva, S.S. (1993) Feeding habits in soil nematode families and genera-An outline for soil ecologists. *J. Nematol.*, **25**, 315-331.

Young, P.T. (1933) Relative food preferences of the white rat. II. *J. Comp. Psychol.*, **15**, 149-165.

Young, P.T. (1941) The experimental analysis of appetite. *Psychol. Bulletin*, **38**, 129-164.

Zhang, Y., Lu, H. and Bargmann, C.I. (2004) Olfactory learning of C. elegans in response to pathogenic bacteria. *West Coast Worm Meeing Abstracts*, **41**.

VITAE

Boris Borisovich Shtonda was born on October 15, 1976 in Kyiv, Ukraine, to parents Olga Igorevna and Boris Grigorievich Shtonda. In 1983 through 1993 he attended school # 141 in the same city. In 1993 through 1998 he studied biology in Kyiv Taras Schevchenko University, majoring in biochemistry. There, he got Bachelor in Biochemistry (in 1997) and Magister in Biochemistry (in 1998) degrees, both with Honors. In 1998, he joined the Graduate school of the UT Southwestern Medical Center in Dallas, TX. In 1999-2001, he was working in the laboratory of Dr. Ilya Bezprozvanny. In March 2001, he joined the laboratory of Dr. Leon Avery.

e-mail: boris@eatworms.swmed.edu

telephone: (214)-520-07-46

web: http://eatworms.swmed.edu/~boris/